RESEARCH & DEVELOPMENT

Re-appraisal of the Specification for Aggregate Base Course (ABC)

Brina Montoya, PhD, PE
Cassie Castorena, PhD
Department of Civil, Construction, and Environmental Engineering
North Carolina State University

Technical Report Documentation Page

1. Report No. FHWA/NC/2016-01	2. Government Accession No.	3. Recipient's Catalog No.
2. Title and Subtitle Re-appraisal of the Specification for Aggregate Base Course (ABC)	5. Report Date January 31, 2018	
	6. Performing Organization Code	
7. Author(s) Brina Montoya and Cassie Castorena	8. Performing Organization Report No.	
9. Performing Organization Name and Address Department of Civil, Construction, and Environmental Engineering North Carolina State University Campus Box 7908 Raleigh, NC 27695	10. Work Unit No. (TRAIS)	
	11. Contract or Grant No.	
12. Sponsoring Agency Name and Address North Carolina Department of Transportation Research and Development Unit 104 Fayetteville Street Raleigh, North Carolina 27601	13. Type of Report and Period Covered Final Report August 1, 2015 – December 31, 2017	
	14. Sponsoring Agency Code RP 2016-01	
Supplementary Notes:		

16. Abstract

   The current specification for acceptance of Aggregate Base Course (ABC) materials consists of a band-type gradation specification, which is essentially a "recipe" that dictates the mass percentages of the individual particle sizes constituting the ABC. These specifications were developed about a half century ago with few adjustments since then and are similar to the majority of the DOTs around the country. The "recipe" specification is based on the assumption that the product will achieve the desired engineering performance as long as it meets the gradation specifications and is placed and compacted properly in the field. A more comprehensive approach to evaluate ABC material is needed. Gradation of the ABC alone is insufficient to adequately capture the performance of the pavement during the service life. Incorporating easy to measure physical characteristics of the ABC (e.g., angularity, shape, and texture) and aggregate packing theory into the material evaluation may aid in linking easily measured ABC properties to observed mechanical behavior and be used in the ME design parameters. The findings of the project indicate that the ABC materials meeting the current NCDOT gradation specification exhibited consistent resilient behavior, even when the material is gap-graded within the specification band. Furthermore, analytical packing theories confirmed that the current gradation band produces material with adequate performance. The surface texture and sphericity are statistically significant morphological properties that affect the resilient modulus of ABC. A regression analysis was performed to establish a predictive resilient modulus model; the inputs to the model include surface texture, and sphericity. Additionally, compaction processes (e.g., impact compaction) can degrade ABC materials that are susceptible to crushing. This in turn affects the resilient modulus of the ABC by changing the fabric of the material. The compaction method used in the laboratory should match the compaction processes in the field for a more representative resilient modulus; for example, if vibratory methods are used in the field, they should also be considered for the laboratory specimen preparation. Finally, the majority of the M_R results for a wide range of degree of saturation are within a relatively narrow band, indicating that the inherent variability of the material may have a higher effect than saturation level on the M_R results for the sources studied.

17. Key Words Aggregate base course, resilient modulus	18. Distribution Statement		
19. Security Classif. (of this report) Unclassified	20. Security Classif. (of this page) Unclassified	21. No. of Pages 160	22. Price

Form DOT F 1700.7 (8-72)   **Reproduction of completed page authorized**

DISCLAIMER

The contents of this report reflect the views of the author(s) and not necessarily the views of the University. The author(s) are responsible for the facts and the accuracy of the data presented herein. The contents do not necessarily reflect the official views or policies of either the North Carolina Department of Transportation or the Federal Highway Administration at the time of publication. This report does not constitute a standard, specification, or regulation.

EXECUTIVE SUMMARY

The current specification for acceptance of Aggregate Base Course (ABC) materials consists of a band-type gradation specification, which is essentially a "recipe" that dictates the mass percentages of the individual particle sizes constituting the ABC. These specifications were developed about a half century ago with few adjustments since then and are similar to the majority of the DOTs around the country. The "recipe" specification is based on the assumption that the product will achieve the desired engineering performance as long as it meets the gradation specifications and is placed and compacted properly in the field. The biggest disadvantage of the "recipe" specification is that it cannot quantify the mechanical behavior of the aggregates under different traffic and weather conditions, which will determine the stress states and moisture content. Recent developments in mechanistic-empirical (ME) pavement design (i.e., Pavement ME Design) utilize mechanical material properties to predict pavement performance, which includes properties of the unbound aggregates. Therefore, understanding the mechanical properties of ABC is critical for the prediction of pavement performance, and consequently pavement design. Unfortunately, the current ABC specification is disconnected with the design process and required parameters (e.g., resilient modulus).

A more comprehensive approach to evaluate ABC material is needed. Gradation of the ABC alone is insufficient to adequately capture the performance of the pavement during the service life. Incorporating easy to measure physical characteristics of the ABC (e.g., angularity, shape, and texture) and aggregate packing theory into the material evaluation may aid in linking easily measured ABC properties to ME design parameters. To assess the ABC specification, a thorough testing program was developed. The testing program was complimented with analytically evaluating the ABC material using aggregate packing theory. The material and behavioral testing and analysis results were used to develop a relationship between the material properties and resilient modulus, which is a key input to Pavement ME Design.

The findings of the project indicate that the resilient behavior of ABC materials was insensitive to the gradation when inside the current NCDOT gradation specification. Furthermore, analytical packing theories confirmed that the current gradation band produces material with adequate performance. The surface texture and sphericity are statistically significant morphological properties that affect the resilient modulus of ABC. A regression analysis was performed to establish a predictive resilient modulus model; the inputs to the model include surface texture, and sphericity. Additionally, compaction processes (e.g., impact compaction) can degrade ABC materials that are susceptible to crushing. This in turn affects the resilient modulus of the ABC by changing the fabric of the material. The compaction method used in the laboratory should match the compaction processes in the field for a more representative resilient modulus; for example, if vibratory methods are used in the field, they should also be considered for the laboratory specimen preparation. Finally, the majority of the M_R results for a wide range of degree of saturation are within a relatively narrow band, indicating that the inherent variability of the material may have a higher effect than saturation level on the M_R results for the sources studied.

TABLE OF CONTENTS

Introduction

The current specification for acceptance of Aggregate Base Course (ABC) materials consists of a band-type gradation specification, which is essentially a "recipe" that dictates the mass percentages of the individual particle sizes constituting the ABC. These specifications were developed about a half century ago with few adjustments since then, and are similar to the majority of the DOTs around the country. The "recipe" specification is based on the assumption that the product will achieve the desired engineering performance as long as it meets the required gradation and is placed and compacted properly in the field. However, the biggest disadvantage of the "recipe" specification is that it cannot quantify the mechanical behavior of the aggregates under different traffic and weather conditions, which will determine the stress and moisture state. Recent developments in mechanistic-empirical (ME) pavement design (i.e., Pavement ME Design) incorporate the mechanical properties of pavement materials, which include the unbound aggregates. Therefore, understanding the mechanical properties of ABC is critical for the prediction of pavement performance, and consequently design. Unfortunately, the current ABC specification is disconnected with the design process and required parameters (e.g., resilient modulus).

The criteria for accepting the ABC material based on the current gradation specifications is insufficient and outdated. A reappraisal of the ABC specification is needed. Gradation alone is insufficient to adequately capture mechanical properties, including stress and moisture sensitivity, of different aggregates. Incorporating physical characteristics of the ABC (e.g., angularity, shape, and texture) and aggregate packing theory into the material specification may provide more justification for the observed mechanical properties. Developing a relationship between the material properties and the mechanical behavior will allow the ABC evaluation process to be directly related to the design parameters.

The primary goal of this research is to develop a new approach to evaluate aggregate base course material. To do this, the following research objectives were to:

- Identify and evaluate the physical properties (e.g., morphology, material, fabric) that influence the ABC performance.
- Characterize the mechanical behavior of the ABC.
- Develop relationships between material properties and mechanical behavior.

The research results in a better understanding of the behavior of ABC in conjunction with resilient modulus. After a summary of the literature review is presented, the materials and methods used to address the research objectives are discussed. Then, a summary of the experimental work to assess the material properties and resilient modulus for all aggregate sources studied, and the corresponding relationship between them is discussed. The band-type gradation specification is evaluated using packing theory frameworks. The effect of compaction methods and saturation levels on aggregate behavior are discussed. Finally, conclusions and recommendations from the research project are then presented.

Results of Literature Review

The ABC layer comprises one of the main structural components of a pavement. The layer, therefore, must possess high stiffness and strength. Materials used in ABC construction are also called unbound granular material (UGM). The unbound granular material derives its high stability from particle interlock and inter-particle friction.

The ABC layer is subjected to repeated load applications due to traffic. With every load repetition, the ABC layer undergoes both elastic (resilient) as well as plastic (permanent) deformations, shown in Figure 1. During loading, strains accumulate. During unloading, resilient strain is recovered but permanent strain remains. The resilient deformation is a complex function of multiple factors.
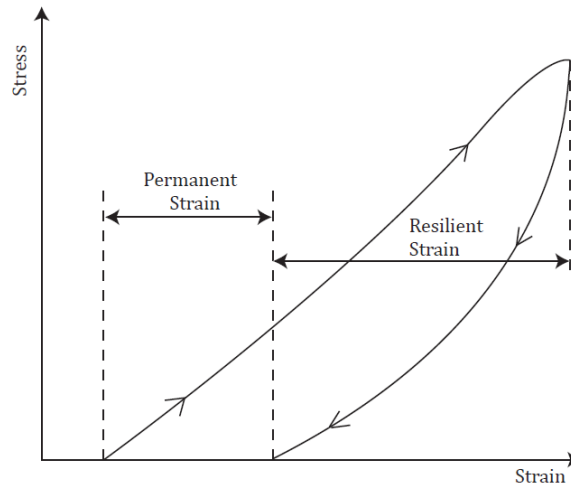
Figure 1 - Strain in ABC during a load cycle (Lekarp et al. 2000)

In a typical ABC layer, the accumulation of permanent deformation for each load repetition gradually decreases with increase in number of load application. The relative magnitude of permanent and resilient deformations in an ABC layer depends on traffic load levels and speed of operation, thickness and quality of overlying pavement layers (if any), quality of aggregates used in construction, and subgrade conditions.

Resilient response of ABC

Ideally, the deformation of an ABC layer during a pavement service life should be largely elastic since the repeated load applied to ABC layer is small compared to the strength of the material. Therefore, the deformation under each load repetition during the service life pavements is mostly elastic and proportional to the load, as shown in Figure 2 (Huang 1993). Accordingly, the elastic or resilient response of ABC has been emphasized in the mechanistic-based pavement design approaches to predict the critical pavement responses under traffic loading.
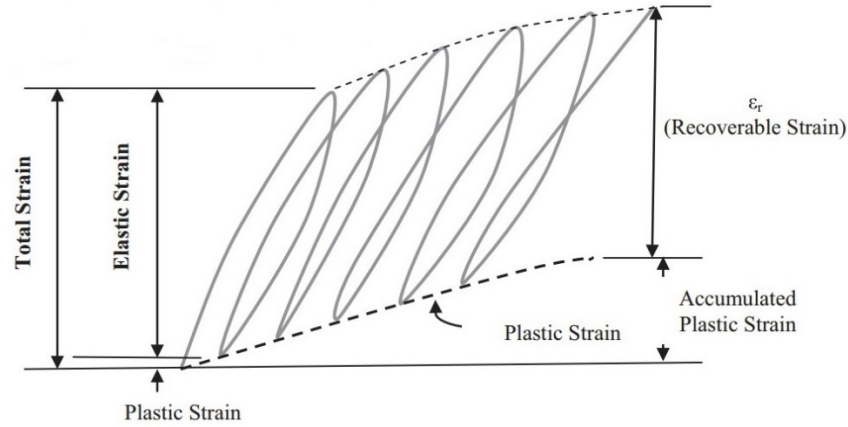
Figure 2 - Permanent and resilient deformation of UGM under repeated traffic loading (Huang 1993)

The most important property for incorporating repeated load behavior of ABC into pavement analysis is the resilient modulus (M_R) (NCHRP 1-37A 2004). M_R is defined as the secant modulus representing hysteretic stress-strain behavior of materials, illustrated in Figure 3.
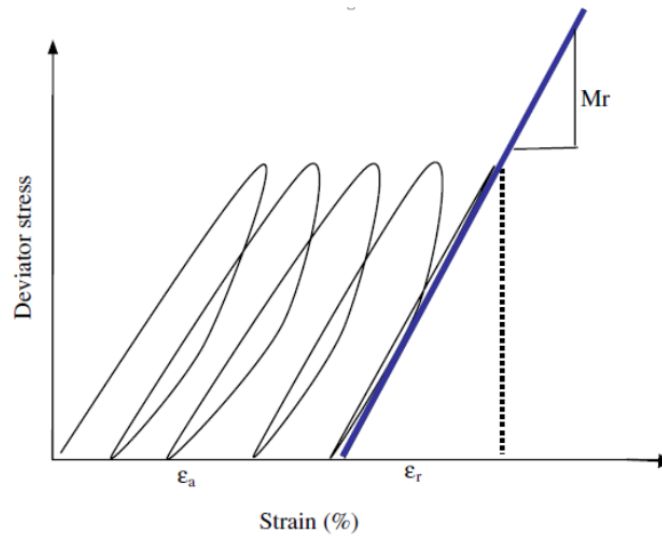
Figure 3 - Resilient modulus illustration (Kim and Kim 2007)

M_R can be obtained by either: 1) directly measuring M_R from a laboratory test, 2) correlating M_R using known ABC material properties, such as the California Bearing Ratio (CBR) (e.g., Hossain et al. 2011), or 3) using typical M_R values for the region (NCHRP 2004).

Factors affecting M_R

The resilient behavior of ABC is affected by several factors. These factors can be categorized to three main factors: (1) particle properties, (2) mass properties, and (3) in-service factors (Saeed et al. 2001). The particle properties consist of the gradation, particle shape, particle texture, particle angularity, specific gravity, chemical durability, mechanical durability, and freeze-thaw durability. The mass properties describe the behavior of the

aggregate layer as a continuum and include the shear strength, stiffness, permeability, frost susceptibility, and degree of compaction. Mass properties are significantly affected by particle properties. In-service performance of ABC is influenced by the moisture condition, state of stress, load duration and frequency. In the following sections, factors influential of ABC behavior and their reported effect of the resilient behavior of ABC are summarized.

Effect of Gradation

Gradation is a key factor that influences the mechanical behavior of ABC (i.e., resilient modulus, shear strength, and permanent deformation) and resistance to weathering (i.e., permeability, frost susceptibility, and erosion susceptibility). Traditionally, it was believed that dense-graded material with the minimum void content and maximum compacted weight would yield the highest shear strength and stiffness; however, more recent literature suggests that open graded material that drains well is preferable to maximize the resistance to damage caused by excessive moisture and frost action (Saeed et al. 2001).

The performance of a blend of aggregate can be greatly affected by the amount of the material passing the No. 200 sieve; however, the effect on performance is not consistent in the established literature. The amount of material passing the No. 200 sieve is typically specified to limit frost susceptibility, ensure sufficient permeability, and prevent the development of pore pressure (Saeed et al. 2001). Thompson and Smith (1990) reported that differences in the mass percentage of ABC material passing the No. 200 sieve yield limited differences in resilient modulus. Also, studies have indicated that increasing the fine content of ABC leads to a decrease in the resilient modulus (Barksdale and Itani 1989; Kamal et al. 1993). According to the current NCDOT specification, the amount of the material passing the No. 200 sieve is between 4 and 12 percent, which is a balance between the desired mechanical and serviceability (e.g., frost susceptibility, permeability, etc.) characteristics (NCODT 2012). Therefore, the effect of material passing the No. 200 sieve was not a focus of the current study.

Barksdale and Itani (1989) found that a finer gradation generally leads to greater plastic deformation and lower resilient moduli as shown in Figure 4. They argued that the coarse aggregates have a greater effect on plastic deformation than fine aggregate.
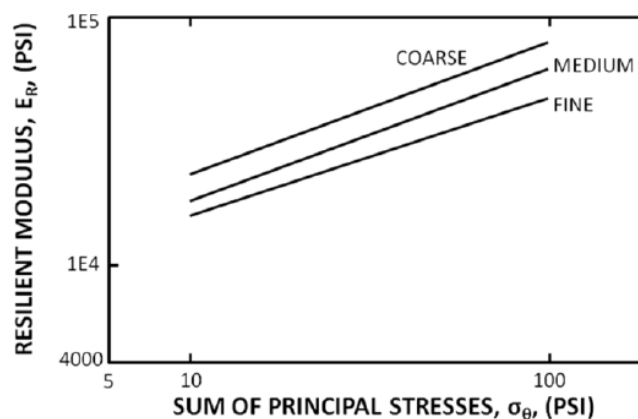

Figure 4 - Effect of gradation on resilient modulus (Barksdale and Itani 1989)

Tian et al. (1998) studied the effect of gradation on the resilient modulus of ABC material. They found that open-graded aggregates result in better drainage, lead to relatively high resilient modulus values. Therefore, open-graded aggregates will likely perform better

under saturated conditions. In addition, they found that finer-graded material tend to have a lower resilient modulus due to the lack of interlocking between large, irregular particles.

Trends among the resilient behavior for coarse and well-graded blends are not clear. Some studies have reported that coarser blends lead to higher resilient moduli (Tian et al. 1998; Zaman et al. 1994). Others have reported that coarse blends yield lower resilient moduli than fine blends (Rada and Witczak 1981, Zeghal 2000). Additional studies have reported little sensitivity (less than 10 percent) in the resilient behavior of ABC to gradation (Zaman et al. 1994). Cunningham et al. (2013) suggested that gradation plays some role in determining the resilient behavior of ABC, especially with changes in the percent passing No. 200 material, but their effect was very little compared to the stress state of the material.

Mishra et al. (2010) studied the effect of plasticity of the fines on unbound aggregate performance. They demonstrated that plastic fines deteriorate aggregate performance significantly. Plastic fines contents in excess of 10 percent by weight at wet of optimum moisture conditions reduce strength substantially. However, an increase in the non-plastic fines content did not decrease strength. At low fine contents, the type of fines is unlikely an important factor in determining the resilient behavior of ABC. According to the current NCDOT specification, the plasticity index less than 6.0 and liquid limit less than 30 are acceptable for the material passing the No. 40. As these values are relatively low, the effect of plasticity index was not a focus of the current study.

Effect of Moisture Content

The behavior of granular material is highly dependent on the degree of saturation (i.e., moisture content). The resilient response of dry and partially saturated granular materials are expected to be similar; however, the resilient behavior may be sensitive to the moisture content at conditions near saturation (Vuong 1992). The literature demonstrates that the resilient modulus decreases as the saturation level increases at high degrees of saturation (Barksdale and Itani 1989; Heydinger et al. 1996; Hicks and Monismith 1971).

Thom and Brown (1985) demonstrated a decrease in the resilient modulus of ABC with an increase in the moisture content, which they attributed to the lubricating effect of the moisture (Thom and Brown 1987). Pore water pressure did not develop as the degree of saturation was increased to 85 percent.

Tian et al. (1998) reported a decrease in the resilient modulus of ABC with increasing moisture content when the moisture content exceeded optimum which they attributed to a decrease in the matric suction. Dawson et al. (1996) reported a similar finding based on the analysis of a range of well-graded unbound aggregates.

Effect of morphological properties

Aggregate morphological characteristics, including particle form, particle angularity, and surface texture (depicted in Figure 5), can influence the resilient behavior and permanent deformation performance of ABC (Barksdale and Itani 1989).
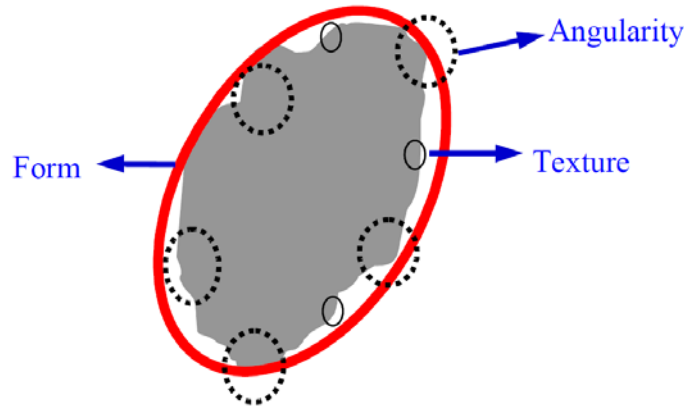
Figure 5 - Physical characteristics of aggregate particles (Little et al. 2003)

The aggregate morphological properties can be assessed using experimental tests. The variations in the proportions of an aggregate particle is considered the particle form. The particle form of coarse aggregates can be examined using proportional calipers to determine the proportion of flat and elongated coarse aggregate particles (ASTM D 4791). These particles can affect compaction and can break under compaction, (which can change the gradation of the aggregate) (Little, et al. 2003). Surface texture is related to an aggregate particle's surface irregularity at a micro-scale. Surface texture does not affect the overall particle shape but does affect the friction between particles. There is indication that increasing particle roughness, (along with particle angularity), increases the resilient modulus and at the same time decreases Poisson's ratio (Tutumluer, 2013). Surface texture is difficult to measure because it relates to the micro-scale. Angularity is the difference in the corners of an aggregate particle. Angularity is critical to the performance of the unbound pavement layer because angularity drive interlocking between particles. Interlocking of particles increases resistance to rutting and fatigue (Saeed, et al. 2001). Angularity increases the contact points between aggregate particles which increases resilient modulus and distributes loads better than less angular particles (Tutumluer, 2013). There are two standards to quantify the angularity of an aggregate particle; AASHTO T 335 and AASHTO T 304. These methods have been shown to be difficult, time-consuming, and subjection (Gates, et al. 2011). Thus, a system was developed to measure aggregate morphological properties by utilizing image analysis in a non-destructive procedure that is rapid and not subjective, called Aggregate Imaging Measurement System (AIMS). The AIMS device can measure the morphological properties of both coarse and fine aggregate. AIMS characterizes coarse aggregate angularity, sphericity, flatness/elongation, and surface texture. AIMS characterizes fine aggregate angularity and particle form.

The AIMS2 device, the second generation of AIMS which has improvements in its imagining process, has a turntable for the aggregate particles which decreases the size requirements of the backlight area. Particles can be loaded directly on the turntable in different slots instead of on specific points within a grid which is simpler and accommodates a greater number of aggregate particles. The tray system also makes cleaning easier. Fine particles can be placed on colored trays to see them with sufficient contrast. A better camera was employed within the AIMS2 as well as LED technology for the lighting. The operator interface was streamlined to address user difficulty. The AIMS2 system is shown in Figure 6. The improvements have made the AIMS2 a viable option for automated determination of

aggregate particle geometric properties in practice, which can further improve specifications in asphalt pavements.

Figure 6 - AIMS2 equipment and set-up (Gates et al. 2011)

Effect of compaction method

Laboratory characterization of ABC (such as resilient modulus, permanent deformation, and moisture-density relationship) can be influenced by compaction method. Furthermore, it's important to align laboratory compaction methods to simulate the field compaction processes. Compaction processes can also alter the original ABC gradation, and this may increase the fine content and result in increase in optimum moisture content of ABC.

There are two common laboratory compaction methods, impact compaction and vibratory compaction. These compaction methods can lead to different particle orientations in a granular mixture (Oda 1972). The impact method has been shown to may break aggregate during the compaction, resulting in a change in the original gradation. On the other hand, the vibratory method has previously shown a minimal change to the original gradation. However, there is no sufficient research on the effect of the compaction methods on the mechanical behavior of ABC (Cetin, et al. 2014).

In this research, the effect of compaction method on the M_r test results was studied by comparing the impact and vibratory compaction methods because the impact compaction is the common compaction method in the material and test unit of NCDOT, and the AASHTO standard for the M_r test suggests compacting the ABC using the vibratory compaction method.

Aggregate Packing theories

Several methods have been developed to design and/or evaluate the grain size distribution (GSD) of ABC materials and asphalt concrete mixtures using particle packing theories. Particle packing theories are a class of methods to analytically evaluate the GSD of granular material. Particle packing is a core research area in particle/powder technology (German 1989). Particle packing is driven by three factors: particle size distribution, particle shape, and particle size. The concept of packing theories was initially used in granular material mixtures in Fuller's equation as follow.

$$P = 100 \times \sqrt{\frac{d}{D}} \tag{1}$$

where,

P: the percent of material by weight passing a given sieve with an opening of size,

D: the maximum particle size of a given aggregate blends, and

n: the fitting parameter for the optimum curve that affects the coarseness or fineness of the gradation, given by the slope. 'n' typically varies between 0.3 and 0.5 where the smaller number correlates to a larger proportion of fine material (Santamarina et al 2001).

It was believed that the particle density drives the mechanical performance of the granular material. Further studies indicated that the densest aggregate does not necessarily perform well (Santamarina et al. 2001). Experimental studies with photoelastic disks of granular material under compression have shown that under an applied external pressure most of the load is transferred through chains of particles, shown in Figure 7, and other particles play the secondary role of preventing the main chain of particles from buckling. Therefore, studies have moved toward evaluating the effect of particle packing with respect to load transfer mechanisms and the material performance (Santamarina et al. 2001).

Three frameworks were recently developed based on packing theory namely Bailey (Vavrik 2002), Dominant Aggregate Size Ratio (DASR) (Kim et al. 2006), and Yideti (Yideti et al. 2014) frameworks. These frameworks either evaluate the performance of the aggregate or identify the load carrying structure in order to predict the performance of the unbound material. In this study, these frameworks are implemented to evaluate the NC gradation band for ABC material. Further description of the three packing theory frameworks are included in the literature review (Appendix A) and the draft packing theory paper (Appendix B).

(a) (b)
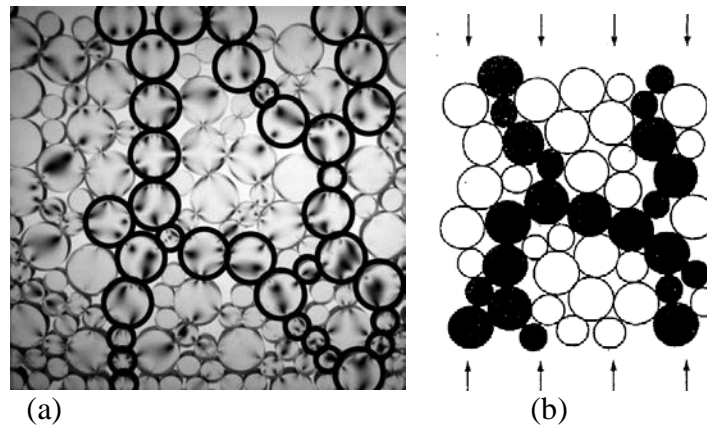
Figure 7 - Particle chain (a) Photoelastic demonstration (b) Schematic demonstration (Santamarina et al. 2001)

Materials and Methods

This section outlines the experimental plan to evaluate the effects of aggregate properties and laboratory preparation methods on the mechanical behavior of ABC.

Research Framework

A research framework was developed to investigate the effect of aggregate properties on the mechanical performance of ABC. Based on extensive review of technical literature and available tools (as summarized in Appendix A), a series of aggregate physical and morphological properties were chosen to be measured which are described in this section. The mechanical properties of ABC were obtained using the resilient modulus (M_R) test, which is widely used to measure the ABC stiffness and is a key factor in mechanistic-

empirical pavement design (e.g., Pavement ME). The research plan implemented in the current study and described herein is depicted in Figure 8.
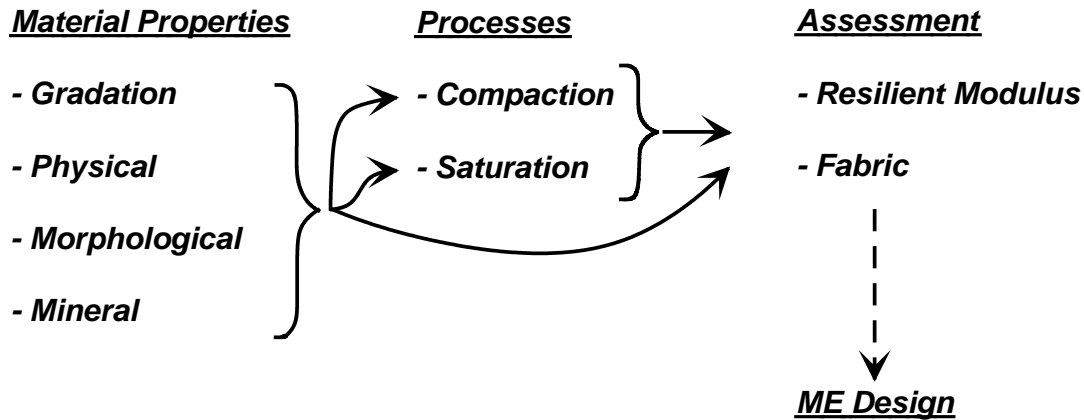
Figure 8 - Research plan for current study, broken down into three categories: material properties, processes, and assessment (connected using solid lines). Current work connection to mechanistic-empirical design is also illustrated (dashed line).

Material source and selected gradations

ABC material was collected from five sources in North Carolina (NC) for evaluation in this study. The aggregate sources were selected to encompass a wide range of aggregate properties and mineralogy. Table 1 shows the selected aggregates and corresponding geological region (Chow, et al. 2014).

Table 1 - ABC sources selected for the research

Quarry	Geology
Arrowood	Piedmont
Jamestown	
Franklin	
Fountain	Coastal Plain
Belgrade	

Every agency has established ABC gradation band specifications. Generally, agencies adopt gradation specifications that fall near those given in AASHTO M147, Table 2. The NCDOT band specification falls close to AASHTO M147 Grading B as shown in Figure 9. All ABC material evaluated was oven-dried for sieve analysis. Sieve analysis was conducted in accordance with ASTM C136. The list of the sieves considered and the NCDOT specification for upper band (UB) and lower band (LB) is shown in Table 3. Sieved materials were recombined to meet the desired gradation for mechanical testing. The UB and LB gradations are the finest and coarsest gradations, respectively, acceptable by NCDOT for ABC materials. In addition to these two gradations, middle band (MB) and gap-graded (GG) gradations were also used in this study. The middle band gradation was obtained from the average percent passing in upper band and lower band gradations. The GG gradation was

created using the MB gradation but excluding aggregate smaller than 12.7 mm and larger than 4.75 mm.

Table 2 - Upper and lower limits suggested by AASHTO M147

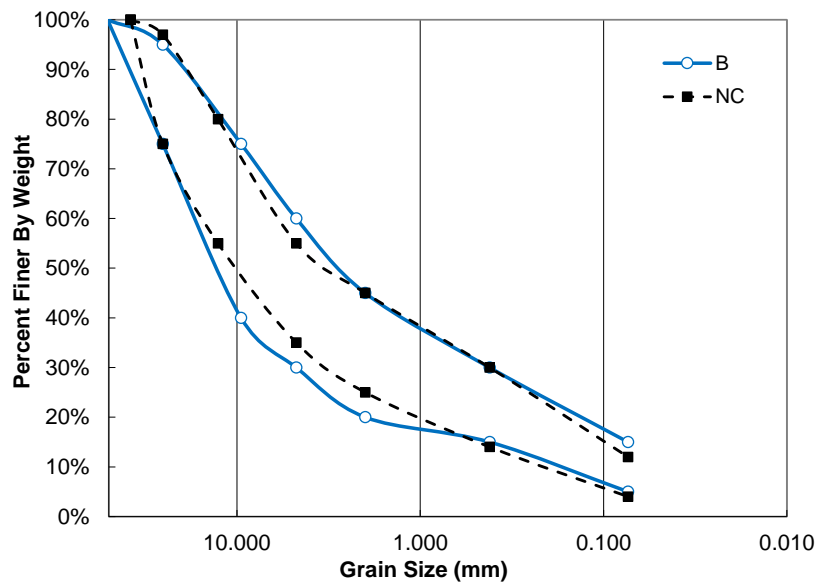| Sieve Designation		Mass Percentage Passing					
Standard, mm	Alternate	Grading A	Grading B	Grading C	Grading D	Grading E	Grading F
50.0	2 in	100	100	–	–	–	–
25.0	1 in	–	75–95	100	100	100	100
9.5	3/8 in	30–65	40–75	50–85	65–100	–	–
4.75	No. 4	25–55	30–60	35–65	50–85	55–100	70–100
2.00	No. 10	15–40	20–45	25–50	40–70	40–100	55–100
0.425	No. 40	8–20	15–30	15–30	25–45	20–50	30–70
0.075	No. 200	2–8	5–20	5–15	5–20	6–20	8–25

Figure 9 - NC gradation band - upper and lower limits

Table 3 - NCDOT upper and lower limits (NCDOT, 2012)

Sieve No.	Diameter (mm)	Percent Passing (%)	
		Upper Limit	Lower Limit
1 1/2"	38.10	100%	100%
1"	25.40	75%	97%
1/2"	12.70	55%	80%
#4	4.75	35%	55%
#10	2.00	25%	45%
#40	0.42	14%	30%
#200	0.074	4%	12%

Laboratory characterization of aggregates

A series of common index tests were conducted to measure the aggregate physical properties. In addition, appropriate tests to assess morphological properties in a non-subjective manner were conducted. These tests are outlined in detail in this section.

Aggregate physical properties

Specific gravity test

The bulk specific gravity of the aggregates was measured in accordance with ASTM D854-14 for the particles finer than 4.75 mm (No.4 sieve), and ASTM C127-15 for the particles coarser than 4.75 mm (No.4 sieve). Two replicate measurements of specific gravity were made for each aggregate source and the blended coarse and fine aggregate specific gravities ($G_{avg@20°C}$) were calculated using Equation 2.

$$G_{avg@20°C} = \frac{1}{\dfrac{R}{100 \times G_{1@20°C}} + \dfrac{P}{100 \times G_{2@20°C}}}$$

(2)

where,

R : the percent of soil retained on the 4.75-mm sieve

P : the percent of soil passing the 4.75-mm sieve,

$G_{1@20°C}$: the apparent specific gravity of soils retained on the 4.75-mm sieve as determined by Test Method C127, corrected to 20°C

$G_{2@20°C}$: the specific gravity of soil solids passing the 4.75-mm sieve as determined by Test Method C854

Atterberg limits

The Atterberg limits, (i.e., plastic and liquid limits), of aggregate passing the No. 40 sieve were measured in accordance with ASTM D4318 to understand the role of the interaction between the fine material and water on ABC behavior. Fine aggregates control the behavior of the ABC within the gradation band used in the research where up to 12% of the total mass can be made of material passing the No. 200 (0.075 mm) sieve based on the Unified Soil Classification System (USCS) classification system (ASTM D2487-11).

Moisture-density relationship

The compaction characteristics of each ABC source and gradation evaluated in this study were measured using a modified version of the modified compaction test specified in AASHTO T-180. Compaction was performed using five layers in a CBR mold with 6-in diameter and 7-in height. A total of 86 blows was applied to each layer with a 10-lb hammer and 18-in drop height. For each gradation, four tests were performed at different moisture contents and used to plot the moisture-density curve. It should be mentioned that the AASHTO standard is 56 blows, and the addition of 30 blows per layer in the compaction test was chosen to be consistent with the procedure traditionally used in NCDOT Material and Testing unit.

Los Angeles Abrasion Test

The abrasion and degradation resistance of the ABC materials was quantified using the Los Angeles Abrasion test specified in ASTM C131-14. Abrasion resistance is anticipated to be an indicator of ABC resistance to degradation under compaction. This test is a measure of degradation of mineral aggregates of standard grading resulting from a combination of actions including abrasion or attrition, impact, and grinding in a rotating steel drum containing a specified number of steel spheres, the number depending upon the grading of the test sample. As the drum rotates, a shelf plate picks up the sample and the steel spheres, carrying them around until they are dropped to the opposite side of the drum, creating an impact crushing effect. The contents then roll within the drum with an abrading and grinding action until the shelf plate picks up the sample and the steel spheres, and the cycle is repeated. After the prescribed number of revolutions, the contents are removed from the drum and the aggregate portion is sieved on a 1.70 mm (No.12) sieve to measure the degradation as percent loss. The abrasion resistance is quantified using the percent loss, calculated using Equation 3.

$$Loss(\%) = (\frac{M_0 - M_1}{M_0}) \times 100$$

(3)

where,

M_0 : mass of original test sample, g,

M_1 : final mass of sample retained on 1.70 mm (No.12) sieve.

Aggregate morphological properties

Aggregate morphological properties, including angularity, texture, and aspect ratios (flat and elongated), were measured using the imaging measurement machine, Aggregate Imaging Measurement System 2 (AIMS2). The AIMS2 was used to measures particles angularity index (AI), surface texture (ST), and sphericity (S) of coarse and fine particles (Table 4). Particle form quantifies the relative from of fine particles from 2D images, ranging from 0 (a perfect circle) to 20. Angularity of particles describes variations at the particle boundary that influence the overall shape, ranging from 0 (a perfect circle) to 10^4. Surface texture describes the relative smoothness or roughness of coarse particles' surface, ranging from 0 (a smooth polished surface) to 10^3. Sphericity of coarse particles describes the overall 3D shape of a particle by measuring the particle's shortest (d_S), intermediate (d_I), and largest (d_L) dimensions. Sphericity is calculated from the following equation:

$$SP = \sqrt{\frac{d_S d_I}{d_L^2}} \tag{4a}$$

Flatness and elongation ratios represent the ratio of a particle dimensions:

$$F \& E = \frac{d_L}{d_S} \tag{4b}$$

In this report, AIMS2 results are presented visually in two manners: bar charts to describe the morphological properties of each particle size, and cumulative distribution as described by Gu et al. (2014). The cumulative distribution is determine by calculating the composite index of different sources and fitting a cumulative Weibull distribution to the data. The cumulative distribution is a particularly meaning method to represent the data in order to implement the AIMS2 results into the statistical analysis of the data, as discussed in the subsequent section of this report.

Table 4 - Measurements performed by AIMS2 on different particles

Test	Coarse Aggregate	Fine Aggregate
Particle form		$\times$
Angularity	$\times$	$\times$
Texture	$\times$	
Sphericity	$\times$	
Flatness and elongation ratios	$\times$	

Aggregate mineralogy

The mineralogical composition of each aggregate source was quantified according to ASTM C25 by an external laboratory, which yields the percentage of Ca, Mg, Fe, Al, and Si within the aggregate mineral structure.

Compaction methods

The effect of the laboratory compaction method on the M_R values of ABC was evaluated by preparing laboratory-fabricated ABC specimens using two different compaction methods: impact compaction (IC) and vibratory compaction (VC).

The IC was performed with a 4.5 kg hammer with 45.7 cm drop (according to AASHTO-T180) in six layers in accordance with AASHTO T-307. The VC method was performed following the procedure described in AASHTO T-307 (Annex B). A Makita Demolition Hammer MODEL HM0810B was used to prepare VC specimens. Each layer was compacted to achieve a target height using the compactor's weight plus pressure applied by the operator were used in combination with the vibratory action from the hammer. The VC specimens were compacted using seven lifts. The resulting moisture-density relationships from the two compaction methods are equivalent.

Change in the sample saturation

In this project, a procedure was used to evaluate the effect of moisture on M_R of ABC that more realistically represents wetting and drying in the field. This procedure is developed from the Canadian standard for M_R test, LC 22-400 MTQ (2004). The Canadian standard is

similar to AASHTO T-307 in terms of loading conditions, but it requires changing a sample's moisture and obtaining the M_R of the sample at three different saturation degrees. Based on the Canadian standard, a M_R test specimen is prepared and tested at a low moisture content (2 percent above aggregate water absorption) (Stage 1), and then the test is performed on the sample on two other saturation degrees: near 100 percent saturation (Stage 2), and gravitationally drained (Stage 3). This standard has been applied and disseminated by a research group at Université Laval, Quebec, Canada (Bilodeau and Dore, 2012).

During Stage 1 the M_R test was carried out on a specimen that was compacted at 2% above the water absorption. At this stage, the degree of saturation was about 41% and 68% for the ABC materials tested (i.e., Arrowood and Belgrade specimens, respectively). After the resilient modulus test was conducted, water was injected into the specimen from the bottom platen, as shown in Figure 10, which is similar to the setup described in LC 22-400 MTQ (2004). In this method, the specimen was saturated using a water reservoir and effluent bucket. Before starting the saturation process, the weight of the empty bucket and full reservoir and tubes were measured. Then, the water reservoir was positioned at an elevation to produce about 20 kPa water pressure at the elevation of the bottom platen while a constant confining pressure of 35 kPa (5 psi) was applied to the sample. While keeping the confining pressure on the sample, the bottom drainage valve was opened so that the water enters the sample from the bottom gradually with an approximately 20 kPa pressure. Then, the top drainage lines were opened, the air bubbles were drained off, and water was collected in the bucket while it was covered to prevent from evaporating. When the reservoir became empty, the weight of the full bucket and empty reservoir and tubes were measured and recorded. The retained water in the specimen was estimated as expressed below:

$$M_{\text{retained water}} = (M_{\text{full reservoir}} - M_{\text{empty reservoir}}) - (M_{\text{full bucket}} - M_{\text{empty bucket}}) \qquad (5)$$

Then, the reservoir was filled again and the previous steps were repeated until the estimated cumulative retained water reached a constant value. Finally, the M_R test was performed on the nearly saturated sample. During M_R testing in stage 2, drained water was collected and weighted in order to back calculate the moisture content and degree of saturation at stage 2. The degree of saturation at stage 2 was greater than 90% based on the oven dried sample, at end of the series of the resilient modulus testing.
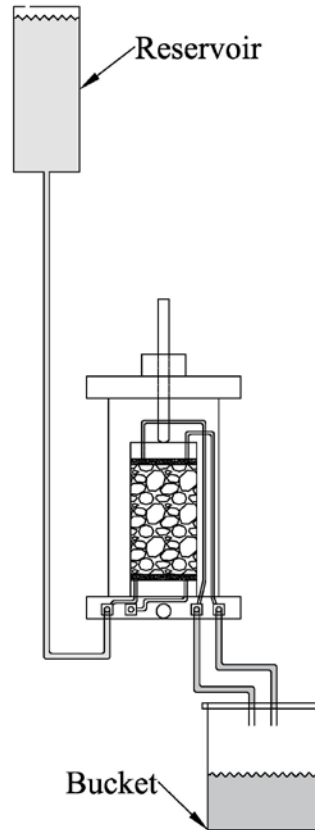
Figure 10 - Saturation setup

After the Stage 2 M_R test was executed, the water was allowed to drain out of the specimen gravitationally by keeping the sample in the cell and on the M_R setup frame which was about 1 meter above the ground, and placing the bucket on the ground (Figure 11). In addition, a confining pressure of about 100 kPa was applied to the specimen. This confining pressure allowed the sample to drain more easily. While the confining pressure was applied, all bottom and top valves were opened and water was allowed to drain from the bottom lines and collected in the bucket that was covered to prevent any evaporation. The cumulated water in the bucket was measured at different time interval until water ceased to drain from the specimen. Finally, the last M_R test (stage 3) was performed on the specimen. The degree of saturation at stage 3 was about 80%.

Figure 11 - Drainage Process

Aggregate mechanical test

The mechanical properties of the ABC was evaluated using the M_R test. The M_R test is performed in accordance with AASHTO T-307. Samples were compacted with impact and vibratory methods to achieve 100% dry density at th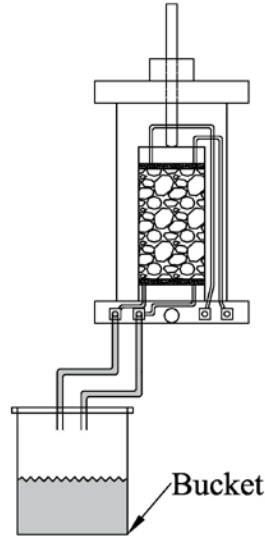e optimum moisture content. Each sample was compacted using multiple layers of equal mass to achieve the desired density by controlling the compacted height. The specimen preparation technique used in this study is consistent with the protocol used within the NCDOT Materials and Testing Unit.

M_R is obtained in the laboratory using the repeated load triaxial test under varying confining pressures. Various regression models for M_R can be used to estimate the modulus for other loading conditions. The regression model used in the Pavement ME Design (Equation 6) and k-θ method (Equation 7) were used herein.

$$M_R = k_1 P_a (\frac{\theta}{P_a})^{k_2} (\frac{\tau_{oct}}{P_a} + 1)^{k_3} \tag{6}$$

$$M_R = k\theta^n \tag{7}$$

where

θ : bulk stress;

τ_{oct} : octahedral shear stress;

P_a : atmospheric pressure; and

k, k_1, k_2, and k_3: regression coefficients.

Evaluation of specimen fabric

Digital image analysis was used to evaluate the aggregate fabric of compacted ABC specimens. To evaluate the fabric, an epoxy resin was used in place of water to prepare bound compacted ABC specimens. The epoxy resin used is Epo-Tek 301 from Epoxy Technology. The epoxy resin acts as a lubricant, similar to water, in the compaction process. Therefore, it was assumed that the epoxy resin acts similar to water and thus, is not anticipated to influence

the fabric of specimens. The resin content added to ABC mixture was equal to the mixture's optimum moisture content to best reflect M_R test specimens. The resin specific gravity is 1.094 and was prepared by mixing a base (G_S=1.15) and hardener (G_S=0.87) using a 4:1 ratio. The viscosity of the mixture is 100 to 200 cPs. It was hypothesized that adding the resin to ABC at the optimum moisture content would result in the maximum dry density of the mixture, which was confirmed experimentally using identical compaction energies. Thus, the relatively high viscosity of the epoxy resin does not appear to affect the compactability.

In addition, the fine aggregates were dyed blue to enhance the contrast between the coarse and fine particles during the image analysis. The bound specimens were sawn vertically into three sections and the faces were photographed using a DSLR Olympus Camera with a macro lens in order to capture high quality photographs of the sample fabric. The images were first processed using Adobe Photoshop CC2017. A perspective warp conducted to remove warping. Auto-contrast, auto-tone, and color balance tools were used to improve the contrast between the blue fines and larger aggregate particles. Subsequently, the image was converted into a grayscale image by increasing the value of red and decreasing the value of blue.

The grayscale image was imported into Matlab to determine the particle orientation and approximate gradation of the observed particles. The Matlab code converts the black and white image to a true binary image. This value was selected by evaluating a histogram of greyscale values and choosing a local minimum that delineated coarse and fine aggregate. Once converted into a binary image, the Matlab regionprops command was used to establish the centroid of each particle, area, and particle orientation.

To determine the number of contact points, the binary images that were created in Matlab were analyzed in the iPas software. The surface distance threshold (SDT) length was set as 4.7 mm because this was the cutoff size between fine and coarse particles. All coarse aggregate particles within 4.7 mm of one another were considered to be in contact. The SDT length was used as a filter to count the number of particles larger than sieve #4 (4.75mm) that were in contact.

Resilient Behavior of various ABC Sources

An objective of the current research study is to relate aggregate physical and morphological properties to the mechanical performance of ABC material. This was achieved by experimentally obtaining the properties and obtaining M_R values and regression coefficients of each tests. Finally, a statistical analysis was performed to obtain the significant of different aggregate physical and morphological properties on the M_R is obtained using nonlinear multivariable regression.

ABC material properties

The mineralogy, physical, and morphological properties of five aggregate sources were assessed. The aggregate mineralogy was obtained by evaluating the aggregate following ASTM C25 procedure. The most common elements measured within all the studied aggregate sources are silica, silicon dioxide, and aluminum oxide. The exception was the material from Belgrade, where the dominant minerals present are calcium, calcium oxide and calcium carbonate. In addition, the Arrowood source has a relatively high presence of iron oxide, though much smaller than the silica, silicon dioxide, and aluminum oxide.

Physical properties of ABC materials are presented in Table 5. The methods used to evaluate the properties are discussed in the Materials and Methods section of this report.

Please note, OWC and MDD refer to optimal water content and maximum dry density, respectively; both values were obtained from the moisture-density relationship. The middle band (MB) of the NC ABC gradation band was chosen as a controlled particle-size distribution to ensure that observed changes in aggregate behaviors could be attributed to the effects of varied aggregate properties (Figure 12).

Table 5 - ABC samples properties

Source	Geology	LA Abrasion Loss (%)	GS	OWC (%)	MDD (gr/cm3)
Arrowood	Piedmont	29%	2.91	4.2	2.46
Jamestown	Piedmont	43%	2.72	5.5	2.28
Franklin	Piedmont	56%	2.71	5.6	2.27
Fountain	Coastal Plain	28%	2.67	5.5	2.27
Belgrade	Coastal Plain	54%	2.56	7.2	2.15

According to Table 5, a similar behavior within the five ABC courses was observed, with Arrowood and Belgrade being the two extremes. Arrowood aggregate has the highest specific gravity, highest maximum dry density, and a relatively low LA abrasion loss, which may be attributed to the high presence of iron oxide in Arrowood aggregate. On the other hand, Belgrade aggregate has the lowest specific gravity and highest percent loss in the LA abrasion test. In addition, Belgrade aggregate has the highest optimum moisture content that may be the result of aggregate breakage during the compaction test, which increases the amount of fine particles in the mixture and consequently increases the required moisture to reach to the maximum density. The physical properties of Belgrade aggregate may be explained by the high percentage of calcium-based minerals. The other tested ABC material, Franklin, Foundation, and Jamestown, have relatively similar physical properties.
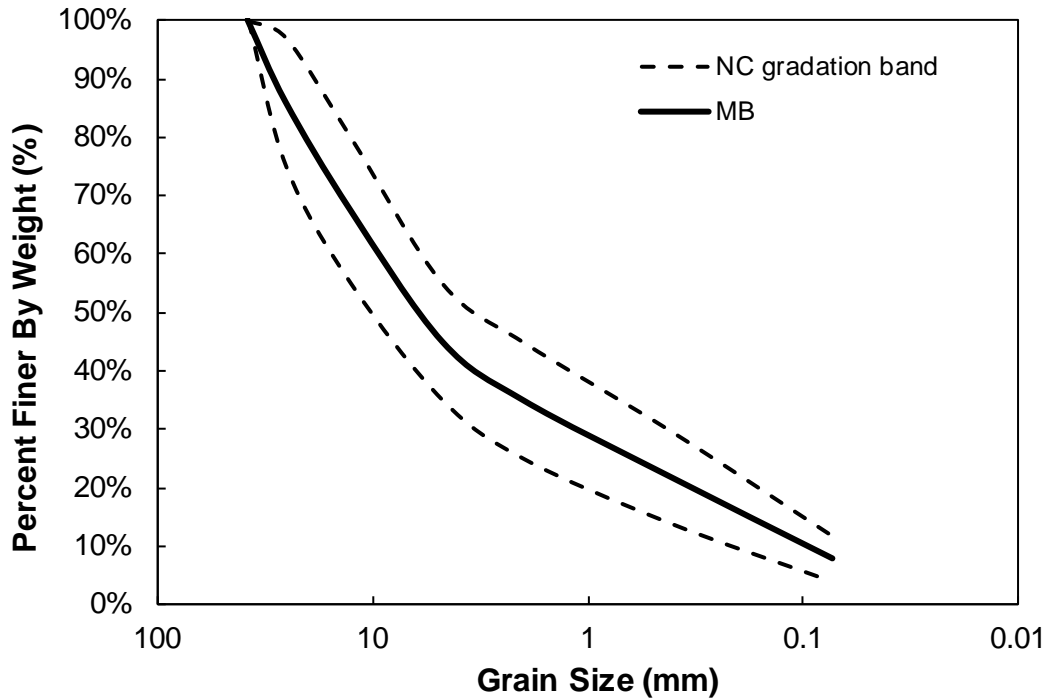
Figure 12 - Selected grain size distribution

The aggregate morphological properties were obtained using an aggregate image measurement system (AIMS2) (Gates et al. 2011), and the method is further described in the previous section. The aggregate properties obtained by AIMS2 are summarized in Table 4 for coarse (larger than 4.75 mm) and fine (smaller than 4.75) particles.

The AIMS2 results are shown in Figure 13 to Figure 17 for each particle size range of each source. The results indicated that morphological properties of the ABC materials are relatively similar with a few exceptions. The fine particles generally have high particle form (non-circular), shown in Figure 13. All of the particle sizes have high angularity, and some of the sizes have extreme angularity (Figure 14). According to Figure 15, the coarse particles have high texture, and some of the Arrowood particle sizes have extreme surface texture. All the coarse particles are high sphericity (almost spherical) (Figure 16). Finally, Figure 17 shows that the coarse particles have a flatness and elongation value between 2 and 3 (i.e., a moderate ratio).
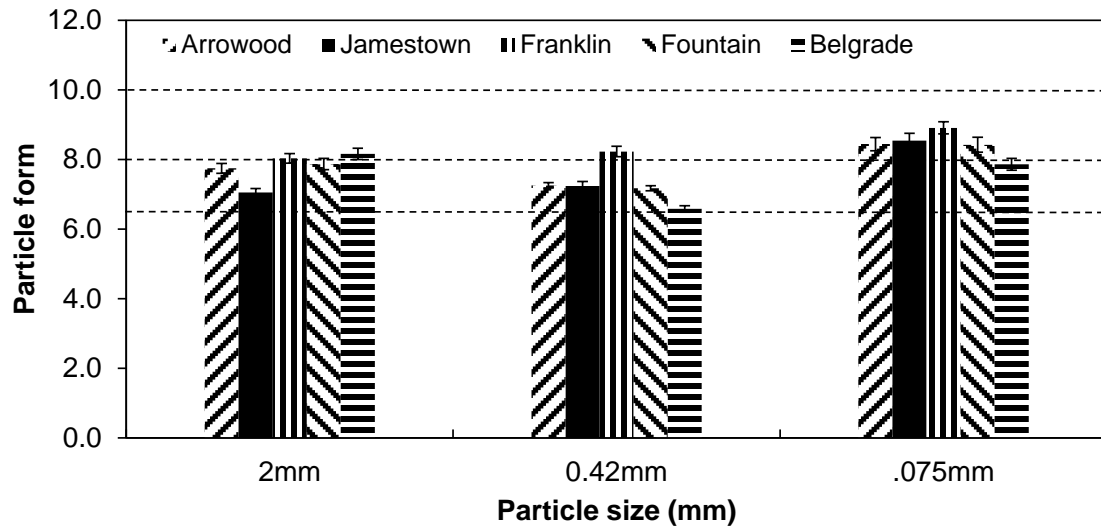
Figure 13 - Particle form - fine particles (smaller than sieve #4)
(0<low<6.5, 6.5<moderate<8, 8<high<10, 10<extreme<20)
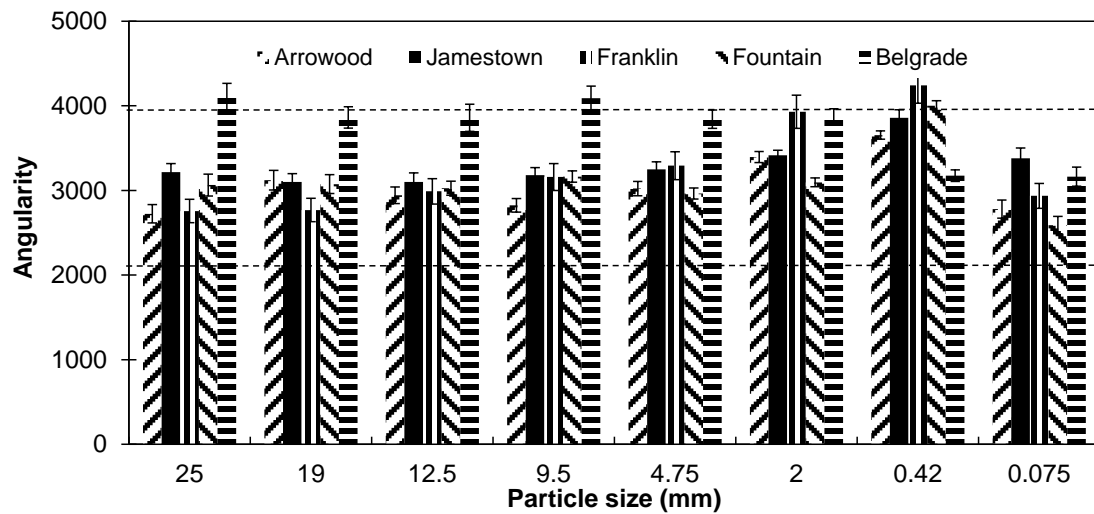
Figure 14 - Angularity index of aggregate
(0<low<2100, 2100<moderate<3975, 3975<high<5400, 5400<extreme<10^4)

25
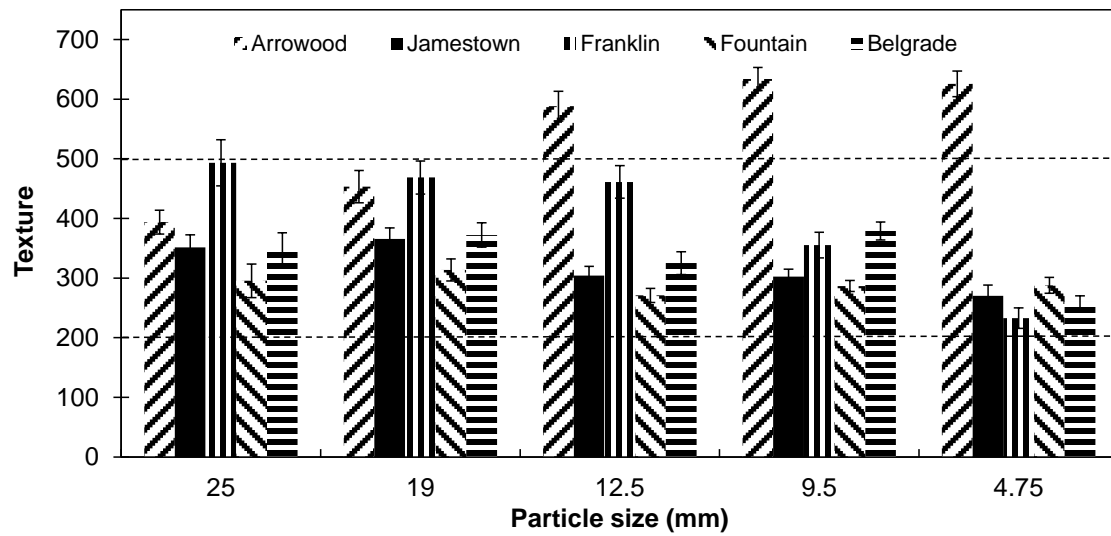
Figure 15 - surface texture of coarse particles
(0<low<200, 200<moderate<500, 500<high<750, 750<extreme<10³)
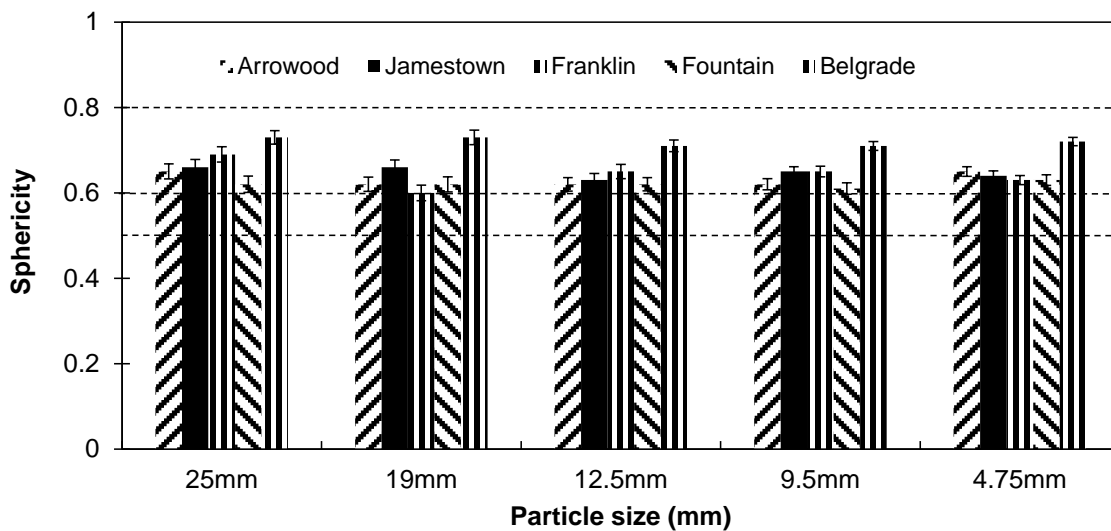
Figure 16 - Sphericity - coarse particles (larger than sieve #4)
(0<low<0.5, 0.5<moderate<0.6, 0.6<high<0.8, 0.8<extreme<1.0)
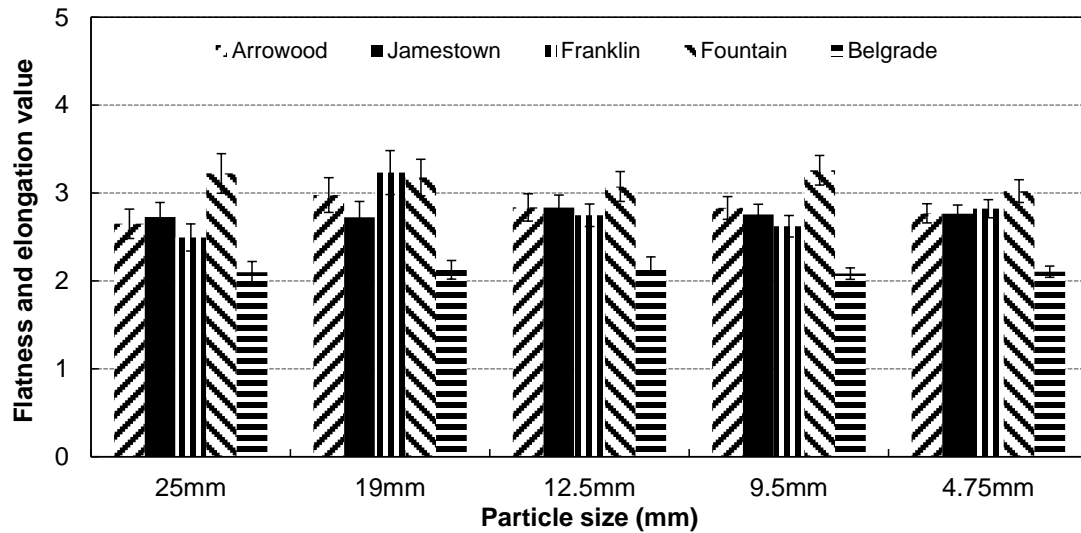
Figure 17 - Flatness and elongation value - coarse particles (larger than sieve #4)

M_R test results

M_R tests were performed on material from five different sources, as previously discussed. Multiple M_R tests were performed on samples from each source. Depending on the variability of the M_R tests results and the material availability, two to four sets of M_R tests were performed, and an average M_R value of all the repetitions for each test is reported. The average properties of the M_R specimens from each source are shown in

Table 6. The M_R results were computed at 15 stress states for ABC materials compacted with a MB gradation. Figure 18 illustrates the average M_R values at each sequence for the ABC materials. Standard errors of the M_R results are also shown in Figure 18 which shows the variability of the obtained moduli. The model parameters for two resilient modulus models, k-θ and Pavement ME models, are listed in Table 7. Both models fit very well to the resilient modulus data, with coefficient of determination (R^2) values often exceeding 0.98.

The results clearly showed the stress hardening behavior of ABC material; the M_R values increased with increase in bulk stress. The M_R increased at different rates for the different aggregate sources, which is described by k_1 parameter in the Pavement ME model (Table 7).

An overall observation shows that Belgrade material had the highest M_R values and Fountain material had the lowest M_R values at the same stress state. Franklin and Jamestown materials resulted in comparable M_R values. Lastly, Arrowood material showed M_R values lower than Belgrade material and higher than Franklin and Jamestown materials. In addition, the results showed that among all the sources Belgrade had the highest variability in the results. Since all of these tests were conducted on material at the same gradation, the differences between obtained M_R values are likely related to physical and morphological properties of aggregates. This relationship is discussed in the present section.

Table 6 - Average values of properties of ABC samples from each source

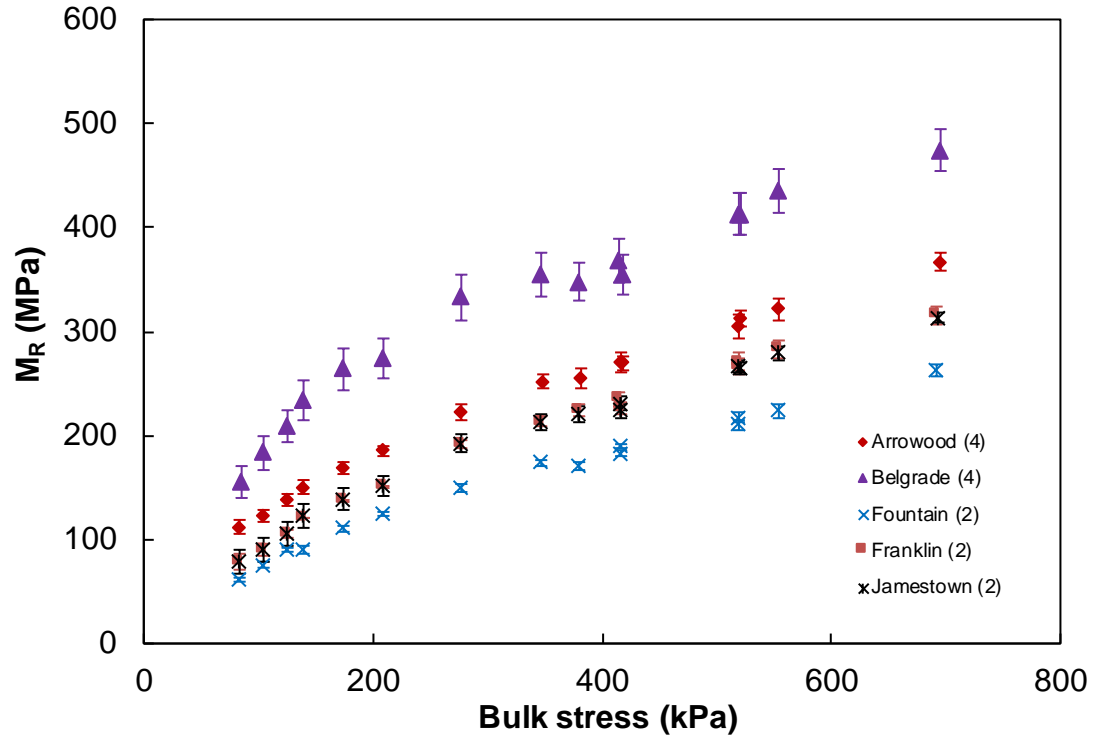| Source	No. of Samples	G_s	MDD (gr/cm³)	OWC (%)	Saturation degree (%)
Arrowood	4	2.91	2.45	4.2	67%
Jamestown	2	2.72	2.26	5.5	78%
Franklin	2	2.71	2.17	5.6	79%
Fountain	2	2.76	2.27	5.5	85%
Belgrade	4	2.56	2.08	7.2	97%

Figure 18 - M$_R$ tests results with the results' variations
(Numbers in parenthesis indicate the number of repetitions)

Table 7 - Regression parameters

Source	Pavement ME model				K-θ model		
	k_1	k_2	k_3	R^2	k	n	R^2
Arrowood	1219	0.558	0.014	1.00	3972	0.561	1.00
Jamestown	944	0.686	-0.159	1.00	3140	0.587	0.99
Franklin	945	0.697	-0.169	1.00	2337	0.654	0.99
Fountain	729	0.623	0.111	1.00	1889	0.652	0.99
Belgrade	1879	0.518	-0.086	0.99	7316	0.490	0.98

Discussion of Experimental Results

The M_R tests were conducted on samples from five aggregate sources. Based on the results, in terms of morphological properties of aggregates, the relatively high M_R values of Arrowood samples may be attributed to the higher texture of some of the aggregate sizes (e.g., aggregate retained on 12.5 mm, 9.5 mm, and 4.75 mm sieves) in this material. This aggregate size range creates the load bearing chain in these samples; therefore, the influence of texture for this size range is meaningful. Moreover, in the Belgrade material, some of the large particles have a relatively higher angularity. Therefore, the high M_R values may be related to the angularity of these aggregates. In regards to the physical properties of aggregates, M_R values tend to increase as the G_S of ABC materials increased. The exception was Belgrade aggregates which show relatively higher M_R values with the lowest G_S. Also, the decrease in the dry density reduced the M_R values, again the exceptions were the coastal materials; Belgrade material with the lowest MDD showed the highest M_R values, and Fountain material which had a relatively high dry density showed the lowest M_R values.

During the specimen preparation using impact compaction, significant aggregate breakage was observed during compaction of Belgrade material; this may be related to the high M_R values of this material. The aggregate breakage is reasonable for Belgrade aggregate because of the high LA abrasion loss (54%), and it was confirmed by the post-compaction grain size distribution of Belgrade samples shown in Figure 19. This indicates that the aggregate breakage during the impact compaction increased fractured faces of Belgrade particles and resulted in higher interlock, tighter packing, and consequently higher M_R values. The effect of aggregate breakage during compaction is further discussed later in this report. It should be mentioned that the grain size distribution of all the other sources were obtained after impact compaction and no significant change in the original gradation was observed for the other four aggregate sources.
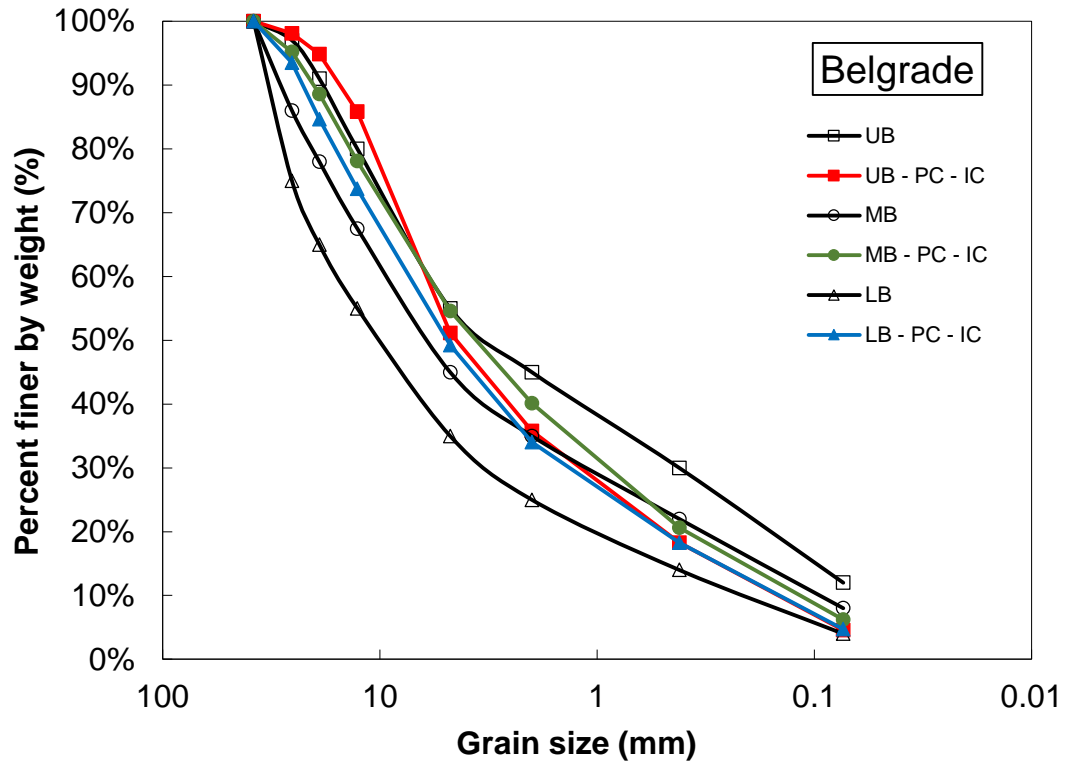
Figure 19 - Post-compaction (PC) grain size distribution of Belgrade samples compacted by impact compaction method (IC)

Statistical analysis to estimate M_R using aggregate properties

M_R is often represented (e.g., in Pavement ME analyses) using regression coefficients (as presented in Equation 6 and Table 7), which are obtained from laboratory tests or empirical estimations. The laboratory test to obtain M_R (and the corresponding regression coefficients) is complex and time consuming and also requires experienced personnel; empirical estimations based on correlations between ABC properties and M_R are simpler and more efficient for design. Therefore, relationships have been proposed to relate the regression coefficients to some simple material properties.

Statistical analyses were performed using linear regression analysis on M_R tests results on the MB gradation using the measured physical and morphological properties to obtain equations to estimate the regression coefficients in Equation 6. The regression analysis was performed using the stepwise method with Statistical Package for the Social Sciences (SPSS) (IBM Corp. 2013) software. In the analysis, all the measured parameters (physical and morphological properties) were chosen as independent variables. The morphological properties inputs were the constants of cumulative Weibull distribution (α, λ). As an example, the cumulative distribution of angularity of Arrowood particles is shown in Figure 20.

The analysis was initially performed to estimate k_1, k_2, and k_3. However, because of using a limited number of laboratory results in the analysis (i.e., only 5 aggregate sources evaluated in current project), no significant regression equations were obtained for k_2 and k_3. Therefore, a conservative approach was taken to select constant values for k_2 and k_3 in the

estimation of the M_R. For k_2, the minimum value of k_2 for the ABC source, shown in Table 7, was selected which was $k_2 = 0.518$. Also, since the k_3 value for ABC material is negligible, k_3 was assumed to be zero for all the ABC sources. Therefore, the statistical analysis was performed to estimate k_1 values for ABC material. In the estimated M_R values, selected k_2 and k_3 values and estimated k_1 values were used.
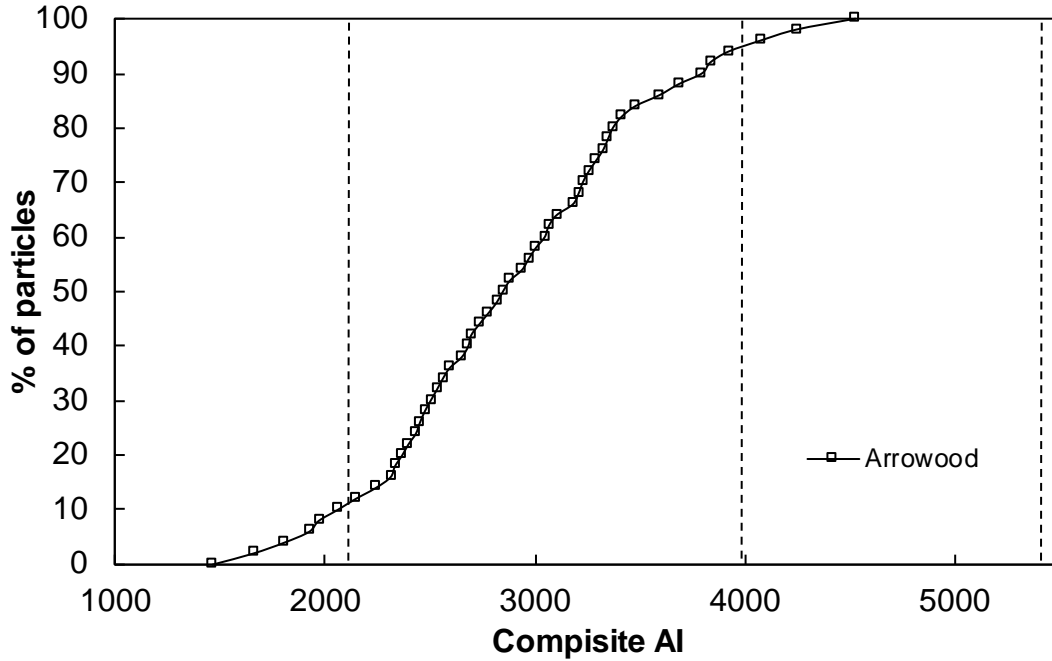

Figure 20 - Angularity index of aggregate
(0<low<2100, 2100<moderate<3975, 3975<high<5400, 5400<extreme<10^4)

Three equations were obtained in the analysis for k_1. The equations are shown in Eq. 8, 9, and 10.

$$K_1 = 6048.22 - 3313.39 \times G_s + 1853.76 \times LA + 390.73 \times ST(a) + 4.70 \times ST(\lambda) \qquad (8)$$

$$K_1 = 81637.16 + 17542.85 \times G_s + 9348.45 \times ST(a) - 39.45 \times ST(\lambda) - 33538.46 \times AI(a) \qquad (9)$$

$$K_1 = -27874.40 + 11.63 \times AI(\lambda) + -6080.68 \times SP(a) + 5051.19 \times ST(a) +$$
$$36300.37 \times SP(\lambda) \qquad (10)$$

As demonstrated in the regression equations shown above, a combination of physical and morphological properties was found to be statically significant in estimating the M_R coefficient. In general, specific gravity, LA abrasion loss, surface texture, angularity, and sphericity were used in one or more of the regression equations. The coefficient of determination for these equations were equal (R^2=0.7). This may be attributed to the limited data used in the analysis. Including more M_R test results form more ABC sources in the analysis can result in regression models with higher R^2, and the significant parameters in the empirical equations may converge, resulting in one "best" equation for North Carolinian aggregates.

These models can be independently used to estimate k_1 for all the sources; however, the relatively low R^2 indicates that the estimation has a different accuracy for different

sources. This is shown for Arrowood and Belgrade in Table 8 and Table 9. As seen in the tabulated results, the three regression equations applied to Arrowood result in very similar values of k_1; however, more variability is observed in the estimated k_1 values for Belgrade aggregate.

Table 8 – Estimating k_1 for Arrowood using obtained regression models

Regression model	Variable	Arrowood	k_1	
			Estimated	Obtained
Eq.	G_s	2.904	1177	1177
	LA_abrasion	0.29		
	ST(a)	4.0		
	ST(λ)	563.6		
Eq. 9	G_s	2.904	1177	
	ST(a)	4.0		
	ST(λ)	563.6		
	AI(a)	4.37		
Eq. 10	AI(λ)	3099	1177	
	SP(a)	8.47		
	ST(a)	4		
	SP(λ)	0.67		

Table 9 – Estimating k_1 for Belgrade using obtained regression models

Regression model	Variable	Belgrade	Value	Prediction Limit
Eq. 8	G_s	2.56	1720	1715.00
	LA_abrasion	0.54		
	ST(a)	3.55		
	ST(λ)	376.7		
Eq. 9	G_s	2.56	1615	
	ST(a)	3.55		
	ST(λ)	376.7		
	AI(a)	4.27		
Eq. 10	AI(λ)	4456	1781	
	SP(a)	11.02		
	ST(a)	3.55		
	SP(λ)	0.74		

The estimated M_R values for Arrowood and Belgrade materials are shown in Figure 21. The results show that even though limited number of laboratory test results were used in this study and k_2 and k_3 values were assumed to be constants, the estimated M_R values are within and slightly lower (conservative) than the range of laboratory measured M_R values. The laboratory measured versus estimated (from one of the repression equations) M_R values

are also shown in Figure 22 for Arrowood and Belgrade materials. Notwithstanding the limited data set used to develop the relationships, the results were promising. This indicates that performing the statistical analysis on a larger data with more aggregate sources will provide regression with higher significant. The research team believes that this can be done with relatively minimal effort, and the Department routinely collects the majority of the data used, and with additional assessment of the morphological properties of more aggregate sources, a more robust regression analysis can be performed.
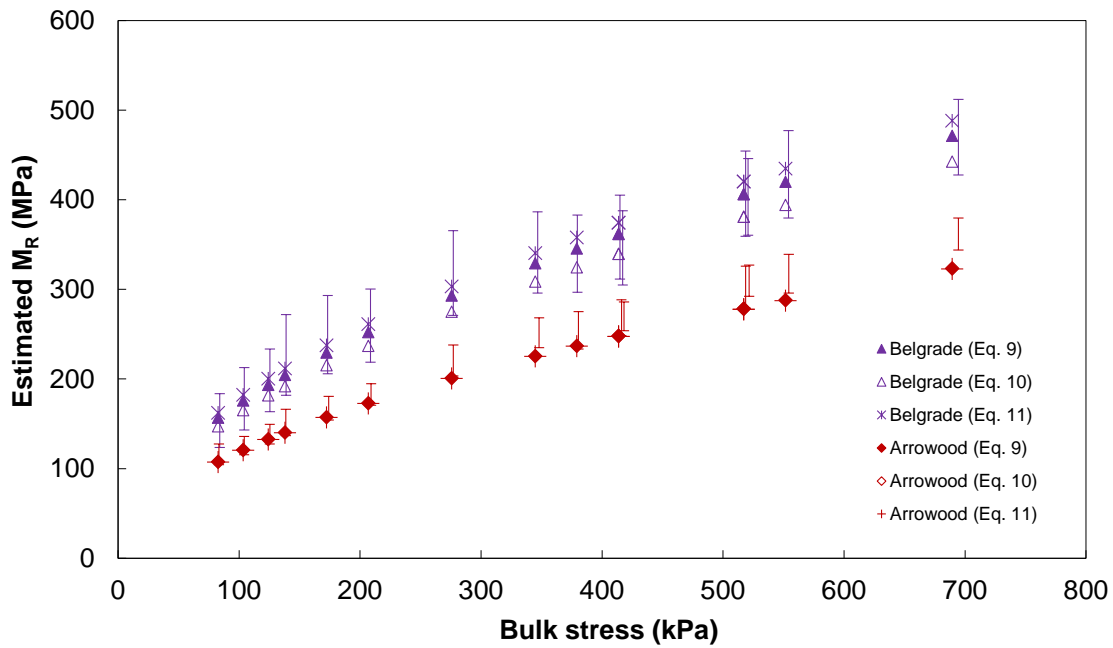

Figure 21 - Estimated M$_R$ versus the bulk stress for Arrowood and Belgrade materials (The bar charts show the range of laboratory measured M$_R$ for Arrowood and Belgrade sources)
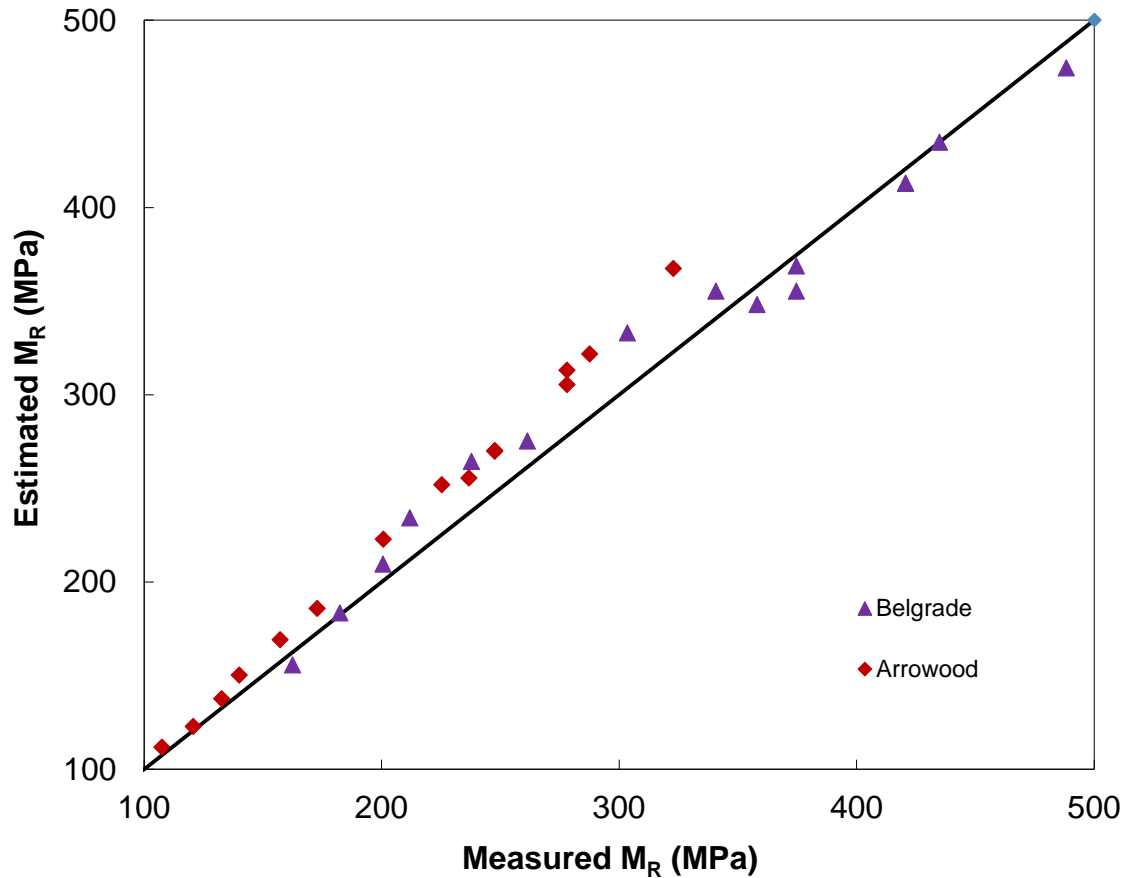
Figure 22 - Estimated versus laboratory measured M_R versus for Arrowood and Belgrade materials – from Equation 9

The low R^2 value can be related to the low number of observations (20 observations). In addition, some of the obtained properties used in the analyses, such as LA abrasion, specific gravity and maximum dry density, are highly correlated. This will decrease the influence of these parameters on k_1 estimation. On the other hand, there is less correlation between the different morphological properties, and the results show that among all the properties, the morphological properties have a higher influence in the estimation of k_1. Therefore, the results indicate that if M_R values are to be estimated, morphological properties (such as those measured with AIMS2) should be included. It is also suggested that conducting additional AIMS2 tests on aggregate sources used by NCDOT outside the five considered in the current study would provide a larger database to develop the statistic equation, resulting in a stronger predictive equation.

Effect of Gradation on Resilient Behavior of ABC

To evaluate the effect of gradation on the resilient behavior of ABC material three ABC sources all within the Piedmont geologic region were used to minimize an influence on different mineralogy (e.g., limestone minerals in Coastal aggregate, such as Belgrade). Within this section of the report, the sources used are Arrowood, Jamestown, and Franklin. The material properties and resilient behavior of these three aggregate sources are evaluated within the packing theory frameworks within this section.

Analytical results based on the packing theories

       The packing theory frameworks were first applied on the three well-graded gradations (e.g., UB, MB, LB) to identify the load-bearing chain (abbreviated as LBC in following tables) and its stability for the three aggregate sources, then the frameworks were applied to the gap-graded gradation.

<u>Bailey method</u>

To evaluate the ABC materials using the Bailey method, a volumetric analysis was performed on the compacted ABC blends using the loose unit weight (LUW) and rodded unit weight (RUW) tests results following the method proposed by Bilodeau and Dore (2013). For all of the gradations evaluated, the boundary between the coarse fraction (CF) and fine fraction (FF) of the aggregate was the #4 sieve, which happens to coincide with the conventional definition of course and fine aggregates used in soil mechanics. The results of the RUW and LUW analyses are shown in Table 10.

       For all of the ABC sources and gradations considered, the percentage of the loose unit weight of CF ($\%LUW_{CF}$) of the LB gradations is higher than 95 percent; therefore, the load-bearing chain in the LB gradations is constructed by coarse aggregate according to the Bailey method. In addition, the results suggest that strong interlocking exists within the load-bearing chain because the $\%LUW_{CF}$ of all the aggregate sources exceed 100% for the LB gradation; this indicates that the particles constituting the load-bearing chain are in contact. Also, the percentage of the rodded unit weight of the FF within the aggregate blend ($\%RUW_{FF}$) of the LB gradations of all the aggregate sources are equal or higher than 100%, which indicates the fine particles are compacted within the voids of the load-bearing structure and thus, are expected to provide stability for the CF. As the gradation becomes finer (i.e., MB and UB), the results suggest that not all of the coarse aggregate will be in contact because the $\%LUW_{CF}$ of all the aggregate sources are less than 95%. Therefore, the Bailey method suggests that the fine fraction of the aggregate constitutes the load-bearing chain for the MB and UB gradations. While the Bailey method does not stipulate whether a coarse or fine load-bearing chain is better, past studies suggest that coarser gradations result in higher resilient moduli (Lekarp et al. 2000). Also, as the gradation becomes finer, the $\%RUW_{FF}$ increases. A higher $\%RUF_{FF}$ indicates that the fine aggregate has greater particle-to-particle connectivity within the aggregate blend which provide more stability for the load-bearing chain.

Table 10 - Volumetric analysis results of ABC materials

Source	GSD	RUW$_{FF}$	LUW$_{CF}$	%RUW$_{FF}$	%LUW$_{CF}$
		gr/cm3	gr/cm3	(>100%)	(>95%)
Arrowood	UB	1.76	1.53	122%	72%
	MB	1.83	1.56	113%	87%
	LB	1.90	1.52	101%	106%
Jamestown	UB	1.50	1.39	132%	73%
	MB	1.57	1.42	122%	89%
	LB	1.64	1.42	103%	103%
Franklin	UB	1.67	1.38	113%	71%
	MB	1.73	1.42	110%	88%
	LB	1.75	1.43	100%	102%

DASR method

The DASR method is based on the analysis of the relative proportion of aggregates with a size ratio of 2:1. Therefore, to apply this method to the gradations in the current study, the tested gradations were first re-evaluated based on 2:1 sieve size ratios using interpolation of measured values. The results are shown in Table 11.

Table 11 - Re-evaluated gradations

1:2 ratio sieves (mm)	Percent passing			Percent retained		
	LB	MB	UB	LB	MB	UB
38.1	100%	100%	100%	0%	0%	0%
19.05	66%	78%	91%	35%	22%	9%
9.53	48%	60%	72%	18%	18%	19%
4.76	35%	45%	55%	13%	15%	17%
2.38	27%	37%	47%	9%	9%	9%
1.19	21%	31%	40%	6%	6%	7%
0.60	16%	25%	33%	5%	5%	7%
0.30	12%	19%	26%	4%	6%	7%
0.15	8%	14%	19%	4%	5%	7%
0.074	4%	8%	12%	4%	6%	7%

The GSD shown in Table 11 was used to construct the interaction diagram shown in Figure 23. The interaction diagram was constructed using the relative proportions aggregates retained on each pair of consecutive sieves. For example, for the LB gradation, 35% and 18%

of particles are retained on the 19.05 mm sieve and the 9.53 mm sieve, respectively; therefore, the relative proportion of the 19.05 mm and 9.53 mm particle sizes is (35%)/(35%+18%) = 66% = 33/50. It should be noted that the relative proportion of particles with a size ratio of 2:1 is only affected by the gradation and is not a function of the material source; therefore, the interaction diagram is identical for all three material sources evaluated in this study. The interaction diagram is used to identify the load-bearing chain (DASR) in the three gradations by observing the aggregate sizes where the relative proportion of particles falls within the bounds of 30/70 and 70/30. Thus, all particles are interacting and forming the primary load-bearing chain (DASR) based on the DASR method. The minimum particle size which can be considered as a part of the load-bearing chain (DASR) was chosen to be 4.75 mm based on the division between fine and coarse particles based on the Bailey method. Therefore, based on the interaction diagram, in all the gradations, the aggregates larger than 4.75 mm were considered to be the load-bearing chain (DASR).
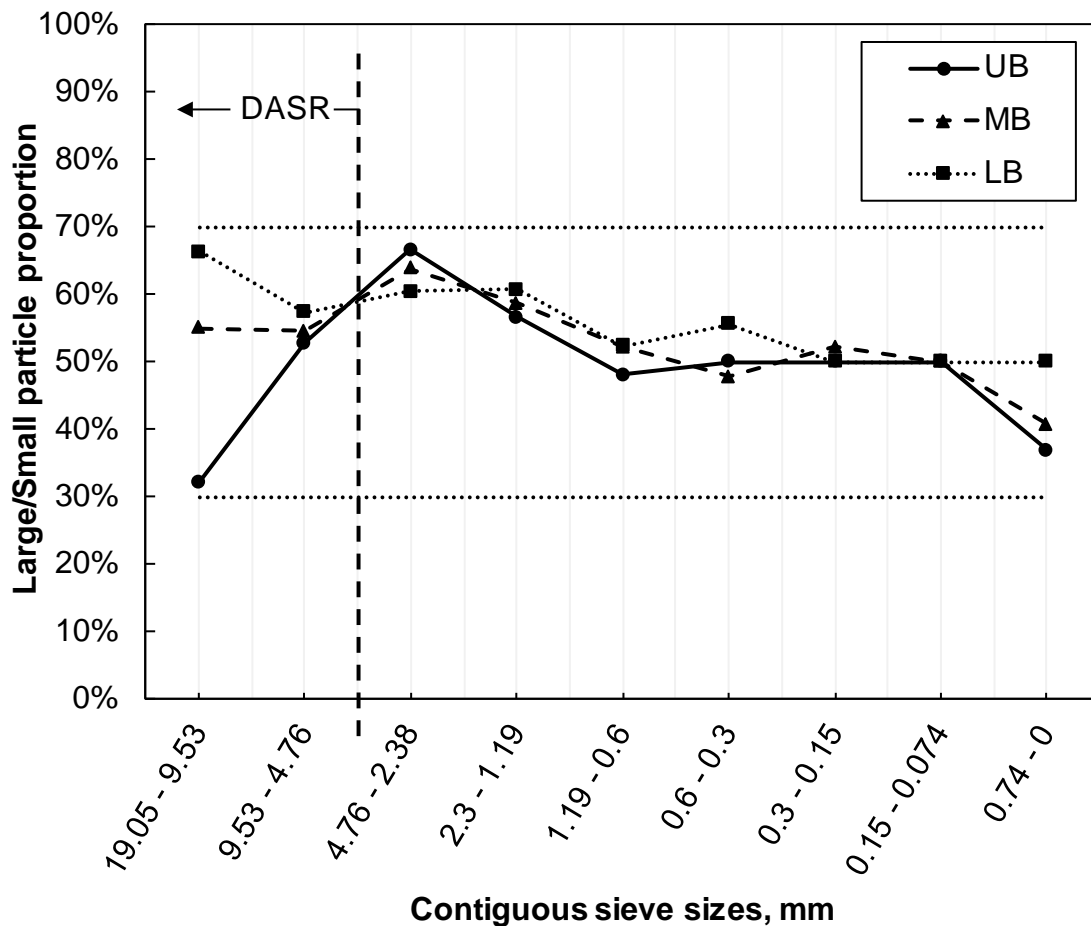

Figure 23 – Interaction diagram for UM, MB, and LB gradations

The porosity of the load-bearing chain (DASR) for each material and gradation was calculated following Kim et al. 2006. In contrast with the interaction diagram, the porosity of load-bearing chain (DASR) is a function of the aggregate specific gravity and maximum dry density and therefore, differs among material sources.

The load-bearing chain (DASR) porosities of the materials and gradations evaluated and shown in Table 12. According to the results, only the porosity of the LB gradation is less than 50 percent for all materials evaluated; a porosity of 50 percent or lower indicates a strong interlock exists between the particles in the load-bearing chain (DASR). It is also observed that the porosity of the load-bearing chain (DASR) of aggregate particles increases and exceeds 50 percent as the gradation becomes more fine. Therefore, the DASR framework suggests that among the three gradations within the NCDOT, only the load-bearing chain (DASR) in the LB gradation possesses a strong interlock, and the chain in the other gradations, MB and UB, have lower degree of interlock and are disrupted by other particles. These results are in agreement with the Bailey method results.

Table 12 - DASR porosity

Gradation	LBC, range (mm)	A	B	C
UB		62.1%	62.1%	63.8%
MB	38.1 - 4.75	53.5%	53.1%	53.4%
LB		44.8%	44.5%	45.8%

Yideti framework

In the Yideti framework, the load-bearing chain of the gradations, called primary structure (PS), is identified following the procedure described by Yideti et al. (2013). The range of particle sizes that comprise the load-bearing chain (PS) and the corresponding load-bearing chain (PS) porosities of all sources and gradations evaluated according to the Yideti framework are shown in Table 13. Similar to DASR method, the load-bearing chain (PS) particle size range is also independent of aggregate properties and is only related to the gradation. The results indicate that the UB gradation load-bearing chain (PS) is comprised of less particle sizes than the MB and LB gradations. In addition, the results indicate that the porosity increases as the gradation becomes finer within the NCDOT specification band; this indicates that better performance is expected with the use of coarser gradations within the NCDOT specification band.

Table 13 – PS and theory porosities for different gyrations and sources

Gradation	LBC, range (mm)	PS porosity		
		Arrowood	Jamestown	Franklin
UB	25.4 - 4.75	63.2%	63.0%	65.3%
MB	38.1 - 2.00	44.1%	46.0%	45.4%
LB	38.1 - 2.00	35.5%	36.9%	36.7%

To evaluate the disruption of the load-bearing chain (PS) by the fine particles, the disruption potential (DP) values were calculated following Yideti et al. (2013) for each gradation and material source evaluated. The DP results are shown in Table 14.

The DP values were between 0.5 and 1.0 for the LB gradations, which shows the stability of the load-bearing chain (PS) for this gradation, and were greater than 1.0 for the MB and UB gradations (except for MB from Jamestown). The later showed that the load-

bearing chain (PS) of MB and UB are disrupted by fine particles (disruptive material), and the disruption is more in UB.

Table 14 – DP of mixtures

Gradation	DP, range (mm)	DP		
		Arrowood	Jamestown	Franklin
UB	4.75 - 2.00	1.46	1.51	1.05
MB	2.00 - 0.42	1.23	0.98	1.05
LB	2.00 - 0.42	0.90	0.77	0.79

Summary of the packing theory frameworks results

The different packing theories lead to some differences in the aggregate size range identified as the load-bearing chain. As summarized in

Table 15, according to Bailey method, the load-bearing chain is constructed in LB gradation by particles larger than 4.75 mm and smaller than 38.1 mm (CF), and in MB and UB gradations, the chain consists of particles smaller than 4.75 mm (FF). This is because Bailey method identifies the chain to be either comprised by CF or FF of a mixture. The DASR method identified similar load-bearing chain for the three gradations as particles smaller than 38.1 mm and larger than 4.75 mm; however, using the Yideti framework, it was found that the load-bearing chain in the three gradation is constructed with different particle sizes; particles smaller than 25.4 mm and larger than4.57 for UB gradation, and particles smaller than 38.1 mm and larger than 2.0 for MB and LB gradations.

The evaluation results, shown in

Table 15, indicate that the Bailey and DASR methods identified LB gradation as the gradation with the load-bearing chain constructed by stable CA and highest degree of interlock, respectively, among others. In addition, the Bailey method showed that load-bearing chains within MB and UB gradations are constructed by FA. Yideti framework results suggested that decreased porosity of the load-bearing chain as the gradation becomes coarser within the NCDOT band specification.

In summary, the results of all of the packing theory frameworks indicate that the load-bearing chain is stronger in coarser gradations within the NCDOT band specification for ABC and that the load-bearing chain becomes (more) porous as the gradation transitions toward the finer gradations within the NCDOT band specification. Therefore, the LB gradation is expected to have better mechanical performance than the MB and the UB gradations.

Table 15 – Summary of the packing theory results

Gradation	LBC, range (mm)			LBC criteria*		
	Bailey	DASR	Yideti	Bailey	DASR	Yideti
UB	< 4.75 (FF)		25.4 - 4.75	%LUW$_{CF}$ = 72%	$\bar{n}$ = 62.7%	$\bar{n}$ = 63.4%
MB	< 4.75 (FF)	38.1 - 4.75	38.1 - 2.00	%LUW$_{CF}$ = 88%	$\bar{n}$ = 53.3%	$\bar{n}$ = 45.2%
LB	38.1 - 4.75 (CF)		38.1 - 2.00	%LUW$_{CF}$ = 104%	$\bar{n}$ = 45.0%	$\bar{n}$ = 36.4%
*The LBC criteria in this table are average values of criterion of all the sources.						

Mechanical performance test results

To evaluate the practical implications of the packing theory framework results, M_R tests were performed. The resilient modulus test results of the different gradations and sources are shown in Figure 24 to Figure 26. Each data point in these figures represent the M_R of each sample at a certain bulk stress. In addition, each test was performed as a duplicate, except the MB gradation of Arrowood which has a total of 4 repetitions, and each plotted point represents the average values of the repetitions. The sensitivity of the M_R to gradation for each aggregate source varies with the bulk stresses. For all of the material sources, the M_R values of the different gradations are close at low bulk stresses but as bulk stress increases, there tends to be more sensitivity in the M_R to gradation. Similar trends were also observed in a previous study within the same gradation band (Cunningham et al. 2013). The packing theory frameworks evaluated all indicate that the LB gradation is expected to perform better than the MB and UB gradations. However, the LB gradation exhibited the highest M_R values for only the ABC material from Franklin. Therefore, packing theory frameworks alone do not have the ability to predict the trends in M_R. Due to the relatively low sensitivity of M_R test results to the gradations evaluated herein, it is recommended that future work investigate other performance measures when evaluating the relative performance of ABC materials (Mishra et al. 2012, Chow et al. 2014).
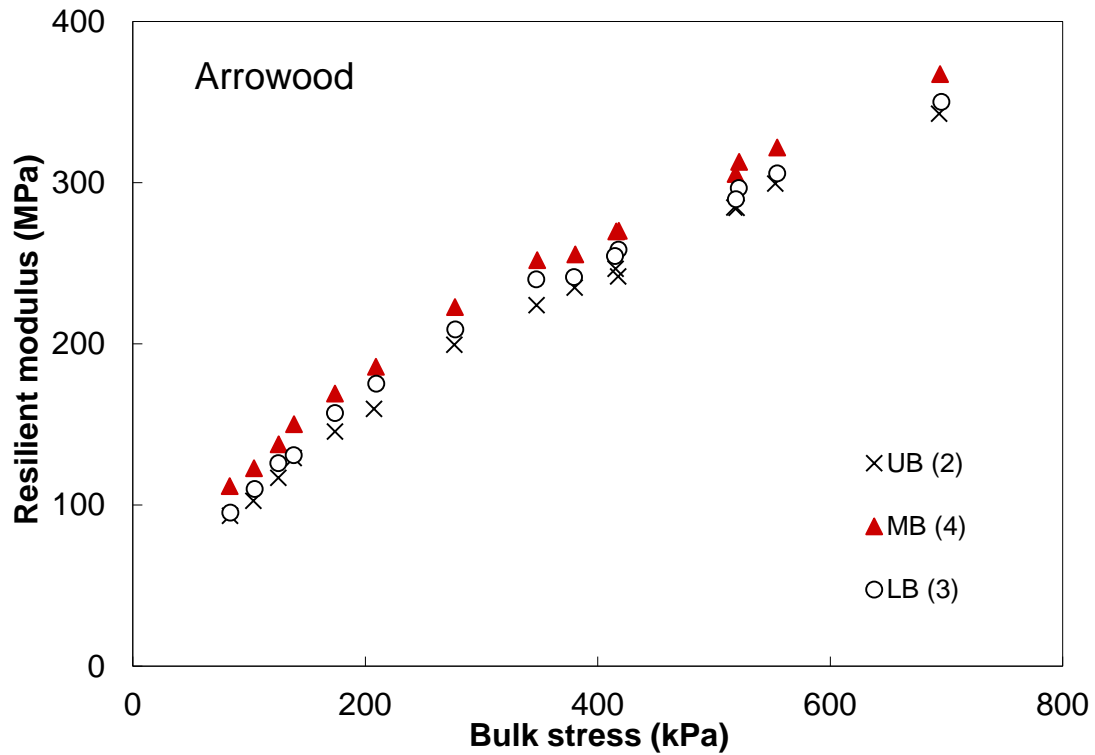
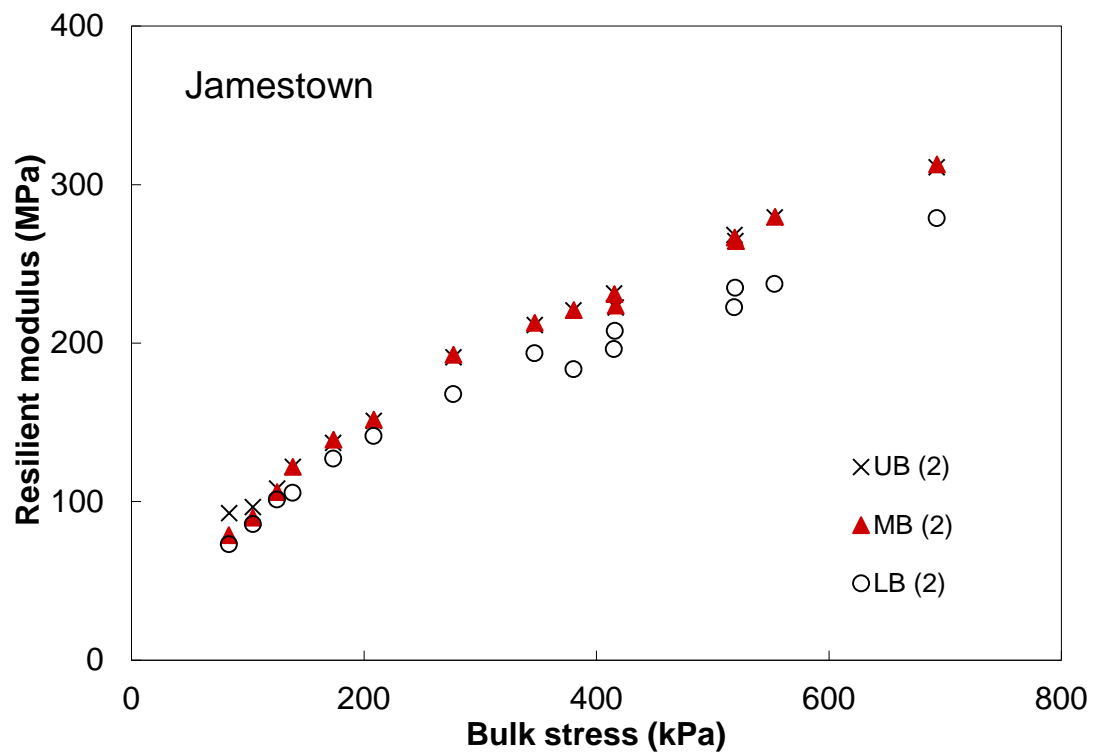**Figure 24 - M$_R$ test results on materials from Arrowood**

Figure 25 - M$_R$ test results on materials from Jamestown
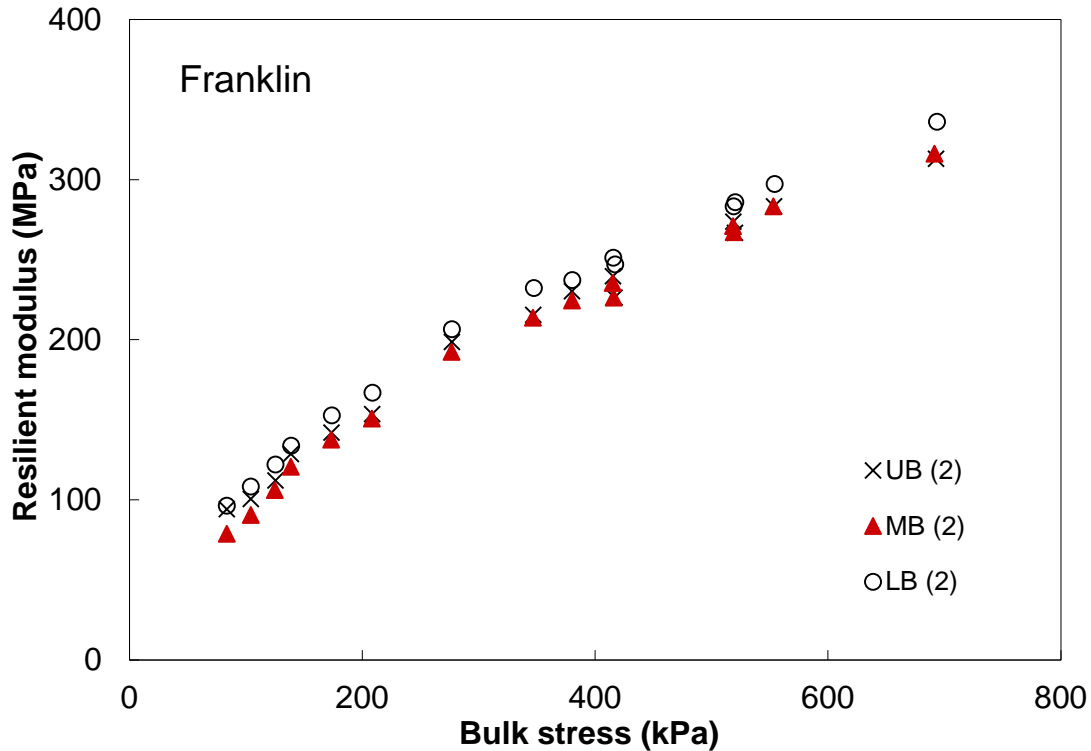
Figure 26 - M$_R$ test results on materials from Franklin

Evaluating a gap-graded gradation

The UB, MB, and LB gradations all represent typical well-graded ABC gradations. Therefore, to further evaluate the relationship between the packing theory frameworks and mechanical performance, a gap gradation comprised of ABC material from Arrowood was designed, evaluated, and tested. The gap gradation (GG) was created using the MB gradation but excluding aggregate smaller than 12.7 mm and larger than 4.75 mm which was found by all the packing theory frameworks to be a large portion of the load-bearing chain. The GG still fell within the NCDOT band specification for ABC.

The Bailey method results of the GG from Arrowood compared to the MB gradations are shown in Table 16. The results show that the %LUW$_{CA}$ of the GG was less than 95 percent which suggests that the coarse fraction in a compacted GG blend is highly disrupted by the fine fraction of the mixture. However, the %LUW$_{CA}$ of GG gradation (71%) is close to the %LUW$_{CA}$ of UB (72%) as shown in Table 10. In addition, the volumetric analysis showed that the fine fraction of GG was highly compacted in the mixture (%RUW$_{FA}$ of 118%). Based on the volumetric analysis on the GG gradation, the load-bearing chain in this gradation is constructed by the FF which is highly compacted (i.e., high density).

Table 16 - Volumetric analysis results on MB and GG gradations – Arrowood

Gradation	RUW$_{FA}$	LUW$_{CA}$	%RUW$_{FA}$	%LUW$_{CA}$
	gr/cm^3	gr/cm^3		
MB	1.79	1.42	107%	88%
GG	1.80	1.42	118%	71%

The interaction diagram resulting from applying the DASR method to the MB and GG gradations is shown in Figure 27. The results indicate that load-bearing is not constructed in the GG gradation because the aggregate larger than the 4.75 mm sieve fall outside of the 70/30 limit for the relative proportion of aggregates from two contiguous sieves with a size ratio of 2:1. The DASR and Yideti framework results for porosity of the load-bearing chain of particles and DP are shown in Table 17. The Yideti framework also suggests a reduction in the range of particle sizes included within the load-bearing chain. It can be seen that the porosity of the load-bearing chain in the GG is significantly higher than 50 percent according the Yideti framework, suggesting poor performance. The expected poor performance was also confirmed by the high DP (1.43) of the GG gradation.
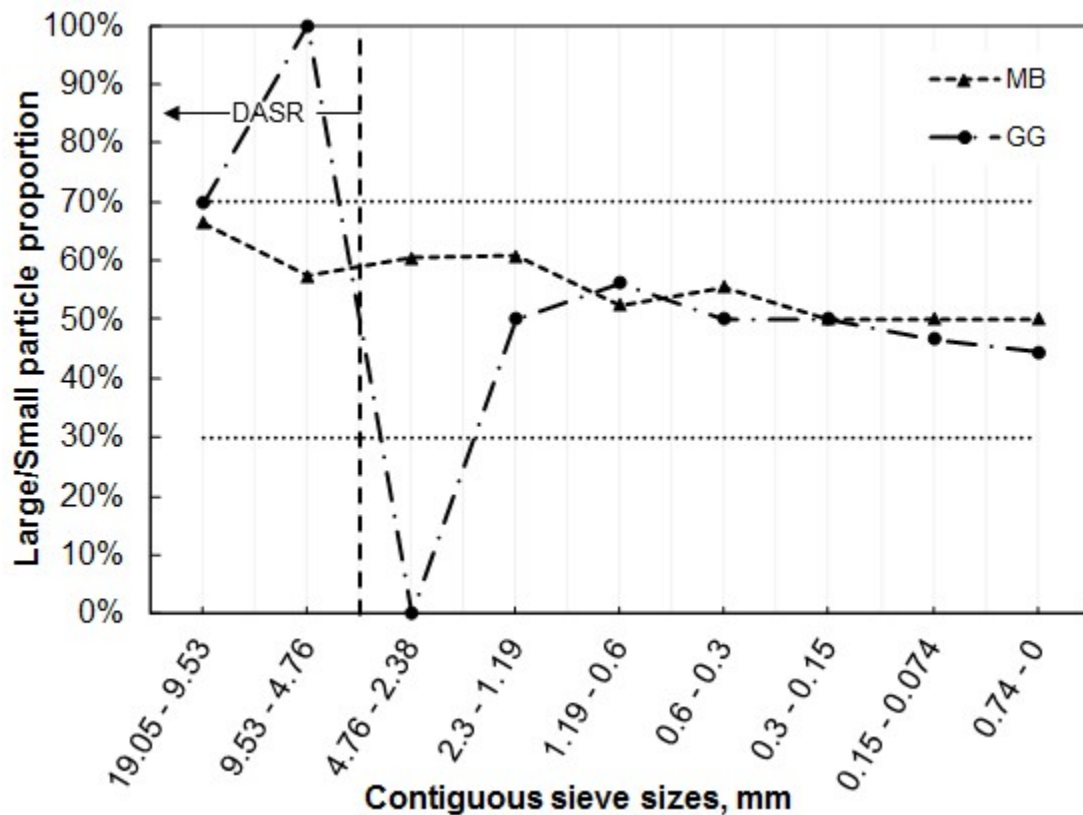

Figure 27 – Interaction diagram, comparing MB and GG from Arrowood

Table 17 – DASR and Yideti frameworks for MB and GG mixtures - Arrowood

Gradation	DASR		Yideti		
	DASR, range (mm)	n (%)	PS, range (mm)	n (%)	DP
MB	38.1-1.19	41.0%	38.1 - 2.00	45.0%	1.23
GG	-	-	38.1 - 12.7	54.9%	1.43

The M_R test results of the GG and MB gradations comprised of materials from Arrowood are shown in Figure 28. The M_R values of the GG are generally very similar to

the MB gradation. Thus, while the packing theory frameworks suggest that the GG gradation does not have a strong load-bearing chain of particles, the performance test results indicate comparable performance to the MB gradation.
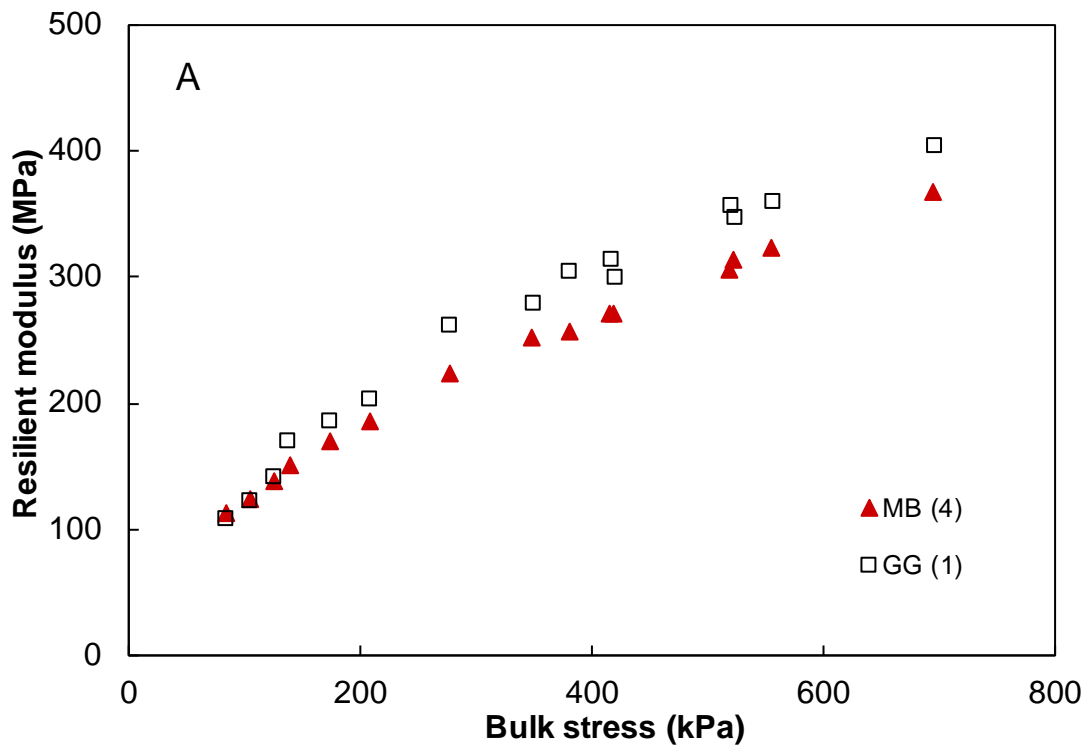

Figure 28 - M_R test results on GG and MB mixtures - Arrowood

The comparison between the packing analysis and M_R test results indicate that within the NCDOT band specification for ABC, the packing theory frameworks do not reflect the experimental M_R results. The experimental results indicate that the variation of M_R is insignificant for all gradations evaluated within the NCDOT band specification. Therefore, packing theory frameworks alone are insufficient to effectively design and evaluate the resilient behaviour of ABC materials falling within typical gradation band specifications.

**Effect of Compaction Method on Resilient Behavior of ABC**

As previously discussed in this report, degradation of Belgrade aggregate was observed during the standard compaction process (i.e., impact compaction), while aggregate degradation in the other sources was negligible. In order to assess the effect of the change in gradation due to aggregate breakage during specimen preparation, two compaction methods were employed, impact and vibratory. In addition, two aggregate sources were studied, Arrowood and Belgrade. The specific objectives for this portion of the study include: 1) evaluating the effect of the compaction method on the M_R results of ABC, and 2) elucidating potential reasons for sensitivity in M_R results to the method of compaction by assessing the changes in ABC fabric.

The results of the experimental study are presented below. The change in physical properties of the ABC is assessed through evaluating the change in gradation and

morphological properties due to the compaction process. In addition, differences in the fabric of the compacted specimens is evaluated using digital image analysis. Finally, the observed M_R behavior of the two aggregate sources compacted using the two methods are presented.

Post-Compaction gradations

The degradation of the two aggregate sources as a result of impact compaction (IC) and vibratory compaction (VC) was evaluated by comparing initial and post-compaction grain size distributions (GSD). The results are shown in Figure 29 with the NCDOT ABC band specification included for reference. The results presented in Figure 29 demonstrate that the Arrowood GSD does not change as a result of IC or VC. It can be seen that the Belgrade GSD does not significantly change under VC; however, the gradation becomes finer with IC, indicating the degradation of coarse particles. It is speculated that the Belgrade aggregate degraded upon impact compaction as a result of its less resistant mineralogy (i.e., calcium-dominant minerals), as demonstrated by the high LA abrasion loss (Table 5). Similar trends in degradation of granular mixtures from different sources were also observed in previous studies (Cetin et al. 2014).
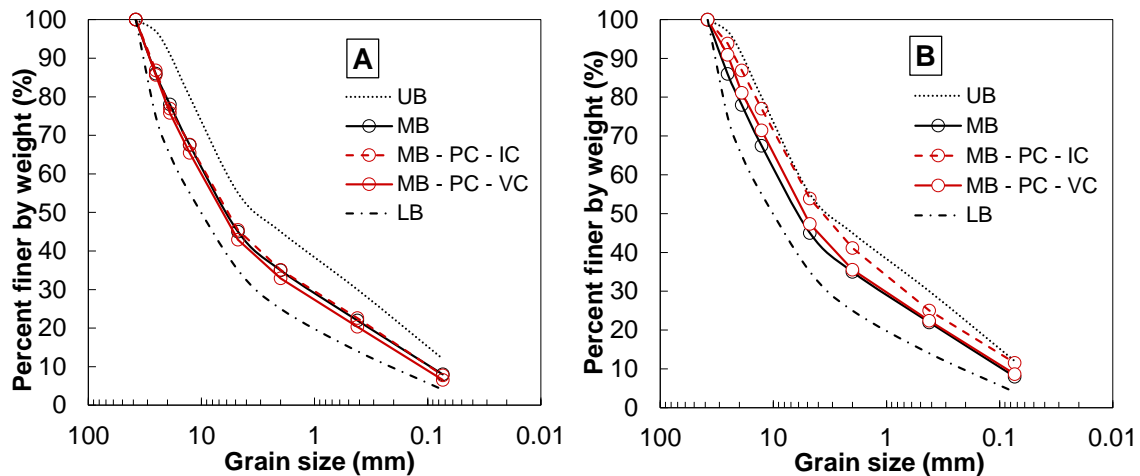
**Figure 29 - Post-compaction gradation of specimens compacted by IC and VC
a) Arrowood and b) Belgrade, post-compaction gradation is denoted by 'PC'**

Aggregate morphological properties

The AIMS2 device was used to determine the aggregate angularity index (AI), surface texture index (ST), and sphericity (SP) of coarse aggregates (retained on #4 sieve). The analysis was initially performed on washed and dried as-received aggregate, as presented earlier. Then, as Belgrade showed a change in its gradation due to compaction, post compacted aggregates from Belgrade were also tested with AIMS2 to evaluate the effect of compaction method on the change in the morphological properties of aggregates. The results presented in Figure 30 are described as the composite indices of the aggregates obtained by the procedure described by Gu et al. (2014). As illustrated in Figure 30, no noticeable changes were observed between the pre- and post-compaction morphological properties no matter which compaction method used.
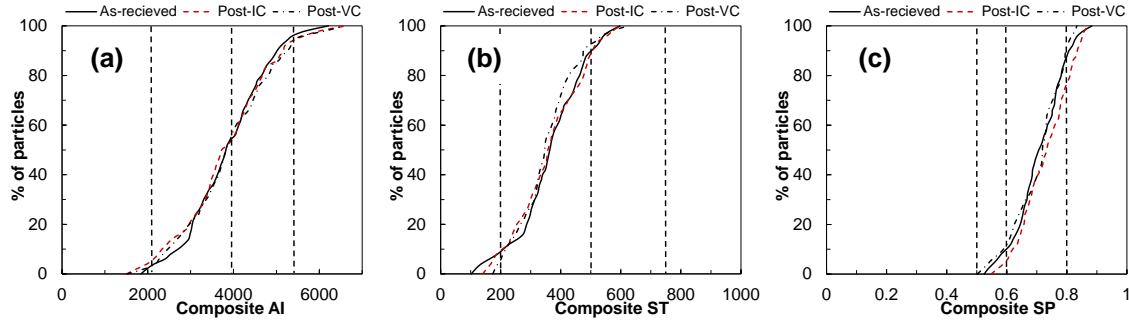
Figure 30 - AIMS2 results for as-received, post IC, and post-VC Belgrade aggregate: (a) distribution of composite AI, (b) distribution of composite ST, and (c) distribution of composite SP

Assessment of compacted ABC specimen fabric

Analyses of digital images were performed to evaluate particle contact points and aggregate orientations in the locked specimens compacted with IC and VC methods. Figure 31 depicts the initial image and processed binary image. The binary image was used to count the number of particles over a range of sizes to compare the gradation of the digital particles to that of the experimentally obtained gradation (e.g., NCDOT middle band gradation) using a rough approximation to determine whether or not the images constituted representative samples for analyses. All of the digital gradations were similar to that of the experimental gradation, indicating that the aggregates captured in the digital image analysis are representative of the specimen. The binary image was then used to measure particle contact points for coarse aggregates (larger than 4.75 mm) (Figure 31c), as described in the Methods section of this report. The particle contacts were determined for both sources, Arrowood and Belgrade, each prepared using both impact and vibratory compaction. A summary of the contact points is presented in Table 18; since the size of the specimens were not identical due to small specimen degradation during extraction from the mold, the number of particle contacts was also normalized per 100 cm^2 of cut surface area for a more straightforward comparison. The measured particle contacts indicate that there is negligible difference between IC and VC for Arrowood aggregate. The number of particle contacts for the Belgrade specimen prepared using VC is similar to the number of particle contacts measured for both Arrowood specimens; however, the Belgrade aggregate demonstrated significant increase in particle contacts for IC compared to VC. The increase in particle contacts agrees with the degradation behavior observed in the post-compaction gradations, where coarser particles broke, creating more smaller particles and in turn increasing the particle contacts.
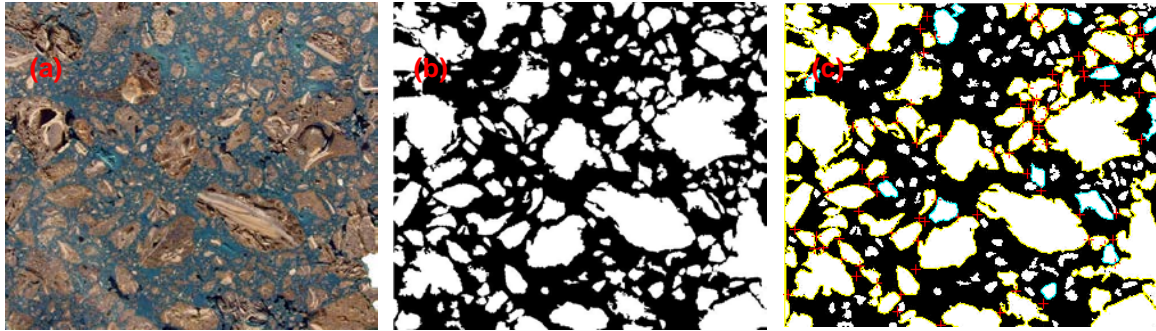
Figure 31 - Example digital images of a Belgrade specimen: (a) initial image (b) binary image, and (c) particle contacts image

Table 18 - Summary of Measured Particle Contacts

Source	Compaction Type	Measured Number of Particle Contacts	Particle Contacts per 100 cm^2
Arrowood	Impact	321	36.8
	Vibratory	310	33.7
Belgrade	Impact	412	59.8
	Vibratory	523	39.2

The calculated angle of orientation to the horizontal of aggregates for each compaction method is shown in Figure 32 in polar diagrams. The results indicated that the compaction method had a small effect on the orientation of the particles for both aggregate sources.
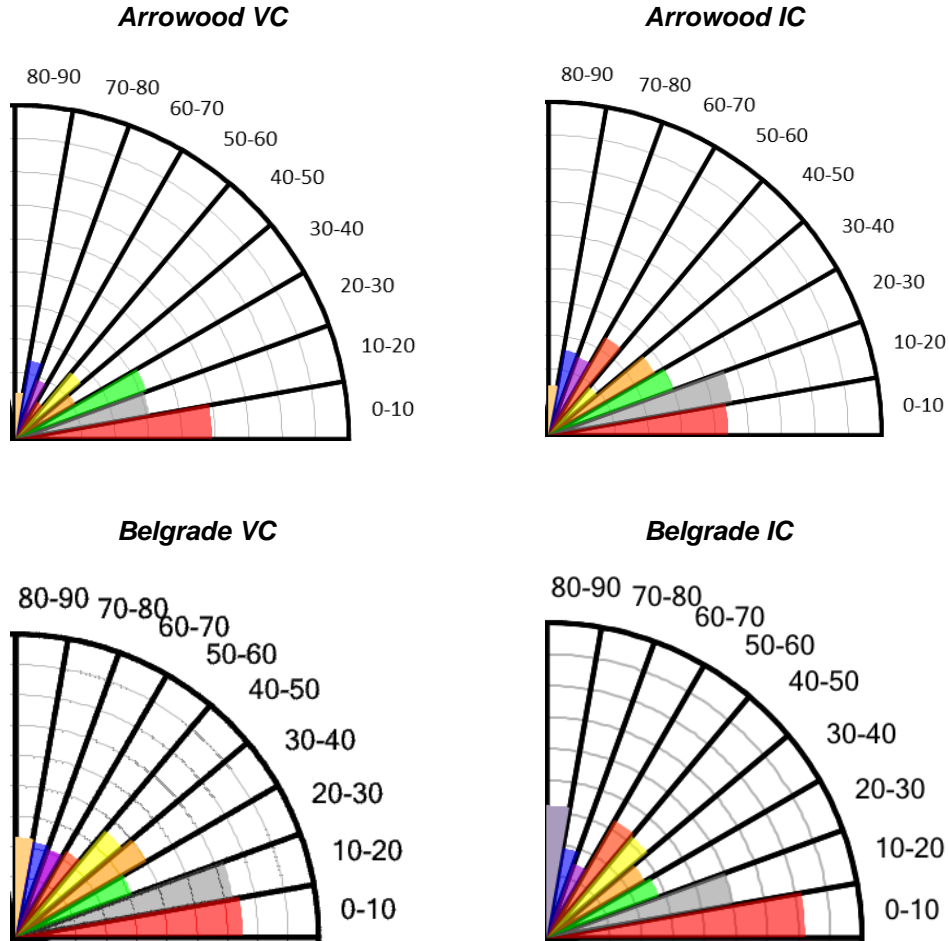
Figure 32 - Particle orientation polar diagrams for IC and VC specimens of both Arrowood and Belgrade sources

The digital image analysis results indicate that although the compaction methods did not affect the particle orientation, the number of particle contact points was higher for IC samples than VC samples for the Belgrade material. A higher number of contact may create a stronger load bearing chain.

M_R behavior

The M_R tests were performed on specimens compacted with the two compaction methods to evaluate their resilient behavior, and the results are shown in Figure 33. Error bars in Figure 33 correspond to the standard error. Figure 33-a and Figure 33-b show the differences in the results of specimens prepared using IC and VC for Arrowood and Belgrade, respectively. Figure 33-a indicates that for Arrowood aggregate, the M_R values specimens compacted by VC are slightly lower than those of specimens compacted by IC at low bulk stresses. However, at higher bulk stresses, the compaction method did not influence the M_R test results. The results presented in Figure 33-b demonstrate that the compaction method had a significant effect on the M_R results for Belgrade aggregate. The specimens compacted by VC exhibit significantly lower M_R values than those compacted by IC. Figure 33-c and Figure 33-d show the comparison between the M_R values of Arrowood and Belgrade when compacted using IC and VC, respectively. Figure 33-c shows that when IC is used,

Belgrade aggregate appears to have significantly higher M_R values than Arrowood; however Figure 33-d shows that the two ABC materials have equivalent M_R values when specimens are prepared using VC, which better mimics field compaction.

Based on these findings, it can be speculated that the IC method, which caused breakage of some of the coarse particles within Belgrade aggregate, resulted in tighter packing of aggregate which consequently resulted in the higher coordination number (analogous to particle contacts). Therefore, the M_R values of specimens made by breakable material (Belgrade) and compacted by IC were significantly higher. However, when the specimens from the two ABC sources were compacted with VC, their gradation was not altered during compaction, and their M_R values were similar.
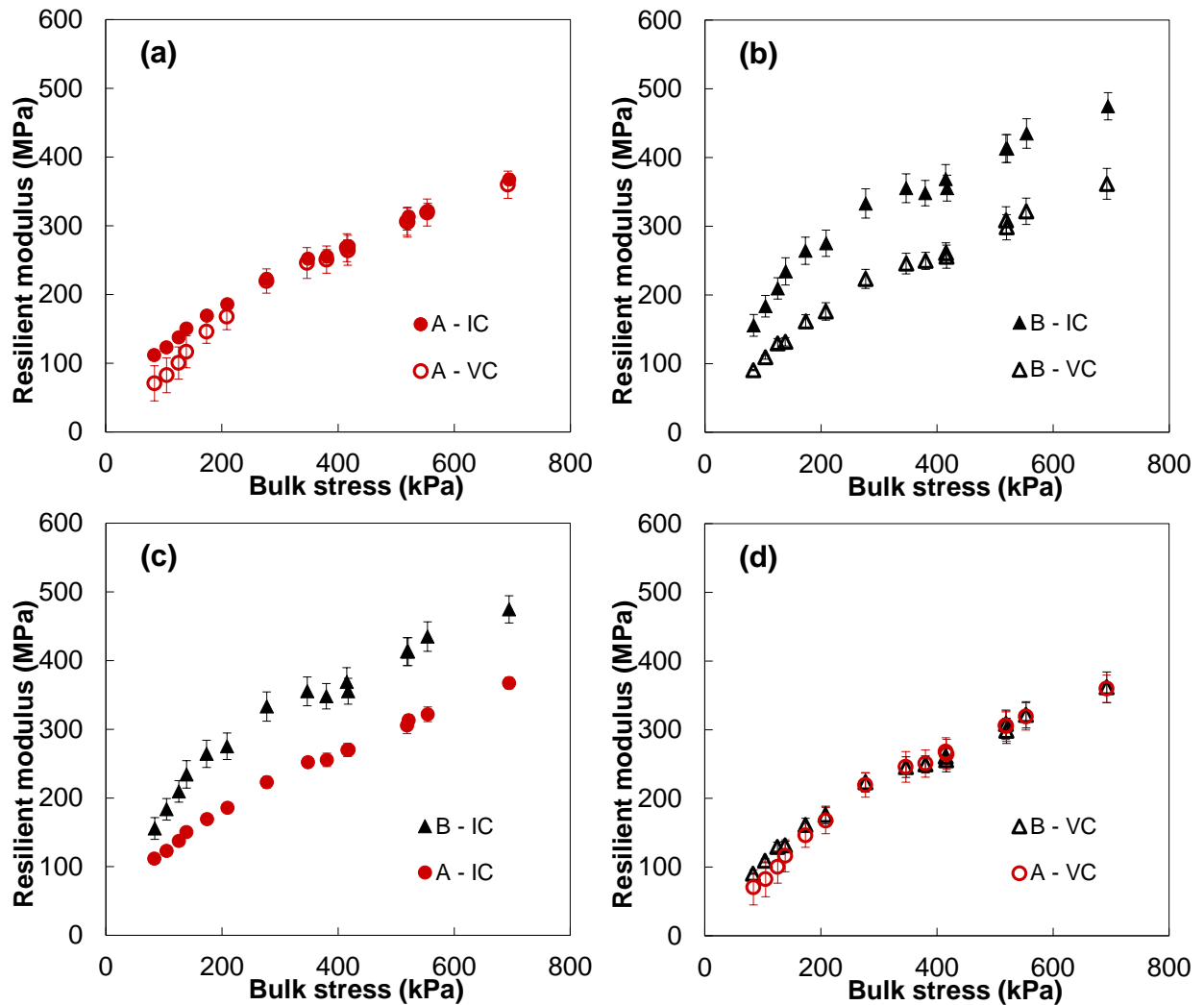

Figure 33 - M_R test results on Arrowood (A) and Belgrade (B) for IC and VC specimens

Effect of Saturation Level on Resilient Behavior of ABC

It has been reported that the degree of saturation can have a major influence on the mechanical performance of ABC mechanical performance, including resilient deformation

(Thom and Brown 1987; Lekarp et al. 2000; Ekblad and Isacsson 2006; Rahman and Erlingsson 2016). An increase in the degree of saturation is expected to lead to a decrease in the resilient modulus of ABC due to the development of pore water pressure and subsequent reduction in the effective stress, lubrication at the water-particle interface, decrease in matric suction, and reduction in internal friction.

ABC resilient modulus tests are generally performed close to the optimum moisture content (OMC). It is speculated that testing is conducted at the OMC because ABC materials are less sensitive to changes in moisture content than other unbound granular material due to their gradation (e.g., less fines) and unsaturated condition in-service (Ekblad 2007). The majority of past studies in the US that have evaluated the effect of moisture content on the resilient deformation behavior of ABC have been performed at moisture contents at or near the OMC (Tian et al. 1998; Khoury et al. 2009; Stolle et al. 2009). During the service life of an ABC layer, there will be cycles of wetting and drying. Therefore, it is crucial to study the effects of moisture content on ABC resilient modulus over a broader range of saturation levels.

M_R Results

In this study, a procedure that realistically represents wetting and drying in the field was used to evaluate the effect of moisture on the M_R of Arrowood and Belgrade ABC materials. The middle-bound gradation was used, and two specimens each of Arrowood and Belgrade sources were tested. The M_R tests on each sample were performed according to the procedure described in the material and method section. After performing the M_R test on a sample compacted at 2% above the water absorption, the sample's saturation degree increased by injecting water, shown in Figure 34, and it was followed by the M_R test was performed on the sample. Then, the water was allowed to gravitationally drain out from the specimen until water ceased to drain from the specimen, as shown in Figure 35. Finally, the last M_R test was performed on the specimen.

The M_R test results at the three moisture conditioning stages are shown in Figure 36 and Figure 37 for Arrowood and Belgrade materials, respectively. The results shown correspond to the average M_R values for each stage. The saturation level for each state of moisture conditioning is indicated in the figure legend. To better illustrate the results, the range of values obtained from replicate M_R tests on MB gradation of each source (compacted with OMC) is shown. The results generally indicate that the M_R test results are not significantly affected by the moisture content given the overlap between the error bars and the results from the different moisture conditions. However, the Stage 1 Arrowood M_R values are significantly higher than the other moisture contents. A higher value of M_R in Stage 1 is expected because moisture contents below the OMC, resulting in increased suction within the specimen; higher suction leads to stiffer material. The effect of the degree of saturation (e.g., between Stage 1 and Stages 2 & 3) becomes more pronounced by increasing the bulk stress. As shown on the Figure 33, the M_R did not change significantly between Stages 2 and 3, where the degree of saturation reduces by about 10% due to gravitational drainage. At the higher level of degrees of saturation (e.g., Stages 2 & 3), the matric suction between the aggregate particles becomes negligible and does not change notably with a slight change in the degree of saturation.
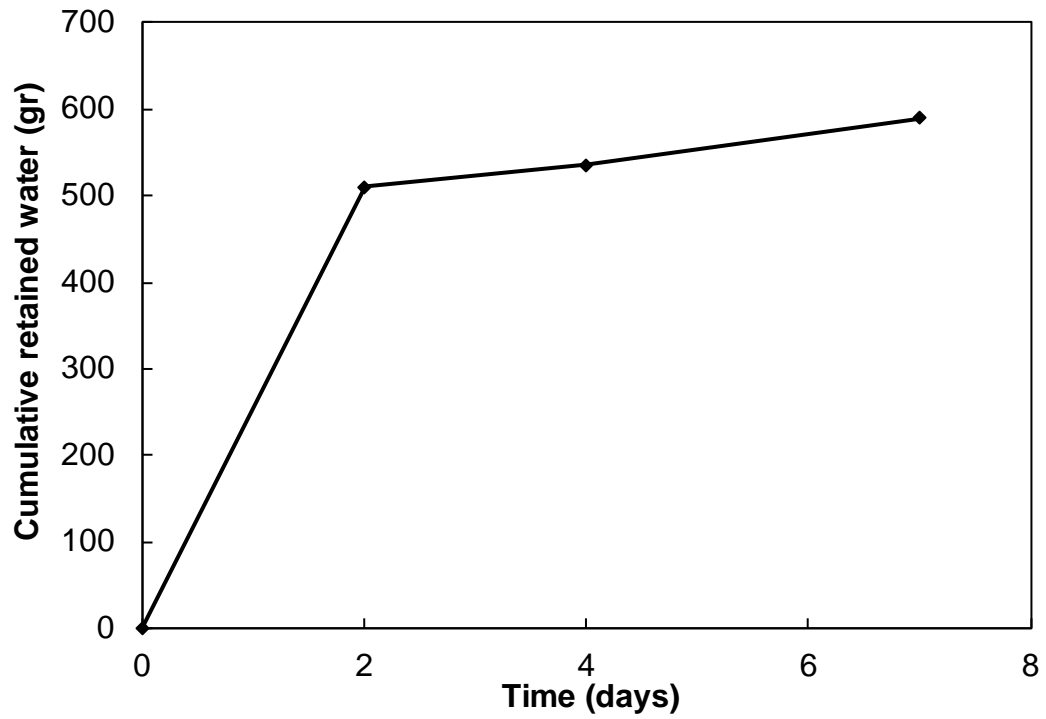
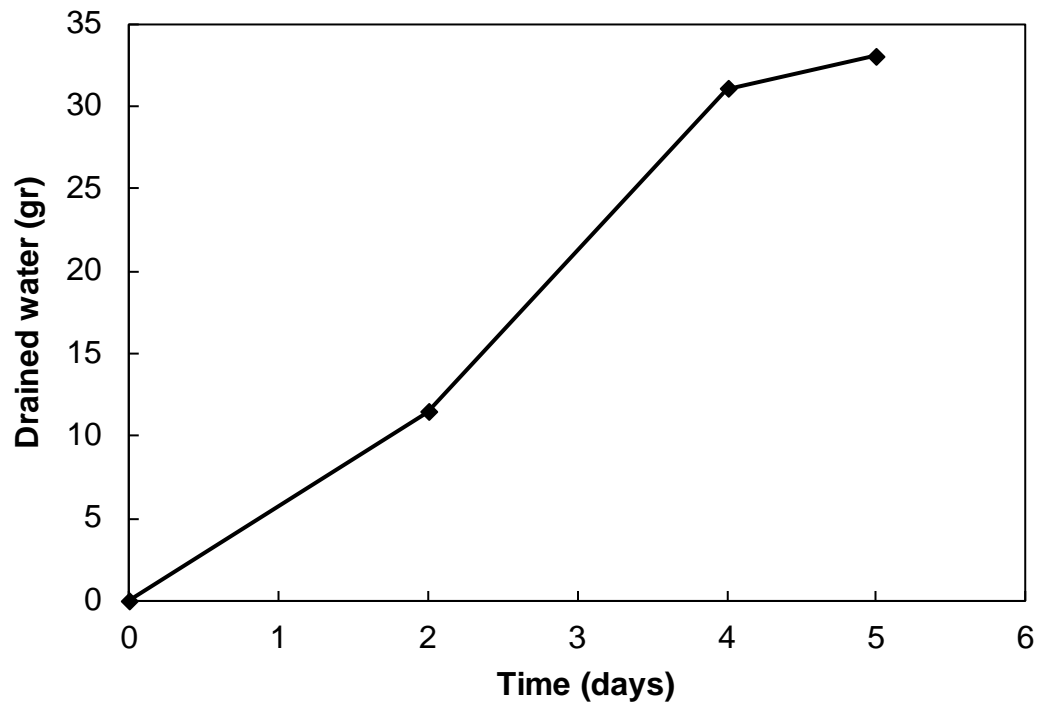**Figure 34 - Saturation phase after Stage 1, estimated retained water vs days**

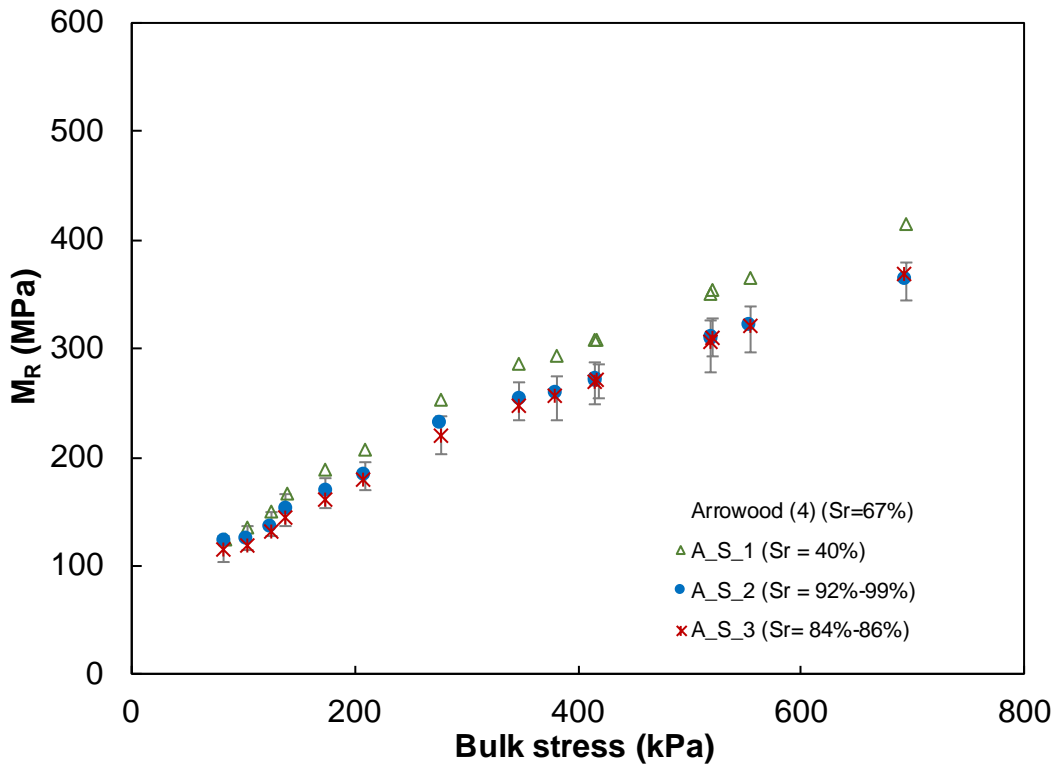**Figure 35 - Drainage phase after Stage 2, estimated drained water vs days**

Figure 36 - M$_R$ test results on Arrowood material - MB gradation - Varying moisture

While the error bars representing the OMC conditions indicate that the differences in M$_R$ at varying moisture conditions are statistically equivalent, Figure 37 shows that the average M$_R$ values increase as the degree of saturation decreases between Stages 1 and 2 for the Belgrade material; however, during Stage 3, an increase in the average M$_R$ values is observed, which may be caused by densification of the ABC sample. Similar trends were observed in Rahman et al. (2016).
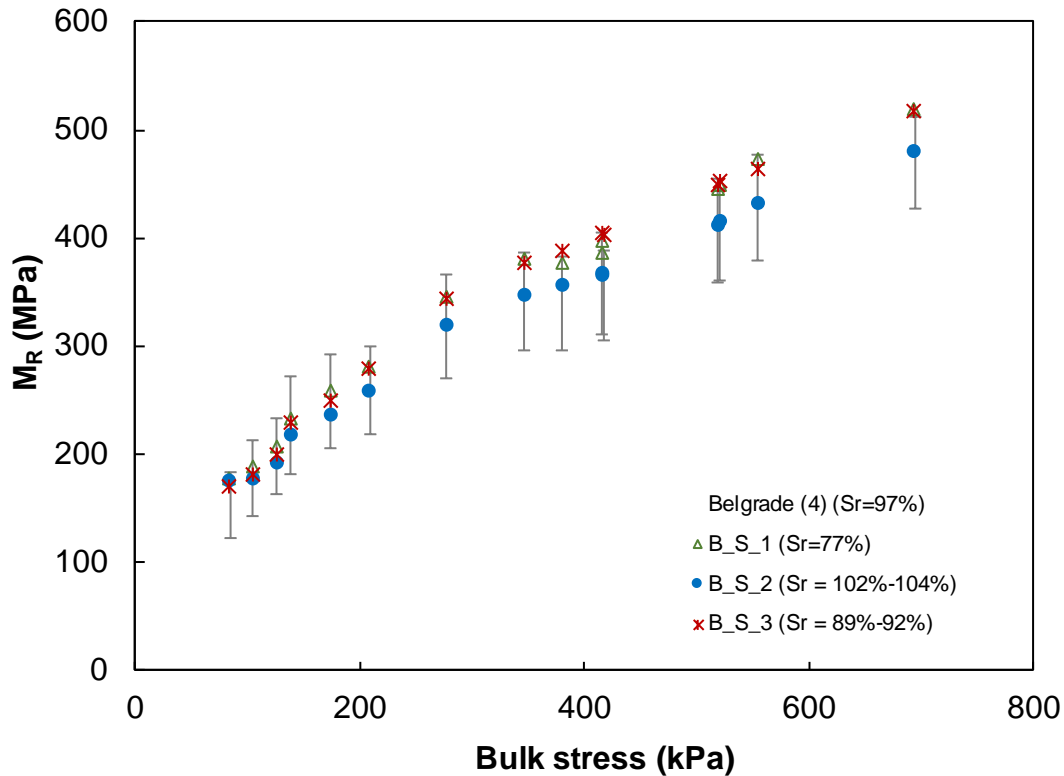
Figure 37 - M$_R$ test results on Belgrade material - MB gradation - Varying moisture

Findings and Conclusions

The specific findings and conclusions for the study presented herein are discussed in this section. ABC materials meeting the current NCDOT gradation specification exhibited consistent resilient behavior, even when the material is gap-graded within the specification band. Furthermore, analytical models confirmed that the current gradation band produces material with adequate performance.

Morphological properties of ABC, such as the surface texture and sphericity, are statistically most significant in predicting the resilient modulus of ABC. Furthermore, assessing the material properties, including angularity, surface texture, and sphericity, allows for a prediction of resilient modulus of the ABC material, which can be used in the design process. If it is deemed important to the NCDOT's objectives, the Department can improve the predictive model by using their existing database of experimental data, including M$_R$, and adding results from AIMS for all aggregate sources of interest.

Compaction processes can degrade ABC materials that are susceptible to crushing. This in turn affects the resilient modulus of the ABC by changing the fabric of the material. The compaction method used in the laboratory should match the compaction processes in the field as best as possible for a more representative resilient modulus.

Varying the degree of saturation results in negligible differences in the measured M$_R$. The majority of the M$_R$ results for a wide range of degree of saturation are within a relatively narrow band, indicating the inherent variability of the material may have a higher effect on the M$_R$ results for the sources studied.

Recommendations

The current band-type specification for acceptance of Aggregate Base Course (ABC) materials results in consistent resilient behavior for the materials tested. These findings indicate that the NCDOT may be able to reduce the amount of experimental resilient modulus tests they perform, as these tests are costly and time consuming. Instead, straightforward morphological tests (e.g., AIMS2) may be able to be used in conjunction with evaluating gradation to confirm the consistency of the ABC material, and provide an assessment of anticipated resilient behavior. Before the Department pursues this, the regression models evaluated herein should be further evaluated with a larger dataset (e.g., NCDOT's current database with the addition of AIMS2 results for each source). The reevaluation of the regression models would result in equations with higher confidence to estimate resilient behavior for design.

Implementation and Technology Transfer Plan

The existing ABC acceptance criteria was evaluated as acceptable over a wide range of stress and moisture conditions. Furthermore, a relationship between easy-to-measure physical properties and the resilient modulus is provided in the final report to allow for reduced laboratory testing and direct connect to the design process. The findings from this study are presented herein and technical papers will be generated from the research project and will be submitted to the *Transportation Research Board* and other appropriate journals for dissemination.

The Materials and Tests Unit can directly use the research products by reducing the amount of resilient modulus testing it is currently conducting, and further developing the relationship between easy-to-measure physical properties and the resilient modulus by implementing the AIMS2 device in conjunction with their existing testing database. This work can enhance their ability to evaluate the base course materials. Additionally, since the material properties can now be correlated with the material behavior, the design unit can use it as reference values for mechanistic-empirical pavement design. The pavement performance should be correlated and evaluated in a more meaningful way, removing some uncertainty of the design resilient modulus input parameter which means the maintenance cost could be more predictable and manageable. Finally, as this research project identifies morphological properties, such as surface texture and sphericity, as the strongest properties influencing resilient modulus, it may lead to a new perspective in evaluating base course materials, which could encourage the construction material industry towards further innovation in a new generation of materials that can meet the engineering functions and satisfy the needs of sustainability.

References

ASTM D2487-11. Standard Practice for Classification of Soils for Engineering Purposes (Unified Soil Classification System), West Conshohocken, PA, 2011, https://doi-org.prox.lib.ncsu.edu/10.1520/D2487-11

Barskale, R.D. and Itani, S.Y., 1989. Influence of aggregate shape on base behavior. *Transportation research record*, (1227).

Bilodeau, J.P. and Doré, G., 2012. Water sensitivity of resilient modulus of compacted unbound granular materials used as pavement base. *International Journal of Pavement Engineering*, *13*(5), pp.459-471.

Cetin, A., Kaya, Z., Cetin, B. and Aydilek, A.H., 2014. Influence of laboratory compaction method on mechanical and hydraulic characteristics of unbound granular base materials. *Road Materials and Pavement Design*, *15*(1), pp.220-235.

Chow, L. C., Mishra, D., Tutumluer, E. Aggregate base course material testing and rutting model delevopment. NCDOT project 2013-18, FHWA/NC/2013-18, 2014.

Cunningham, C.N., Evans, T.M. and Tayebali, A.A., 2013. Gradation effects on the mechanical response of crushed stone aggregate. *International Journal of Pavement Engineering*, *14*(3), pp.231-241.

Dawson, A.R., Thom, N.H. and Paute, J.L., 1996. Mechanical characteristics of unbound granular materials as a function of condition. *Gomes Correia, Balkema, Rotterdam*, pp.35-44.

Ekblad, J. and Isacsson, U., 2006. Influence of water on resilient properties of coarse granular materials. *Road materials and pavement design*, *7*(3), pp.369-404.

Ekblad, J., 2007. Influence of water on coarse granular road material properties. Doctoral dissertation, KTH University, Sweden.

Gates, L., Masad, E., Pyle, R. and Bushee, D., 2011. Aggregate imaging measurement system 2 (AIMS2): final report: FHWA-HIF-11-030. Pine Instrument Company, http://www.fhwa.dot.gov/hfl/partnerships/aims2/aims2_00.cfm (Last accessed 15 Oct 2011).

German, R.M., 1989. Particle packing characteristics. Princeton, N.J.. Metal Powder Industries Federation, c1989.

Gu, F., Sahin, H., Luo, X., Luo, R. and Lytton, R.L., 2014. Estimation of resilient modulus of unbound aggregates using performance-related base course properties. *Journal of Materials in Civil Engineering*, *27*(6), pp.04014188.

Gu, F., Sahin, H., Luo, X., Luo, R. and Lytton, R.L., 2014. Estimation of resilient modulus of unbound aggregates using performance-related base course properties. *Journal of Materials in Civil Engineering*, *27*(6), pp. 04014188.

Heydinger, A., Xie, Q., Randolph, B. and Gupta, J., 1996. Analysis of resilient modulus of dense-and open-graded aggregates. *Transportation Research Record: Journal of the Transportation Research Board*, (1547), pp.1-6.

Hicks, R.G. and Monismith, C.L., 1971. Factors influencing the resilient response of granular materials. *Highway research record*, (345).

Hossain, Z., Zaman, M., Doiron, C. and Solanki, P., 2011. Characterization of subgrade resilient modulus for pavement design. In *Geo-Frontiers 2011: Advances in Geotechnical Engineering*, pp. 4823-4832.

Huang, Y. H. Pavement Analysis and Design. Princeton, New Jersey, 1993.

IBM Corp. Released 2013. IBM SPSS Statistics for Windows, Version 22.0. Armonk, NY: IBM Corp

Kamal, M.A., Dawson, A.R., Farouki, O.T., Hughes, D.A.B. and Sha'at, A.A., 1993. Field and laboratory evaluation of the mechanical behavior of unbound granular materials in pavements. *Transportation Research Record*, pp.88-88.

Khoury, N., Brooks, R., Zaman, M. and Khoury, C., 2009. Variations of resilient modulus of subgrade soils with postcompaction moisture contents. *Transportation Research Record: Journal of the Transportation Research Board*, (2101), pp.72-81.

Kim, D. and Kim, J.R., 2007. Resilient behavior of compacted subgrade soils under the repeated triaxial test. *Construction and Building Materials*, *21*(7), pp. 1470-1479.

Lekarp, F., Isacsson, U. and Dawson, A., 2000. State of the art. I: Resilient response of unbound aggregates. *Journal of transportation engineering*, *126*(1), pp. 66-75.

Masad, E. and Fletcher, T., 2005. Aggregate imaging system (AIMS): Basics and applications (No. FHAWA/TX-05/5-1707-01-1). Texas Transportation Institute, Texas A & M University System.

Ministere des Transports du Quebec, 2004. Détermination du module réversible et du coefficient de poisson réversible des matériaux granulaires al'aide d'une cellule triaxiale achargement déviatorique répété (LC-22-400). *Procedure de laboratoire, Ministere des Transports du Quebec, Quebec.*

Mishra, D., Tutumluer, E. and Butt, A., 2010. Quantifying effects of particle shape and type and amount of fines on unbound aggregate performance through controlled gradation. *Transportation Research Record: Journal of the Transportation Research Board*, (2167), pp. 61-71.

NCDOT, 2012. Standard specifications for roads and structures. North Carolina Department of Transportation.

NCHRP, P., 2004. Chapter 1: Guide for mechanistic-empirical design of new and rehabilitated pavement structures: Final Report for Project 1-37A, Part 1, Chapter 1, Washington, DC, National Cooperative Highway Research Program. *Transportation Research Board*.

Oda, M., 1972. Initial fabrics and their relations to mechanical properties of granular material. *Soils and foundations*, *12*(1), pp. 17-36.

Pan, T., Tutumluer, E. and Anochie-Boateng, J., 2006. Aggregate morphology affecting resilient behavior of unbound granular materials. *Transportation Research Record: Journal of the Transportation Research Board*, (1952), pp. 12-20.

Rada, G. and Witczak, M.W., 1981. Comprehensive evaluation of laboratory resilient moduli results for granular material (No. 810).

Rahman, M.S. and Erlingsson, S., 2016. Moisture influence on the resilient deformation behaviour of unbound granular materials. *International Journal of Pavement Engineering*, *17*(9), pp. 763-775.

Saeed, A., Hall Jr, J.W. and Barker, W., 2001. Performance-related tests of aggregates for use in unbound pavement layers (No. Project D4-23 FY'96).

Santamarina, J.C., Klein, A. and Fam, M.A., 2001. Soils and waves: Particulate materials behavior, characterization and process monitoring. *Journal of Soils and Sediments*, *1*(2), pp. 130-130.

Stolle, D., Guo, P. and Liu, Y., 2009. Resilient modulus properties of granular highway materials. *Canadian Journal of Civil Engineering*, *36*(4), pp. 639-654.

Thom, N.H. and Brown, S.F., 1987. Effect of moisture on the structural performance of a crushed-limestone road base (No. 1121).

Thompson, M.R. and Smith, K.L., 1990. Repeated triaxial characterization of granular bases. *Transportation Research Record*, *1278*, pp. 7-17.

Tian, P., Zaman, M. and Laguros, J., 1998. Gradation and moisture effects on resilient moduli of aggregate bases. *Transportation Research Record: Journal of the Transportation Research Board*, (1619), pp. 75-84.

Tutumluer, E., 2013. Practices for Unbound Aggregate Pavement Layers: A Synthesis of Highway Practice. *Transportation Research Board of the National Academies, Washington, DC, Rep. NCHRP Synthesis*, *445*.

Vuong, B., 1992. Influence of density and moisture content on dynamic stress-strain behaviour of a low plasticity crushed rock. *Road and Transport Research*, *1*(2).

Yaghoubi, M. and Shukla, S.K., 2018. A universal gradation for highway pavement base course materials. *International Journal of Geotechnical Engineering*, *12*(2), pp. 166-171.

Zaman, M., Chen, D.H. and Laguros, J., 1994. Resilient moduli of granular materials. *Journal of Transportation Engineering*, *120*(6), pp. 967-988.

Appendix A – Literature Review

The literature review included within Appendix A was submitted to the NCDOT in 2016, and copied here for completeness in the final report.

Aggregate Base Course Resilient Modulus Behavior

The Aggregate Base Course (ABC) layer comprises one of the main structural components of a flexible pavement. The layer, therefore, must possess high stiffness and strength. Materials used in ABC construction often include unbound granular material. The unbound granular material derives its high stability from particle interlock and inter-particle friction. The deformation in ABC consists of permanent deformation and recoverable (resilient) deformation. The permanent deformation results from an accumulation of irrecoverable strains in the ABC layer. In parallel, during loading and unloading of the pavement, the resilient deformation takes place in ABC layer. The resilient deformation is a complex phenomenon and function of multiple factors.

Aggregate properties affecting ABC's performance under repeated loading

The resilient behavior of ABC is affected by several factors. These factors can be categorized to three main factors: particle properties, mass properties, and in-service factors. The particle properties consist of the gradation, particle shape, particle texture, particle angularity, chemical durability, mechanical durability, freeze-thaw durability, and specific gravity. The mass properties describe the behavior of the aggregate layer as a continuum like shear strength, stiffness, degree of compaction, permeability, and frost susceptibility. Mass properties are also significantly affected by particle properties. In-service performance of ABC factors is influenced by moisture condition, state of stress, load duration and frequency.

Effect of Aggregate Type and Particle Shape

Aggregate characteristics including shape, angularity, surface roughness, and roundness have an important influence on the resilient behavior and permanent response of ABC (Barksdale and Itani 1989). In a study conducted by Heydinger et al. (1996), gravel was shown to have a higher resilient modulus than crushed limestone. However, many researchers (Barksdale and Itani 1989; Hicks and Monismith 1971; Thom and Brown 1988) have reported that crushed aggregate, having angular to sub-angular shaped particles, provides better load spreading properties and a higher resilient modulus than uncrushed gravel, with sub-rounded or rounded particles. Mishra et al. (2010) believes that the most important parameter at low fines contents is the aggregate type (i.e., crushed or uncrushed particles). Unless all voids in aggregate matrix were completely filled with fines, particle angularity typically governs the shear strength.

Effect of Gradation

Gradation is a key factor influencing not only the mechanical response behavior characterized by resilient modulus, shear strength, and permanent deformation but also permeability, frost susceptibility, and susceptibility to erosion. Traditionally, it was believed that dense-graded material with the minimum voids and maximum compacted weight has the highest shear strength and stiffness; however, more free draining, open graded material began to be utilized to reduce damages due to excessive moisture and frost action (Saeed et al. 2001).

The gradation of a blend can be greatly affected by the amount of the material passing the No. 200 sieve. Limiting the amount of material passing sieve No. 200 has been usually specified to reduce frost susceptibility, to ensure sufficient permeability, and to prevent the development of pore pressure (Saeed et al. 2001). Thompson and Smith (1990) reported that for gradations that differ only in the permissible amount of material passing sieve No. 200, limited differences in resilient modulus were noted among the various granular material. Also, studies have indicated decrease in the resilient modulus with increase in the amount of fines content (Barksdale and Itani 1989; Kamal et al. 1993). Adding cohesive fines to a crushed aggregate have been reported to initially improve the stiffness as pore space is filled, and then it leads to considerable stiffness reduction because gradually, excess fines displace the coarse particles so that the mechanical performance relies only on the fines, and stiffness decreases (Jorenby and Hicks 1986).

Barksdale and Itani (1989) found that a finer gradation tends to show greater plastic deformation and a smaller resilient modulus, shown in Figure A-1. They argued that the coarse portion of the aggregates is the dominant factor in the amount of plastic deformation while the fine portion has a relatively small effect.
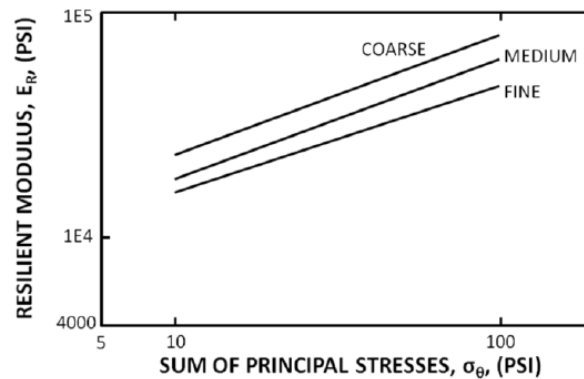

Figure A-1 - Effect of gradation on resilient modulus (Barksdale and Itani 1989)

Tian et al. (1998) studied the effect of gradation on the resilient modulus of ABC material (Tian et al. 1998). He stated the open-graded aggregates result in faster drainage, so it produces relatively higher resilient modulus values. Therefore, the open-graded aggregates are less likely to induce damage in pavements under saturated conditions and lead to more durable pavements. Also, he found that the resilient modulus is lower in finer material because interlocking of large, irregular shaped particles is reduced.

Trends toward coarse and well-graded blends are not clear. On the one hand, it has been argued that coarser blends produced the largest resilient modulus (Tian et al. 1998; Zaman et al. 1994). On the other hand, it has been also reported that coarse blends gave the lowest resilient moduli (Rada and Witczak 1981; Rada and Witczak 1982; Zeghal 2000). In contrast, it has also been stated that gradation has very little, less than 10%, effect on the resilient properties of the material. Cunningham et al. (2013) suggested that it can only be concluded from the previous researches that the gradation plays some role in the resilient values, especially when fines were involved, but their effect was very little when compared with the stress state of the material, which almost every author cited as the major factor in the resilient response (Cunningham et al. 2013).

Mishra and et al. (2010) studied the effect of plasticity of the fines in a blend on the unbound aggregate performance (Mishra et al. 2010). The results of their tests confirmed the common observation that plastic fines deteriorate aggregate performance significantly. High amounts of plastic fines (in excess of 10% by weight) at wet of optimum moisture conditions quickly destroyed the aggregate load transfer matrix, resulting in drastic reductions in strength. However, in the case of non-plastic fines, increased amount of fines did not cause significant decreases in aggregate strength. It was stated that at low fine contents, the type of fines is not likely to play an important role.

Effect of Moisture Content

The behavior of granular material is highly dependent on the degree of saturation or moisture content of the material. It is believed that the resilient response of dry and most partially saturated granular materials is similar, but as complete saturation is approached, the resilient behavior may be affected significantly (Vuong 1992). The result of studies on the resilient behavior of ABC have shown that at high degrees of saturation the resilient modulus is highly dependent on the moisture content, and the modulus decreases with the increase in saturation level (Barksdale and Itani 1989; Heydinger et al. 1996; Hicks and Monismith 1971).

Some researchers believe that the effect of moisture condition is dependent on the analysis. The excess pore water pressure developed in the saturated granular material due to repeated loading results in the decrease in the effective stress in the material, which subsequently decreases the strength and stiffness of the material. It has been reported that the a decrease in the resilient modulus due to saturation is obtained only if the analysis is based on total stresses; however, it has been observed that if the test results are analyzed on the basis of effective stresses, the resilient modulus remains approximately unchanged (Lekarp et al. 2000)

The reduction in the stiffness with increasing the moisture content in a blend has been argued to be related to the lubricating effect of the moisture. Thom and Brown (1985) confirmed the decrease in stiffness (resilient modulus) with increase in the water content, but they argued this reduction in stiffness is related to the lubricating effect of the moisture (Thom and Brown 1987). Increasing the degree of saturation in the samples (up to 85 percent) did not result in developing the pore water pressure. The test results showed a reduction to the resilient modulus with increasing moisture content, and this was related to the lubricating effect of water.

Tian et al. (1998) also studied the effect of moisture on the resilient modulus of ABC material. It was stated that the decrease in the matric suction with increasing moisture content can be a cause of the decrease in resilient modulus with increasing the moisture content. This was also confirmed by Dawson et al. (1996) who studied a range of well graded unbound aggregates and found that below the optimum moisture content stiffness tends to increase with increasing moisture level, apparently due to development of suction (Dawson et al. 1996). Beyond the optimum moisture content, as the material becomes more saturated and excess pore water pressure is developed, the effect changes to the opposite and stiffness starts to decline fairly rapidly.

Effect of Stress

Past investigations indicate that stress level is the factor that has the most significant impact on the resilient modulus of granular materials (Hicks and Monismith 1971; Kolisoja

1997; Rada and Witczak 1981). Resilient modulus increases significantly with an increase in confining pressure and sum of principal stresses.

In pavements, base course materials derive their resistance to stress-induced deformation from interparticle friction; therefore, their stiffness depends on the intergranular (effective) confining stress existing at the location of interest as well as on the applied deviatoric stress. The effect of confining stress is more pronounced on granular non-cohesive soils than on cohesive fine-grained soils because non-cohesive granular soils develop interparticle friction from effective confining stress, whereas cohesive granular materials derive loading resistance from cohesion as well as confining stress.

In addition, the degree to which the confining stress affects resilient modulus depends on other material properties. Resilient modulus of fine-grained cohesive soils increases only slightly with increased confining stress. In coarse grained materials (such as ABC), confining pressure can significantly influence the resilient modulus (Rada and Witczak 1981). The resilient modulus of fine-grained cohesive soils generally decreases with increasing deviatoric stress, referred to as stress softening behavior. For coarse grained soils, the resilient modulus increases with increasing deviatoric stress which indicates a strain hardening effect due to the reorientation of the grains into a denser state.

Kolisoja (1997) explained the mechanisms by which confining pressure and deviatoric stress affect the behavior of granular material. As the confining stress increases, soil particles are compressed against each other. Therefore, the number of contact points between particles and forces acting on the contact points of the particles increases. In addition, increased inter-particle forces at contact points increases frictional forces. Therefore, the particles resistance to slide past one another will be increases. Consequently, deformations will decrease as confining stress increases.

Evans et al. (2009) described the effect of confining pressure and deviatoric stress on the resilient modulus within the framework of Mohr-Coulomb theory. As shown in Figure A-2, increasing the confining pressure shifts the stress state toward the zone, resulting in less permanent deformation and consequently a higher resilient modulus. Increasing the deviatoric stress causes the resilient modulus to decrease. As illustrated in Figure A-3, the stress state is in the linear zone at low stress levels. As the deviatoric stress increases at a constant confining pressure, the stress state tends towards the elasto-plastic zone and then reaches the failure envelope if the deviatoric stress increases to a sufficiently high level. This results in higher permanent deformation as the Mohr's circle grows larger, which implies a reduction in the resilient modulus.
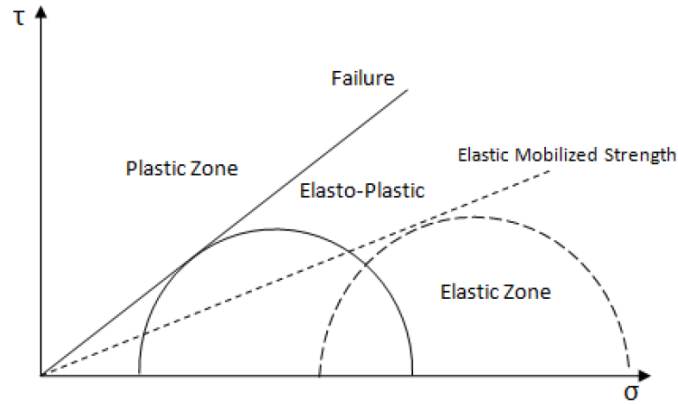
Figure A-2 - Effect of confining pressure on resilient modulus (Evans et al (2009))
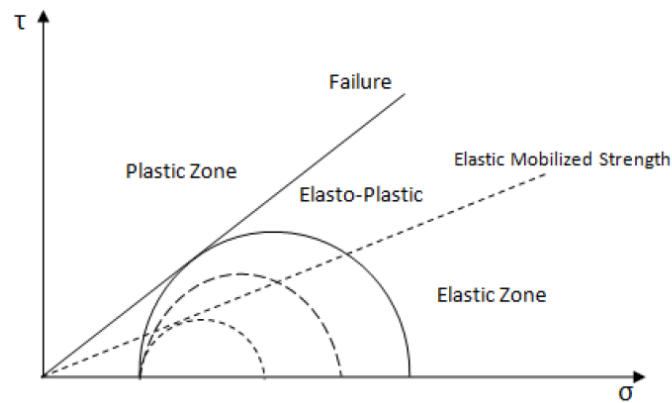

Figure A-3 - Effect of deviatoric stress on resilient modulus (Evans et al (2009))

The effect of deviator stress on the resilient modulus of unbound aggregates is less pronounced than that of confining pressure. Morgan (1996) reported a slight decrease in the resilient modulus when the deviator stress is increased under constant confinement.

Hicks and Monismith (1971) studied the factors influencing the resilient response of granular soils and found that the most important factor in determining the resilient modulus was the stress level. They found that the resilient modulus increased with confining pressure, and slightly with the repeated axial stress, as shown in Figure A-4.
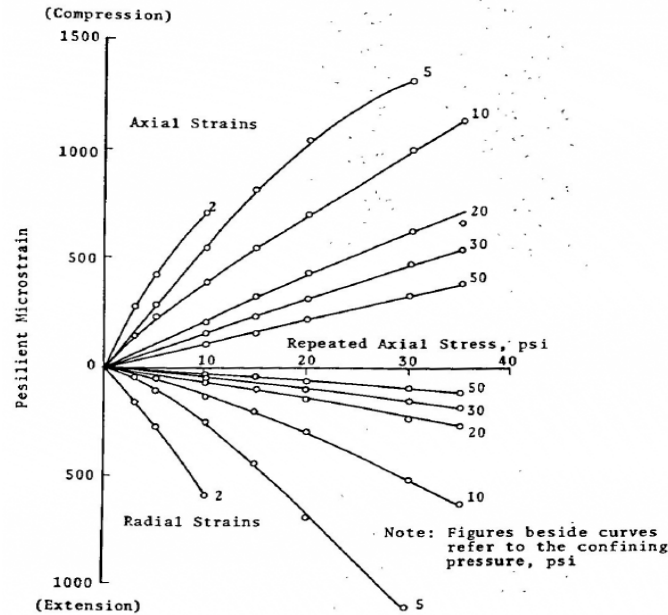
Figure A-4 - Variation in axial and radial strains with axial stress and confining pressures (Partially crushed aggregate, low density, coarse grading, dry) (Hicks and Monismith (1971))

The stress history also can affect the resilient response of the unbound granular material. Changes in resilient modulus with stress history are a consequence of progressive densification and particle rearrangement under repeated loading. Some studies reported that the effect of stress history can be reduced by preloading of the current loading regime and avoiding high stress ratios in tests for resilient response. Others believed that this effect is minimal after the application of a number of repeated loading of the same stress amplitude (i.e., a steady state resilient response is achieved). Therefore, researchers suggest a prescribed number of cycles ranging from 100 to 1000 load repetitions to eliminate stress history effects (Lekarp et al. 2000).

Aggregate Packing Theory

Aggregates are the major components of granular materials either in bound material like asphalt mixture and concrete or in unbound material like ABC. One of the major factors affecting the performance of these structures formed by aggregate is the grain size distribution. Different methods are developed to achieve the ideal blend in granular materials based on the grain size distribution. Fuller and Thompson, pioneers in this area of study, in 1907 proposed a relationship for an aggregate blend that provided the minimum void ratio for the aggregate particles in the mix (Cunningham et al. 2013).

It was believed that the particle density plays the main role in the performance of the granular material. The size distribution of spheres to obtain the maximum possible density was developed by Talbot and Richard as follow:

$$P = 100(\frac{d}{D})^n \tag{A-2}$$

where 'P' is the percent of material by weight passing a given sieve with an opening of size 'd', 'D' is the maximum particle size of a given aggregate blend, and 'n' is the exponent that affects the coarseness or fineness of the gradation, given by the slope (Talbot and Richart 1923).

Further studies indicated that the densest aggregate does not necessarily perform well. Experimental studies with photoelastic disks of granular material under compression have shown that under an applied external pressure most of the load is transferred through chains of particles, shown in Figure A-5, and other particles play the secondary role of preventing the main chain of particles from buckling. Therefore, studies have moved toward evaluating the effect of particle packing and the material performance.

In the following parts, methods developed based on the packing theory in order to either evaluate the performance of the aggregate or identify the load carrying structure and predict the performance of the unbound material will be discussed.
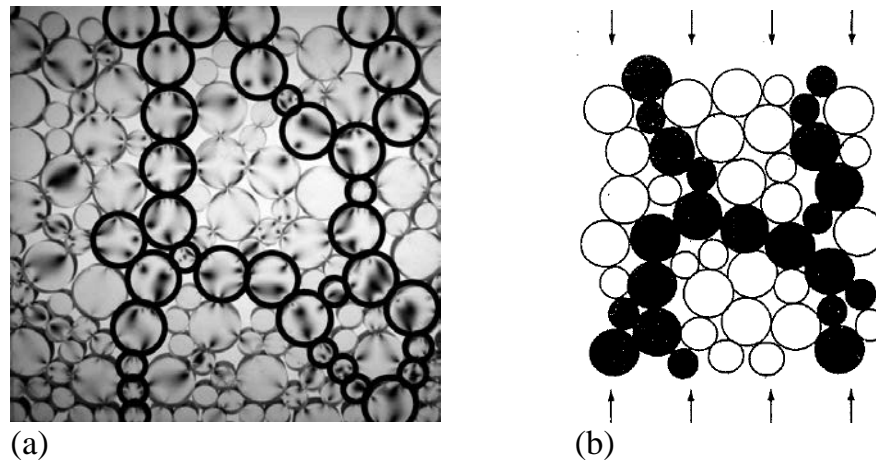

(a)   (b)

Figure A-5 - Particle chain (a) Photoelastic demonstration (b) Schematic demonstration (Santamarina 2003)

Bailey method

The Bailey Method was initially developed by Robert Bailey, now retired, who worked with the Illinois Department of Transportation. The purpose was to design a tool to help better understand the mechanics of aggregate packing and its contribution to the compressive strength of asphalt pavement (Vavrik 2002).

The Bailey Method looks at particle packing based on particle size. The goal is to design a blend that uses the coarse particles efficiently, meaning that there is a balance of coarse particles and fine particles. Such a balance allows the coarse aggregate to interlock, meaning each (relatively) large aggregate is transferring its load to as many other large aggregate as possible. Also, this method allows the fine aggregate to fully support the coarse aggregate by filling the void spaces fully without over filling them, which would push the coarse particles apart.

The particle packing theory used by Bailey method starts by looking at the definition of course and fine aggregate which is different from the geotechnical conventional definition. In geotechnical engineering, the definition of course and find aggregate has been globally accepted; aggregates retained on the 4.75 sieve are considered course. This division between course and fine aggregate is independent of the distribution of aggregate size in the mixture.

In Bailey method, it is necessary to change this definition to properly analyze a mixture gradation and determine the packing and aggregate interlock provided by the combination of all aggregates in the mixture. Therefore, a different approach to divide the coarse and fine fraction in a blend is used. According to this method:

- Coarse Aggregate: Large aggregate particles that when placed in a unit volume create voids.
- Fine Aggregate: Aggregate particles that can fill the voids created by the coarse aggregate in the mixture.

In these definitions of coarse and fine aggregates, there is no aggregate size associated with the words coarse and fine. Therefore, it is possible to have fine aggregate in a traditional coarse aggregate material as well as coarse aggregate in a traditional fine aggregate material. The division between coarse and fine aggregate depends on the nominal maximum particle size (NMPS) of the mix. NMPS is one sieve larger than the first sieve that retains more than 10% (as defined by Superpave terminology).

In addition to the definitions, to have a basis for dividing aggregates to course and fine, the Bailey method uses the result of two dimensional and three dimensional analysis of aggregate packing theory. The two dimensional analysis of aggregate shape consists of four combinations of geometry which yield a particle size ratio. This ratio is the diameter ratio of course aggregate creating the void and the fine aggregate perfectly filling the void. In this analysis which all the particles have the same size and are perfectly circular, maximum density is achieved when each particle is surrounded by 6 particles, shown in Figure A-6 (a). The void between each 3 particles can be fit with circular particle with diameters 0.155 times the diameter of large particles, shown in Figure A-6 (b). In a real blend, aggregates are not perfectly circular, irregularity of aggregates expands the void between the particles, so a larger small particle is needed to fill the void. Therefore, considering irregularity, the particle diameter ratio ranges from 0.155 (all round) to 0.289 (all flat) with an average value of 0.22 (Vavrik 2002). The three dimensional analysis results to the similar results ranging from 0.15 (hexagonal close-packed spheres) to 0.42 (cubic packing of spheres). Therefore, based on theoretical results, it has been observed that the analysis of gradation is not affected if the value ranges from 0.18 to 0.28, so the 0.22 factor is chosen as an average condition; however, it may not be exact.

The Bailey method used the ratio of small to large particles based on two dimensional and three dimensional analysis of aggregate packing to define 4 sieves as follow:

- The Half Sieve is defined as the sieve closest to 0.5 times the NMPS (also known as Nominal Maximum Size Aggregate, NMSA),
- Primary Control Sieve (PCS) which is defined as the sieve closest to 0.22 times the NMPS,
- Secondary Control Sieve (SCS) is defined as the sieve closest to 0.22 times the PCS, and
- Tertiary Control Sieve (TCS) is defined as the sieve closest to 0.22 times the SCS.
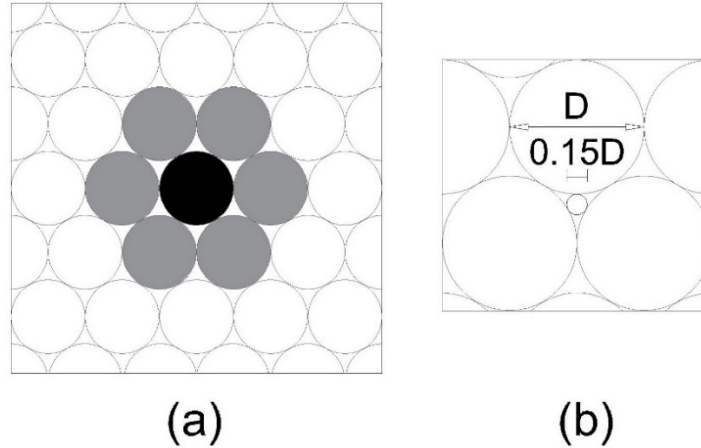
Figure A-6 - (a) Maximum density configuration of uniformly sized, (b) Fine particle filling the void created by coarse aggregate

These virtual sieves categorize the aggregate in Bailey method. Everything larger than PCS is considered "course", and everything smaller is considered "fine". Within fine portion, aggregate larger than SCS is considered "course part of fine aggregate", and everything smaller is considered "fine part of fine aggregate". Similarly, the TCS also separate the fine part of the aggregate. Course aggregates which are smaller than Half sieve are considered fine portion of course aggregates and referred to "interceptors". In the following figure graphical representation of these sieves is depicted. A schematic view of these sieves is depicted in Figure A-7. The control sieves based on different NMSPs are shown in Table A-1.

Fine			Coarse		
Fine		Coarse	Fine (Interceptors)	Coarse	
Fine	Coarse				Sieve Sizes

TCS   SCS   PCS   Half   NMSA

Figure A-7 - Bailey Method sieves (Daniel and Rivera 2009)

Table A-1 - Control Sieves for Various Asphalt Mixes (Vavrik 2002)

	NMSP (mm)					
	37.5	25	19	12.5	9.5	4.75
Half size	19	12.5	9.5	6.25	4.75	2.36
PCS	9.5	4.75	4.75	2.36	2.36	1.18
SCS	2.36	1.18	1.18	0.6	0.6	0.2
TCS	0.6	0.3	0.3	0.15	0.15	0.75

Bailey method uses the density of course aggregate to achieve the balanced blend in terms of particle size. The balanced blend is defined as a blend in which the course aggregates form the complete skeleton and has enough fine aggregates to fill the voids created by course aggregates, without over filling. The density of course aggregate, Chosen Unit Weight (CUW), is a percentage of the measured loose unit weight (LUW) of the course aggregate. The LUW of an aggregate is the amount of aggregate that fills a unit volume without any compactive effort applied. CUW results in calculating the amount of void in the blend which affect the distribution of the amount of aggregate in each section between the control sieves. Bailey Method uses these weights to calculate three weight ratios that help to understand and predict the aggregate behavior. These ratios are defined: Course Aggregate ratio (CA), Fine Aggregate Course Ratio (FA_c), Fine Aggregate Fine ratio (FA_f). Using these parameters, Bailey method controls the aggregate blend with controlling the void in the blend. The definition of these ratios are shown in Table A-2. Also, the range for the parameters are shown in Table A-3.

Table A-2 - Bailey method parameters

Parameter	Formula *
CA ratio	$= \dfrac{Half - PCS}{100 - Half}$
FAc ratio	$= \dfrac{SCS}{PCS}$
FAf ratio	$= \dfrac{TCS}{SCS}$

*Formulas are based on percent passing the control sieves

Table A-3 - Recommended Ranges of Aggregate Ratios (Vavrik 2002)

	NMSP (mm)					
	37.5	25	19	12.5	9.5	4.75
CA ratio	0.80-0.95	0.70–0.85	0.60–0.75	0.50–0.65	0.40–0.55	0.30–0.45
FA_c ratio	0.35–0.50	0.35–0.50	0.35–0.50	0.35–0.50	0.35–0.50	0.35–0.50
FA_f ratio	0.35–0.50	0.35–0.50	0.35–0.50	0.35–0.50	0.35–0.50	0.35–0.50

Changed in CA influences the mixture structure. The packing of the coarse aggregate fraction, observed with the CA ratio, is a primary factor in the constructability of the mixture. For dense-graded mixtures, this ratio is desired to be between 0.40 and 0.80 to ensure balance in the coarse portion of the aggregate structure. As the CA Ratio decreases, compaction of

the fine aggregate fraction increases because there are fewer interceptors to limit compaction of the larger coarse aggregate particles. Therefore, a mixture with a low CA ratio requires a strong fine aggregate structure to maintain adequate mixture volumetric. Experience with mixtures designed under these concepts has shown that mixtures with a low CA ratio also tend to segregate during construction. As the CA ratio increases and approaches 1.0, the coarse aggregate fraction becomes "unbalanced" because the interceptor size aggregates are attempting to control the coarse aggregate skeleton. Although this blend may not be as prone to segregation, it contains such a large quantity of interceptors that the coarse aggregate fraction packs differently than desired. The result can be a mixture that is difficult to compact in the field, as it tends to move under the rolling compaction. With larger NMPS mixtures, it becomes possible for the CA ratio to increase considerably above 1.0, which can cause problems in design and construction. With an increasing CA ratio, it becomes possible for the fine portion of the coarse aggregate to actually dominate formation of the coarse aggregate skeleton. At this point, the fine portion of the coarse aggregate creates the aggregate skeleton. The coarse portion of the coarse aggregate is then considered as "pluggers," as the coarse particles do not make up part of the aggregate skeleton and instead float in a matrix of finer particles.

Moreover, change in FA_c and FA_f affects the blend. The FA_c and FA_f ratios compare the fine and course parts of the fine aggregates and fine part of fine aggregate, respectively. The course part of fine aggregate fills the void created by course aggregate of the blend. Similarly, the fine part of fine aggregate fills the void created by course part of fine aggregate of the blend. Also, the finer portions of the fine aggregate act as a dry lubricant to the larger particles allowing easier compaction. If either the FA_c or the FA_f ratio increases, above 0.5, then the fine aggregate push their way between the larger ones, overfilling the gaps in the coarse aggregate. Therefore, the blend will be too flexible and easily deformable as the large particles slide around on their coating of tiny particles. When the FAc or FAf ratios drop too low, then the small gaps are under filled. This causes the VMA to rise, but also deprives the mix of the lubricating effect of the fine particles, which may make it difficult to compact the mix to the proper level.

In this method, a unit weight (CUW) is chosen as a fraction of loose unit weight (LUW) to ensure the course aggregate interlock, then based on that, the voids in the coarse aggregate of the blend. Then, evaluation of aggregate gradation with the given ratios helps to provide insight into packing of the aggregate structure. In Figure A-8, the upper bound of the aggregate unit weight is also depicted which is the rodded unit weight (RUW). The RUW of an aggregate is the amount of aggregate that fills a unit volume with compactive effort applied, and it is considered the upper limit of course aggregate interlock.

Figure A-8 represents how the selection of a chosen unit weight affects the mixture in terms of aggregate size. The LUW is the lower limit of coarse aggregate interlock. Theoretically, it is the dividing line between fine-graded and coarse-graded mixtures. If the mix designer chooses a unit weight of coarse aggregate less than the loose unit weight, the coarse aggregate particles are spread apart and are not in a uniform particle-to-particle contact condition. Therefore, a fine aggregate skeleton is developed and properties for these blends are primarily related to the fine aggregate characteristics. The RUW is generally considered to be the upper limit of coarse aggregate interlock for dense-graded mixtures. This value is typically near 110-125% of the loose unit weight. As the chosen unit weight approaches the rodded unit weight, the amount of compactive effort required for

densification increases significantly, which can make a mixture difficult to construct in the field.
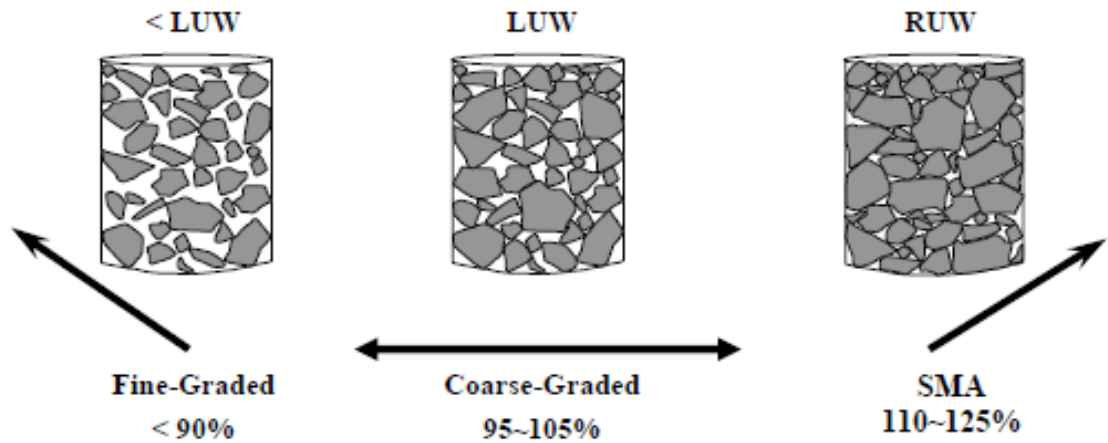

Figure A-8 - Determination of Mix Type (Kim 2006)

Dominant aggregate size ranges (DASR)

The Dominant Aggregate Size Range (DASR) aggregate packing theory was developed by Kim et al (2006), initially for the evaluation of aggregate gradations used in asphalt mixtures. The DASR theory was developed based on two dimensional packing theory of spherical particles of multiple sizes. The DASR approach identifies the size particle size which interact to form the primary load bearing structure of an aggregate blend, termed the "dominate aggregate size range". Correspondingly, the approach allows for identification of the porosity within the DASR, which is assumed to control deformation resistance of the aggregate blend. The theory states that porosity of the DASR must be below 50% for the particles to be in contact with each other and hence, have sufficient loading resistance.

The DASR method is based on the well-known fact in soil mechanic that the porosity of granular material in a loose state is generally between 45% to 50%, regardless of size or gradation. This implies that for particles within an aggregate mixture blend to be in contact with each other the porosity of the blend must not exceed 50%. It also indicates that the porosity can be used to evaluate the contact between large particles within a blend that contribute to resistance to deformation. As discussed, the Bailey method uses the same general approach, which requires the density to be a percentage of loose density which is based on laboratory result. This method and its criterion would preclude the need for laboratory compaction of coarse aggregate.

The DASR can either consist of a single particle size or a range of particles sizes in the blend. Thus, the porosity is calculated for the dominant sieve size or any two or more dominant contiguous sieve sizes within the blend. The porosity of a range of particle size in a blend can be determined based on the definition given in soil mechanics, which is the ratio of the volume of voids to total volume. The total volume of the blend consisting of particles that are equal to or smaller than the size of interest is determined as:

$$V_{T(i-1<Agg<i)} = V_{TM} - V_{(Agg \geq i)} \qquad (A-3)$$

where i = the size of interest; $i-1$ = smaller aggregate size next to i sieve; $V_{T(i-1<Agg<i)}$ = total volume available for particles retained on the $i-1$ sieve and passing the i sieve ; V_{TM} = Total volume of blend; $V_{(Agg \geq i)}$ = Volume of particles larger than the i sieve.

The volume of voids within $V_{T(i-1<Agg<i)}$ includes the volume of aggregates passing the $i-1$ sieve, and the volume voids can be determined as follows:

$$V_{V(i-1<Agg<i)} = V_V + V_{(Agg<i-1)}$$ (A-4)

where $V_{V(i-1<Agg<i)}$ = volume of voids within $V_{T(i-1<Agg<i)}$; V_V = Total volume of voids in the blend (referred to Voids in Mineral Aggregate (VMA) in asphalt concrete volumetrics); $V_{(Agg<i-1)}$ = volume of particles passing the $i-1$ sieve.

Correspondingly, the porosity of this range of aggregate sizes is calculated as follow:

$$n_{(i-1<Agg<i))} = \frac{V_{V(i-1<Agg<i)}}{V_{T(i-1<Agg<i)}} = \frac{V_V + V_{(Agg<i-1)}}{V_{TM} - V_{(Agg \geq i)}} = \frac{V_{TM} - V_{(Agg>i-1)}}{V_{TM} - V_{(Agg \geq i)}}$$ (A-5)

where $V_{(Agg>i-1)}$ = Volume of particles retained on the $i-1$ sieve. Similar calculations can be performed for any other particle size (or range of particle sizes) within the blend.

As a preliminary evaluation of how the porosity criterion relates to the performance of aggregate blends within asphalt concrete, three aggregate blends with known performance in asphalt concrete were utilized. The aggregate gradations considered included coarse–graded (C1), fine-graded (F1), and Stone Matrix Asphalt (SMA) as shown in Figure A-9. The porosity of each individual particle size in the blends was calculated and results are shown in Figure A-10.
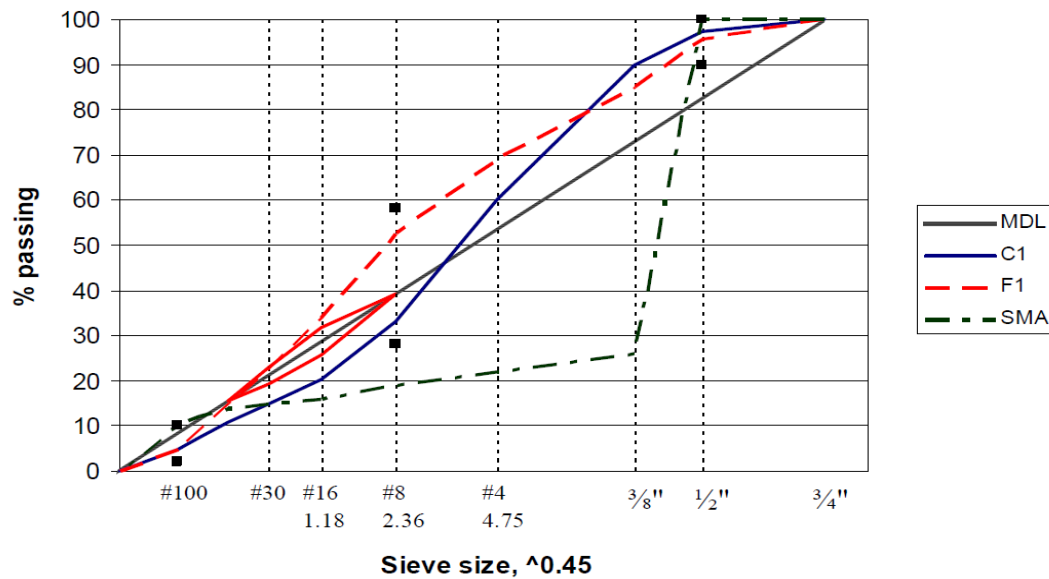
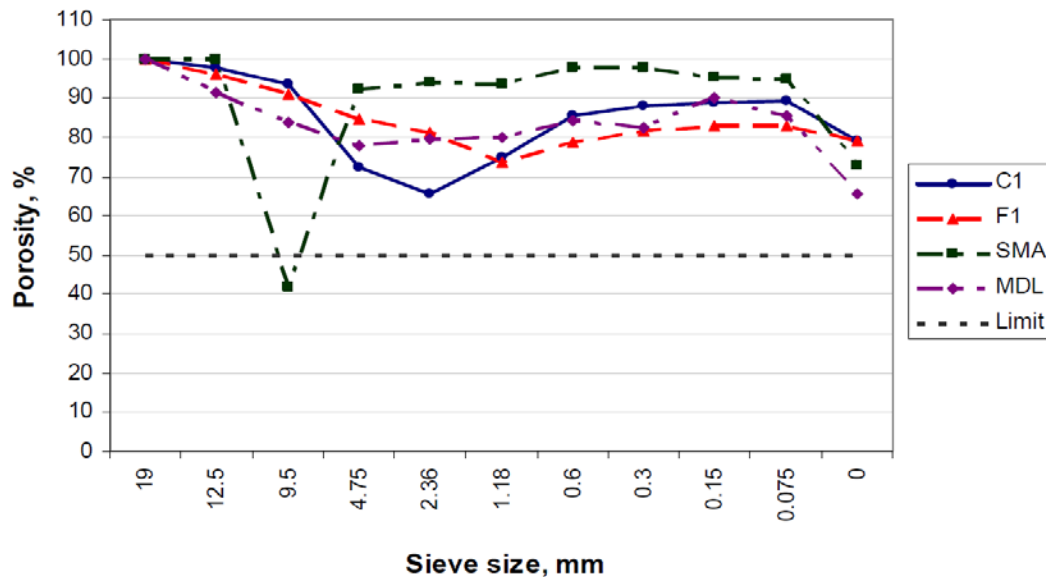**Figure A-9 - Example Gradations (Kim 2006)**

Figure A-10 - Individual Porosity Results (Kim 2006)

The results showed that with the exception of the 9.5 mm particle size in the SMA, none of the individual particle sizes in these gradations had a porosity less than the 50% criterion. The coarse gradation is known to perform well within asphalt concrete. Therefore, it was concluded it is not logical that the coarse aggregate in this blend exists in a state where the particles are not in contact with each other as reflected by the porosity being much greater than 50%. Rather, there must be a range of contiguous coarse aggregate particle sizes that form a network of interactive particles with a porosity less than 50% (i.e., form the DASR). Note that the 50% porosity criterion is equally applicable to a range of interactive particle sizes as to single size particles.

To develop the method to define the DASR , a physical model was used to describe the asphalt mixture, depicted in Figure A-11. The model includes the following components:

- *Dominant Aggregate Size Range (DASR)*: the interactive range of particle sizes which has the particle-to-particle contact and forms the primary structural network of aggregates. It was assumed that the porosity of the DASR must not be greater than 50%

- *Interstitial Volume (IV)*: aggregates and voids existing within the interstices of the DASR. The components within this volume are referred to Interstitial Components (IC). This volume serves to hold the DASR together.

- *Interstitial Surface (IS)*: This surface is defined by an approximately straight plane taken through the interstitial volume. The characteristics of this surface, including its roughness, protrusion of different size aggregate particles, and presence of fines strongly influence the mixture's performance. Rougher interstitial surfaces with larger particle protrusions will result in mixtures with greater shear resistance. Therefore, determination of the characteristics of this interstitial surface, which are controlled by gradation, should provide useful parameters for asphalt mixture evaluation and design. An example of an Interstitial Surface is shown in Figure A-12.

(a) SMA   (b) Coarse dense   (c) Fine dense
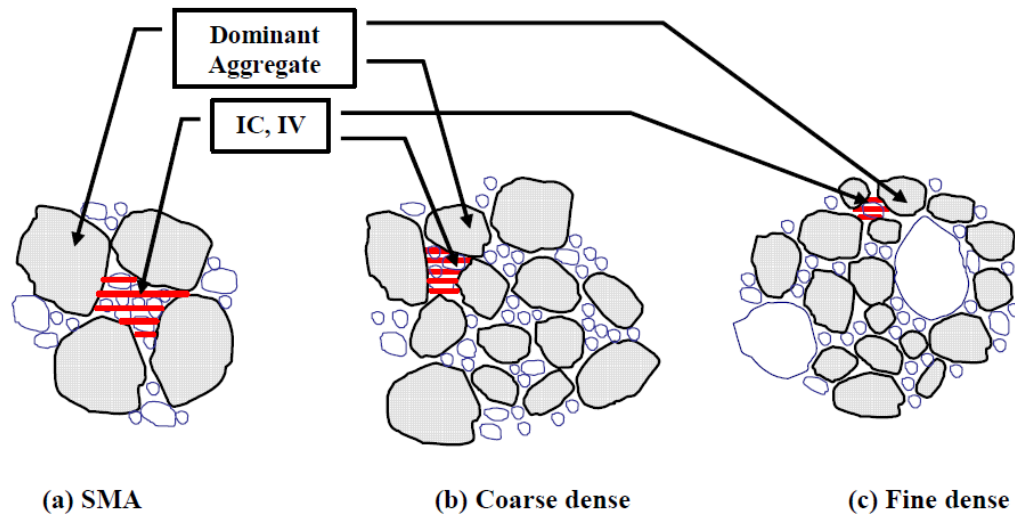
Figure A-11 - DASR and IV in (a) SMA, (b) C1, (c) F1 (Kim 2006)

Figure A-12 - The Interstitial Surface on a Broken Sample (Kim 2006)

The process to determine the aggregate sizes comprising the DASR of an aggregate blend consists of two steps: (1) analyzing the spacing of the particles to detect the contiguous sizes interacting as a unit, and (2) calculating the porosity of the interacting particle size ranges to determine the DASR.

Spacing analysis

The analysis used to define contiguous sizes of interacting particle is based on the particles' center-to-canter spacing on the interstitial surface. A theoretical procedure is developed to determine the spacing for specified gradations and thus determine which particles within the gradation interact to form the DASR. The procedure assumes that particles are distributed according to a hexagonal pattern on the interstitial surface with the larger particles uniformly distributed over the entire area and smaller particles distributed within the remaining area between the larger particles, as shown in Figure A-13. Under this assumption, the particle spacing (s) can be calculated using the following equation:

$$s = (\frac{2}{2n_t + 1})\sqrt{\frac{2A_h}{3\sqrt{3}}}$$ (A-6)

where n_t is the number of hexagonal layers required to accommodate the particles, and A_h is the area of the hexagonal.

(a)   (b)
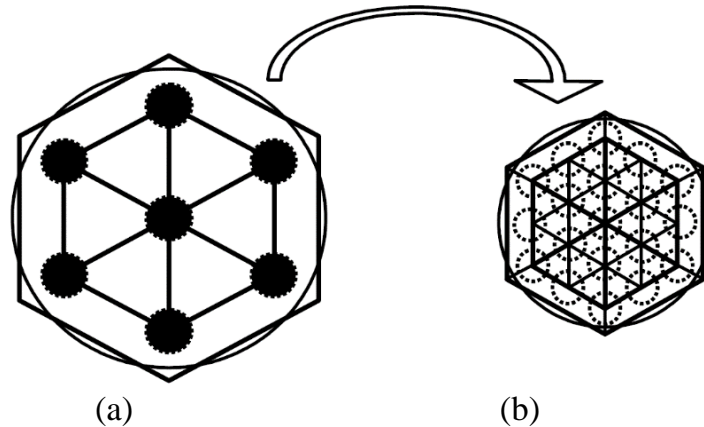
**Figure A-13 - The representative areas based on the hexagonal pattern (Kim 2006) (a)
The biggest particles distribution, (b) The 2nd size particles distribution
(Kim et al. 2006)**

The procedure is based on the fact that in a uniform aggregate blend, where all particles have the same size, the spacing between particles is equal to the diameter of the particles. Uniformly distributing particles with the smaller diameter to the uniform mixture affects the spacing of its initial particles. In the new blend with two particle sizes, the center-to-center spacing of the larger particles is influenced by the proportion of larger/smaller particles. In other words, particle spacing is influenced by the ratio of the larger to smaller particles. Decreasing this ratio, increases the center-to-center spacing of the larger particles. This phenomena is shown in Figure A-14, where the effect of increasing particles with diameters of 4.75 mm on the spacing between particles with diameters of 9.5 mm is depicted. It can be seen that the spacing of one group starts to increase dramatically once the relative proportions of different sized aggregates reaches a critical level. The effect of the ratio of particle sizes can be best understood from Figure A-15, which depicts the slope of the spacing of large (small) particles versus the percent of the small (large) particles in the blend.

Note that results shown for the spacing analysis of particles 9.5 mm and 4.75mm applies to any blend of particles of two different sizes with a size ratio of 2:1, which is generally the size ratio used between consecutive size sieves in asphalt mixture design. Therefore, it can be concluded that in any two particle sizes having a size ratio of 2:1, one particle size will significantly disrupt the ability of another particle size to interact once the relative proportions of the particle sizes is about 70/30. In other words, once the proportions exceed this value, the spacing of the particles with the smaller proportion increases so much that these particles are simply floating in the matrix and are no longer an effective part of the aggregate structure, which means the particles are not part of the DASR. Conversely, at proportions less than 70/30 (e.g., 40/60, 50/50, 60/40), as shown in Figure A-14 and Figure A-15, each particle size maintains a fairly stable spacing, so both are part of the DASR. All contiguous particle sizes determined to be interactive are considered part of the DASR, and are considered to act as a unit for determination of porosity.
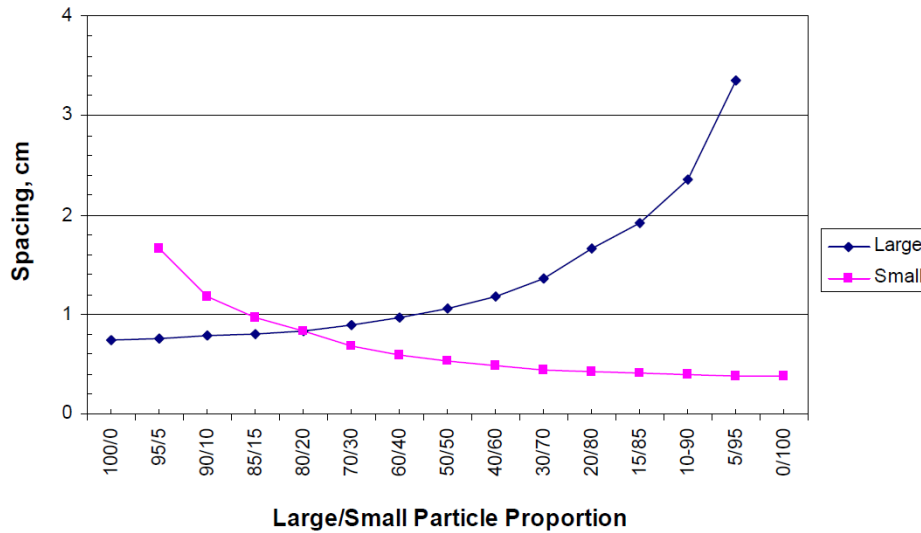
Figure A-14 - Spacing Result for the Binary Blend with 9.5, 4.75mm (Kim 2006)
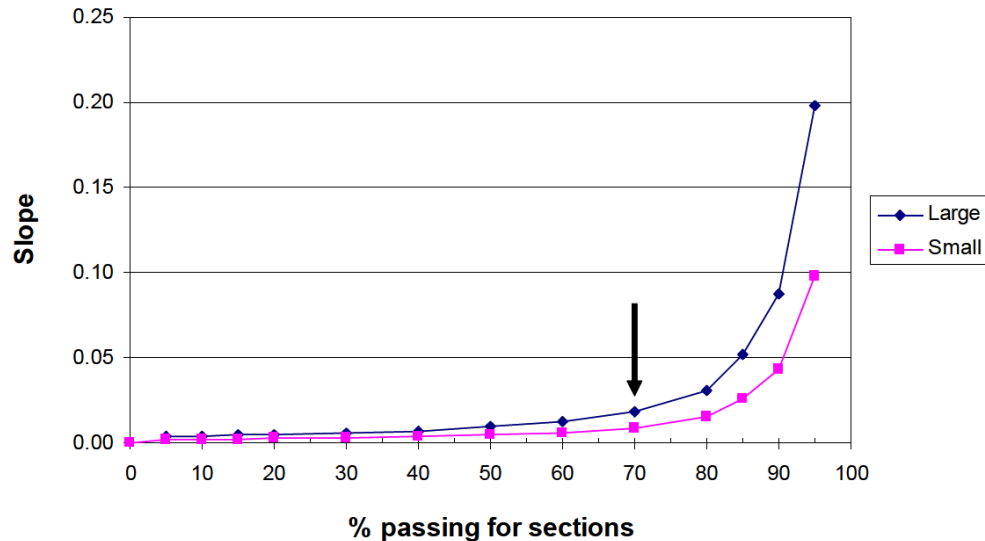

Figure A-15 - Slope (spacing change) for the Binary Blend (Kim 2006)

Based on the findings presented in Figure A-15, identification of all particle sizes contained within the DASR is accomplished using a diagram entitled the "Interaction Diagram". The Interaction Diagram consists of plotting the relative proportion of particles corresponding to successive sieve sizes. Figure A-16 presents the interaction diagram for the three blends described in Figure A-9. Based on the Figure A-15, contiguous particle sizes interact if their relative proportion is between 30/70 and 70/30. Therefore, based on Figure A-16, it can be concluded that the following contiguous particles sizes interact in the blends:
- Coarse-graded and SMA:
    - The aggregate passing 4.75 mm sieve and retained on 2.36 mm, and
    - The aggregate passing 2.36 mm sieve and retained on 1.18 mm
- Fine-graded:
    - The aggregate passing 9.5 mm sieve and retained on 4.75 mm,
    - The aggregate passing 4.75 mm sieve and retained on 2.36 mm, and

77

- The aggregate passing 2.36 mm sieve and retained on 1.18 mm.
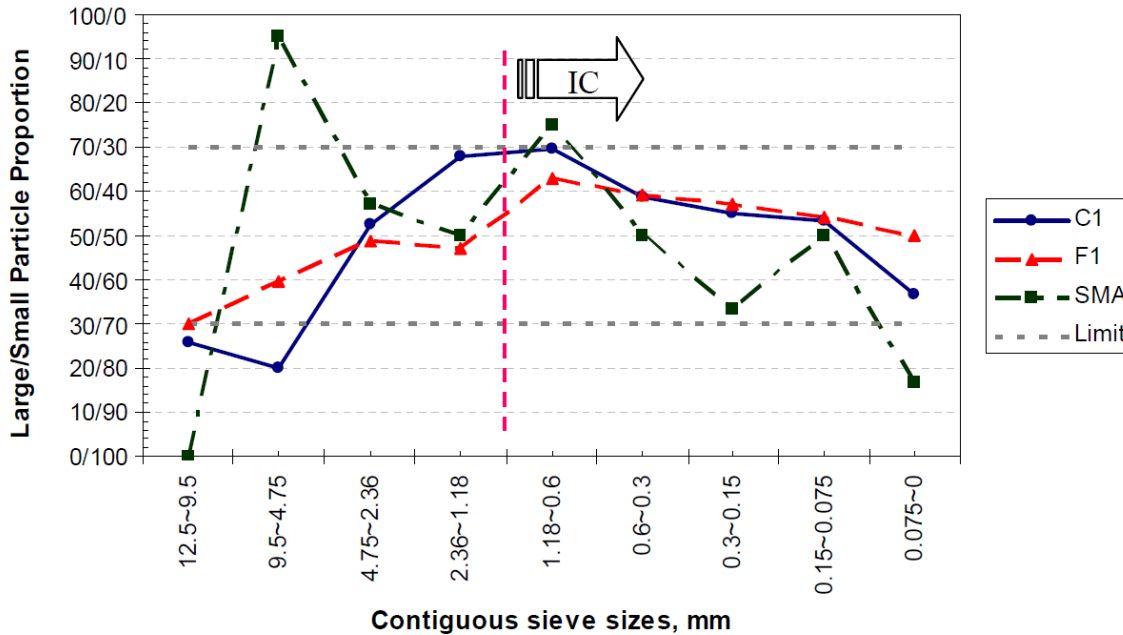
Figure A-16 - Interaction Diagram (Kim 2006)

It should be mentioned that the smallest particle coarse enough to contribute to aggregate interlocking was selected as the particle size passing the 2.36 mm sieve and retained on the 1.18 mm sieve because generally, in asphalt mixtures, coarse and fine aggregate are separated at the 2.36 mm sieve. Also, based on soil mechanics, particles finer than 1.18 mm have little internal friction. In addition, in the Bailey method, for a nominal maximum particle size (NMPS) of 12.5mm, the PCS is 2.36mm, based on a packing factor of 0.22.

Evaluating the Porosity criterion

The DASR of a blend is the set of interactive (or single) particles that results in the lowest porosity in the blend. The porosity of the detected interactive range of particles in the blend is calculated using Equation A-. The porosities of the interactive ranges of particles corresponding to the coarse, fine, and SMA aggregate blends previously discussed is shown in Figure A-17 which also includes the minimum porosities in the blends without considering the DASR. The dramatic effects of interaction on the porosity of DASR are clearly evident. For example, the minimum porosity of the coarse-graded material without considering the DASR is 65%, shown in Figure A-10. However, when the DASR and interaction is taken to account, the porosity of the dominant aggregate is 36% which meets the 50% porosity criterion.
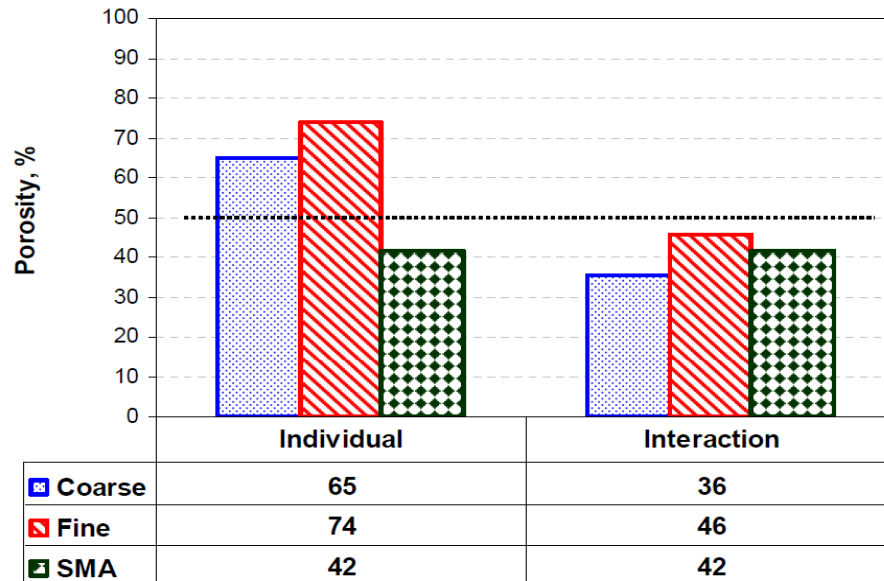
	Individual	Interaction
Coarse	65	36
Fine	74	46
SMA	42	42

Figure A-17 - Porosity Result before and after Considering Interaction (Kim 2006)

It should be noted that the DASR approach is based on packing theory of spherical particles of multiple sizes in two dimensions. Consequently, the criteria developed is probably most applicable to aggregates that are not flat or elongated. However, the authors saw no reason why it would not be possible to extend the concepts and theoretical calculations developed to particles that are not spherical. In addition, it is recognized that aggregate angularity and texture can affect the quality of aggregate interlock and these factors were considered. However, gradations that result in better interlock are beneficial regardless of the aggregate angularity or texture.

Guarin et al. (2013) expanded on the work of Kim et al. (2006) and proposed a means to evaluate the stability of the DASR. It was stated that the stability of the DASR is related to the volume of the particles larger than the DASR voids. Guarin (2013) studied the effect of interstitial component (IC) which includes particle sizes smaller than the DASR and binder. The DASR disruption was analyzed from two perspectives, local and global. A disruptive factor (DF) was introduced to evaluate the potential of IC aggregate to disrupt the DASR structure. The particle packing theory and volumetric properties of aggregates were used as the basis to define the DF, which is the ratio between the potentially disruptive IC particles and the volume of DASR voids. The volume of potentially disruptive IC particles consists of particles smaller than DASR and bigger than the voids of DASR, and it is calculated using volumetric relationships. The volume of DASR voids is determined as a function of the type of DASR structure (cubical or hexagonal) and the number of DASR particles. The type of packing arrangement (simple cubic or close hexagonal) is selected according to the DASR porosity. Figure A-18 shows how the IC plays a role in the disruption of the DASR structure.
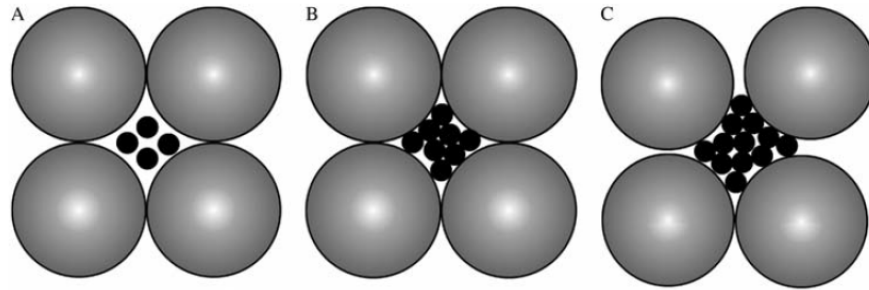
Figure A-18 - Disruptive Factor (DF) representation: (A) Low DF, (B) optimal DF, (C) high DF (Guarin et al. 2013)

Gradation-based framework

Lira et al. (2013) developed an alternative, generalized framework to identify the range of aggregate sizes which form the load carrying structure in asphalt concrete and assess its quality. The method consists of a numerical procedure based on packing theory. Parameters including porosity and coordination number, which is the number of contact points of each particle with its neighbors, can be determined and used to evaluate the quality of the load carrying structure as related to rutting resistance. Similar to the previously discussed method, aggregates are divided to three functional groups as follow:

- *Primary Structure (PS)*: interactive grains that form the main network which provides the load bearing capacity for the blend.
- *Secondary Structure (SS)*: smaller particles (than the PS) that fill in the gaps between the particles in the Primary Structure. Contributes to stability of the aggregate skeleton
- *Other*: particles larger than the PS that essentially float in the matrix. They have the ability to transmit shear forces to the PS without distributing it first.

As discussed, the DASR method was developed based on two dimensional packing and the relation between contiguous sieve sizes defined in accordance with the AASHTO sieve system. In the AASHTO system, gradations are assumed to be formed by discrete particle sizes having a size ratio of 2:1 between contiguous sieve sizes. Lira et. al's (2013) framework removes the limitation of the 2:1 size ratio assumption and extends the methodology of Kim et al. (2006) to three dimensional analysis.

In Lira et al.'s (2013) analysis, it is assumed that the stability of a structure formed by a group of particles is dependent on the particle arrangement which dictates the number of contact points between particles. The current framework is based on the two types of packing arrangement in three dimensional space: a densest and a loosest possible packing as shown in Figure A-19. These packing arrangements are broadly known as rhombohedral (densest) and simple cubic packing (loosest). The densest configuration has a packing density of 74% and coordination number of 12. In contrast, the loosest possible packing (simple cubic packing) of spheres has a packing density of 52% and coordination number of 6.
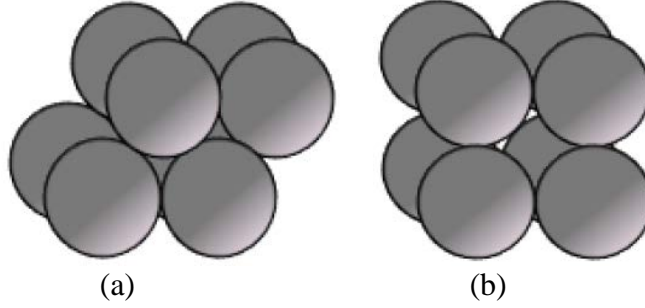
Figure A-19 - packing arrangements: a) Densest Packing, b) Loosest packing (Yideti 2014)

Using the aforementioned three dimensional packing theory, Lira et al.'s (2013) analysis framework is built upon the percent of aggregate retained on each sieve size using the following assumptions:
- All particles are spherical.
- Within each sieve size, there will be a continuous size distribution which is uniformly distributed, so for the sieve size D_n with material retained at D_{min} (opening of the sieve) and smaller than D_{max} (opening of the previous sieve), the mean size ($\bar{D}_n$) in the sieve will be defined as:

$$\bar{D}_n = (D_{min} + D_{max})/2 \tag{A-7}$$

- The maximum concentration of spheres of two different sizes is equivalent to a rhombohedral packing type ($\varphi_{D_n \& D_{n+1}}^{max} = 0.74$)
- Aggregate particles are uniformly distributed in the total volume

Note: The concentration of aggregate retained on any given sieve size is defined as the ratio of the weight of the aggregate retained at the sieve (W_{ret}^n) to the total weight of aggregates (W_{total}) as follows:

$$\varphi = \frac{W_{ret}^n}{W_{total}} \tag{A-8}$$

Consider an aggregate gradation, φ_n and φ_{n+1} as the concentration for two consecutive sieves with mean particle size $\bar{D}_n$ and respectively $\bar{D}_{n+1}$ ($\bar{D}_n > \bar{D}_{n+1}$). The weighted average size (D_{avg}) can then be calculated as:

$$D_{avg} = \frac{\bar{D}_n \cdot \varphi_n + \bar{D}_{n+1} \cdot \varphi_{n+1}}{\varphi_n + \varphi_{n+1}} \tag{A-9}$$

In the analysis to determine the PS, the contact of the aggregate between any two consecutive sieves is evaluated. This is done using the percent retained on each of the sieves and the weighted average size of the consecutive sieves. There two different limiting configurations for any two consecutive sieves in the PS as shown in Figure A-20, which are as follows:

- *Densest configuration*: the bigger particle ($\bar{D}_n$) are in their loosest state, and the voids are filled with the next size particle ($\bar{D}_{n+1}$), so the result will be the densest state of the two consecutive sieve sizes.

- *Loosest configuration*: the spacing between a particle of bigger size ($\bar{D}_n$) and its closest neighbor of the same size is equal to the diameter of the smaller spheres ($\bar{D}_{n+1}$).

The corresponding equation for determining the interaction between particles retained on two continuous sieve sizes which takes into account the two limiting configuration is:

$$0.311\bar{D}_n + 0.689\bar{D}_{n+1} \leq D_{avg} \leq 0.703\bar{D}_n + 0.297\bar{D}_{n+1} \qquad \text{(A-10)}$$
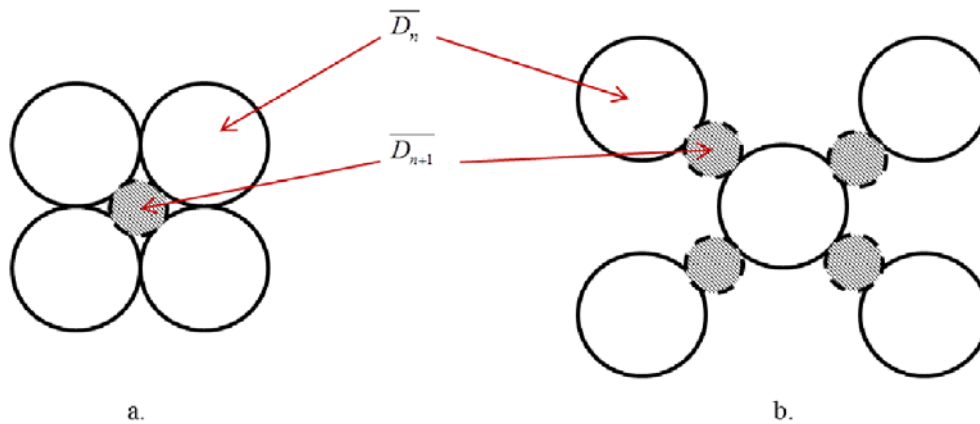
**Figure A-20 - configurations of the Primary Structure: (a) densest (b) loosest
(Lira et al. 2013)**

In a blend of aggregate, the interactive ranges of aggregate should meet the criterion in Equation A-9 The analysis is conducted in a systematic way to check interaction of the material between any two successive sieves until the last sieve size. The obtained interaction range might include several sieve sizes and in some cases these ranges can be interrupted by a non-interactive range. This gives several possible ranges for the primary structure. To select the primary structure among the obtained interactive ranges, the concentration of material at each range is calculated. Then, the range of particle that has the highest concentration will be the Primary Structure.

Rutting data from different sources were used to validate the framework. The proposed framework satisfactory distinguished between good and bad performance of asphalt mixtures when related to permanent deformation.

Packing theory-based framework

Yideti et al. (2013; 2014) presented a packing theory to permanent deformation and resilient modulus of unbound granular materials based on their gradation. Their framework, unlike the previously discussed theories, generalizes the theory to the performance evaluation of unbound granular materials, without the presence of bitumen.

Similar to the previously described frameworks, Yideti et al. (2013) propose a methodology to identify the load carrying aggregate from the aggregate size distribution. Their method takes into account the porosity and contact points between the aggregate

particles in evaluating performance. A modified DF was developed, entitled disruption potential (DP), to investigate the stability nature of load carrying aggregate particles. Finally, the authors demonstrate that the developed framework is related to the mechanical properties of unbound materials: resistance to permanent deformation and resilient modulus.

The basic concept and assumption of the framework is that aggregates of different sizes contribute differently to the load carrying capacity of the granular mix. Fine grained particles fill the gaps between coarse particles and provide stability for the load carrying structure. The interactive range of coarse aggregate particles is called primary structure (PS). A range of grain sizes smaller than the PS is called secondary structure (SS) which resides in between the PS particles and depending on its proportion may provide stability to the load carrying skeleton or in case of excessive amount of SS it will compromise the load carrying capabilities of the PS as shown in Figure A-21. In order to ensure good performing load carrying structure, the porosity limit for PS particles not exceed 50%, assuming the shape of the particles as spherical.
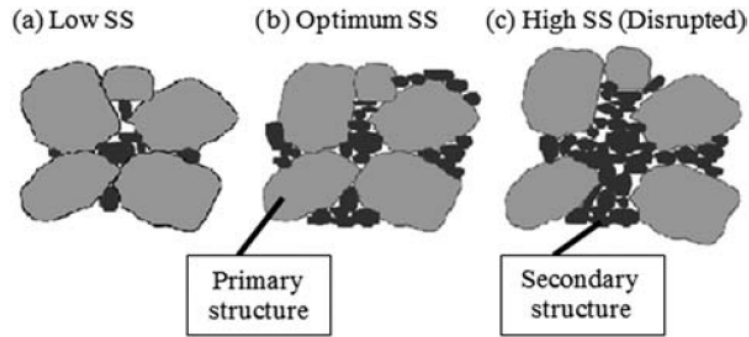
Figure A-21 - Interplay between PS and SS particles (Yideti et al. 2013)

A packing theory was used to identify the interactive PS aggregate particles. Similar to the framework developed by Lira et al (2012) for asphalt mixtures, the particle-to-particle interaction analysis was performed for two consecutive sieve sizes, and the densest and loosest possible packing arrangements in three dimensional space were used (shown in Figure A-20). To ensure stone-to-stone contact between particular sieve size in the PS, the porosity of the particles must not be greater than the simple cubic packing arrangement. Also, the maximum concentration of spheres of two consecutive different particle sizes was assumed to be equivalent to hexagonal/cubic close packing.

As mentioned previously, PS was defined as a range of interactive coarse grain sizes that forms the main load carrying network in unbound granular materials. Secondary structure (SS) is a range of grain sizes smaller than the PS, providing stability to the aggregate skeleton. There are also oversized particles larger than the PS, which are not playing a relevant role in the load carrying system.
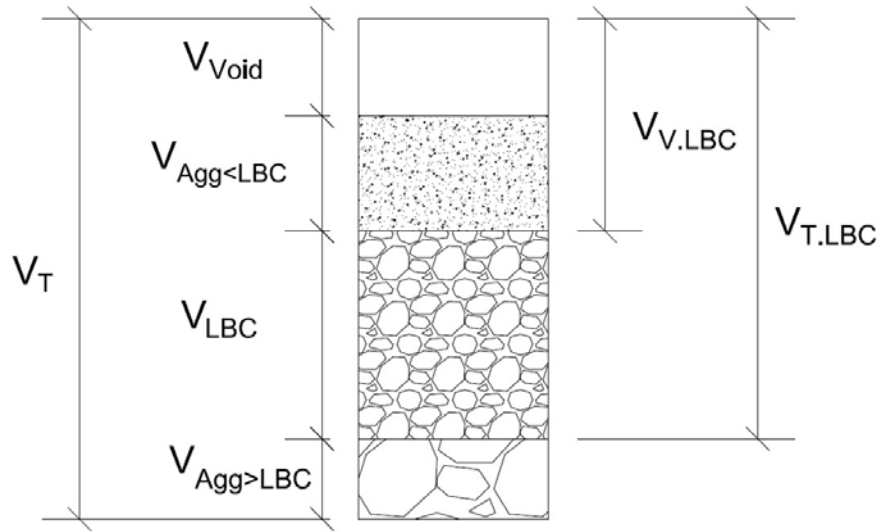
Figure A-22 - Schematic diagram for volumetric composition of unbound granular material

The interaction analysis determines the upper and lower limit of PS particles. This analysis was conducted between two contiguous sieve sizes to be able to interact rather than to have one size to dominate in the mix. Equation A-A-11 defines the analytical upper and lower limits for the interaction between particles on two contiguous sieve sizes.

$$\frac{1.1 \times D_1 D_2}{\sqrt[3]{D_2^3 + 2.36 \times D_1^3}} \le d_{w,avg} \le \frac{1.1 \times D_1 D_2}{\sqrt[3]{2.36 \times D_2^3 + D_1^3}} \qquad (A\text{-}11)$$

Where $d_{w,avg}$ is the maximum void size between the weighted average PS spherical particles ($D_{w,avg}$) in three-dimension simple cubic packing which are defined as follow:

$$d_{w,avg} = 0.732 D_{w,avg} \qquad (A\text{-}12)$$

$$D_{w,avg} = D_1 D_2 \sqrt[3]{\frac{\phi_{1+}\phi_2}{\phi_1 D_2^3 + \phi_1 D_1^3}} \qquad (A\text{-}13)$$

where $d_{w,avg}$ = Weighted average void diameter (particle diameter within PS); $D_{w,avg}$ = weighted average particle diameter; D_1 and D_1 = consecutive sieve sizes; ϕ_1 and ϕ_2 = the percentage retained on the two consecutive sieve sizes

The stability of unbound granular materials can be affected by several factors. In addition to the shape of the grains, grain size distribution, and type of the granular material, porosity of the aggregate and the number of particle to particle contact points have major impacts on the stability of the blend. In this framework, similar to the previous packing theory based frameworks, it is assumed that to ensure the contact of the PS, the PS porosity (n_{PS}) must not exceed 50%. The particle contact point between aggregates in a granular blend can largely influence the bearing capacity of the overall structure. The porosity of spherical particles depends on the arrangement of the spheres. According to Table A-4, the theoretical porosities of spherical particles are shown. In addition, the number of contact points per

particle and their unit cell volume for the four major packing arrangements (Cubic, Orthorhombic, Tetrahedral and Rhombohedral) are calculated.

The PS porosity (n_{PS}) is defined as the fraction of the void volume in the PS over the total volume of the blend (skeleton). The volume of the granular skeleton can be calculated by subtracting the volume of the particles larger than PS from the total volume of the blend. The volume of voids in the PS is everything in the skeleton that is not considered to be part of PS, which includes the volume of SS and the volume of voids in the mix. In the volumetric calculations, a constant dry density and specific gravity of aggregates throughout each sieve size should be assumed.

$$n_{PS} = \frac{V_V^{PS}}{V_T^{PS}} = \frac{V_{agg}^{SS} + V_V}{V_T - V_{agg(>PS)}} \tag{14}$$

Table A-4 - Characteristics of Packing of Uniform Spheres

Packing type	Coordination number	Porosity
Cubic	6	47.64
Orthorhombic	8	39.54
Tetrahedral	10	30.19
Rhombohedral	12	25.95

In the current framework, a relationship between the PS porosity and PS coordination number (cn_{PS}) was developed by fitting the theoretical number of contact points per particle to their corresponding porosities. The theoretical porosities and their corresponding coordination numbers for materials having porosity between 25.95 % and 47.64 % are presented in Table A-4. The developed mathematical relationship and the fitting curve are shown in Equation A-A-15 and Figure A-23, respectively.

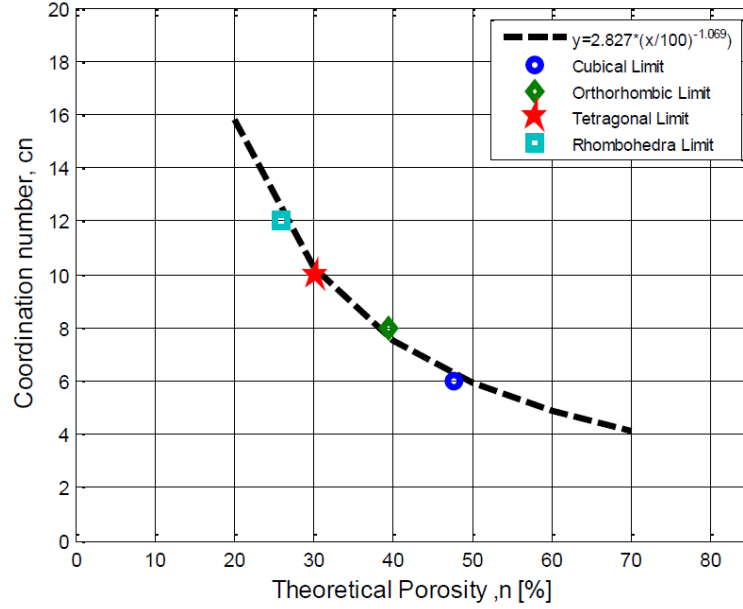$$cn_{PS} = 2.827 \times [\frac{n_{PS}}{100}]^{-1.069} \tag{A-15}$$

Figure A-23 - Relationship between the coordination number and porosity for theoretical porosities (Yideti et al. 2014)

The volume of the SS particles can affect the stability of the PS particles. As shown in Figure A-21, small percentages of the SS particles may fail to provide an adequate support to the PS particles, while too high percentages of SS particles may result in PS particles losing contact with each other, thus reducing load carrying capacity of the materials and eventually the PS aggregates likely to disrupt. The disruption potential (DP) evaluates the ability of SS to disrupt the PS. DP is defined as the ratio of the volume of potentially disruptive SS over the free (available) volume within the PS. The volume of potentially disruptive SS includes the SS particles larger than 0.225 times the smallest grain size of the PS. The Bailey method also used this factor to establish control sieves to separate coarse and fine aggregates. The DP can be obtained for any material regardless of its porosity. Equation A-A-16 mathematically illustrates the DP.

$$DP = \frac{V_{DM}^{SS}}{V_{free}^{PS}} \tag{A-16}$$

where V_{DM}^{SS} is the volume of the disruptive material and V_{free}^{PS} is the free volume within the primary structure.

Evaluation of the framework

As discussed, the authors believed that the porosity and contact points of the load carrying aggregate particles combined with the DP should provide sufficient information to evaluate unbound material resistance to permanent deformation and resilient modulus. In order to validate the framework, the physical and mechanical properties of nineteen unbound granular materials were collected from two different countries (Sweden and USA). Among these, seven materials data were collected from the results of the experiments performed on Swedish originated materials composed of granite (Granite 1-4, GR), sand and gravel (S&G)

and crushed concrete materials (CONC). Sand and gravel materials typically used as a subbase materials but the remaining materials are mainly used ABC. The experimental data for the remaining thirteen USA granular base materials, including three Louisiana State base materials and ten Missouri base materials were used in the model validation. The maximum grain size for the different gradations were between 25 mm and 90 mm. The PS of the collected gradations were defined using Equation A-A-11. Subsequently, the porosity and coordination number of the PS and the DF of the blends were calculated.

It was hypothesized that increasing DP values negatively influences the stone to stone contact between the load carrying particles and leading to higher permanent deformation. However, when there are insufficient fine particles there will not be enough fines material that can support the load carrying particles and eventually the granular material composition becomes less resistant to permanent deformation. Figure A-24 shows the relationship between the normalized permanent strains values with respect to compressive resilient strain in the blends and the DF. Results demonstrate that the DP values are a predictor of the materials' resistance to permanent deformation. Low resistances to permanent deformation were exhibited by granular materials having very low and high DP value whereas blends with the optimum DP values demonstrated lower permanent deformation.

Figure A-25 shows how the volume of SS can affect the permanent deformation. High and low values of SS leads to poor performance in terms of permanent deformation. Good performance is reached with optimum amount of SS to support the PS.
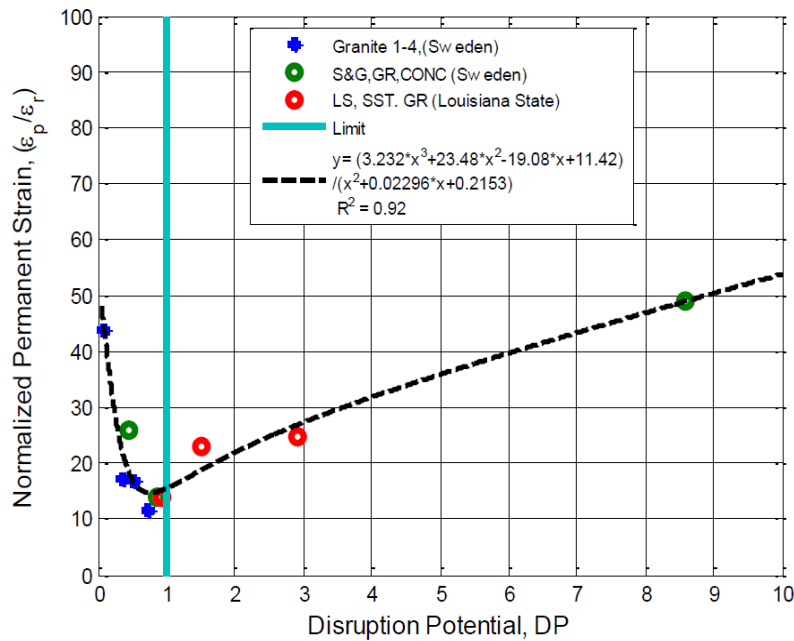

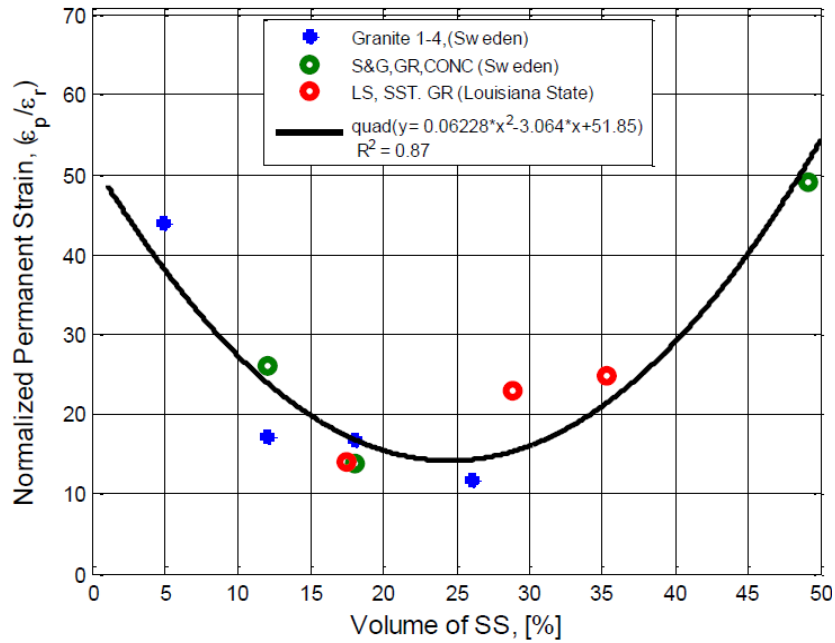**Figure A-24 - Relationship between the disruption potential and permanent deformation (Yideti et al. 2013)**

Figure A-25 - Relationship between the volume of Secondary structure and permanent deformation (Yideti et al. 2013)

The framework can also be used to evaluate the resilient modulus of unbound granular material. The PS porosity and PS coordination number are used to predict the resilient modulus. As discussed, the porosity of the load carrying PS approximately should not be greater than 50% to ensure the contact between aggregates in PS. In Figure A-26, the measured resilient moduli of the materials are plotted versus the PS porosity. The result confirms that increasing the PS porosity resulted in the lower resilient modulus values. In addition, Figure A-27 depicts how change in PS coordinate content is related to resilient modulus. As expected, higher PS coordination numbers correspond to lower PS porosity which leads to higher resilient moduli.
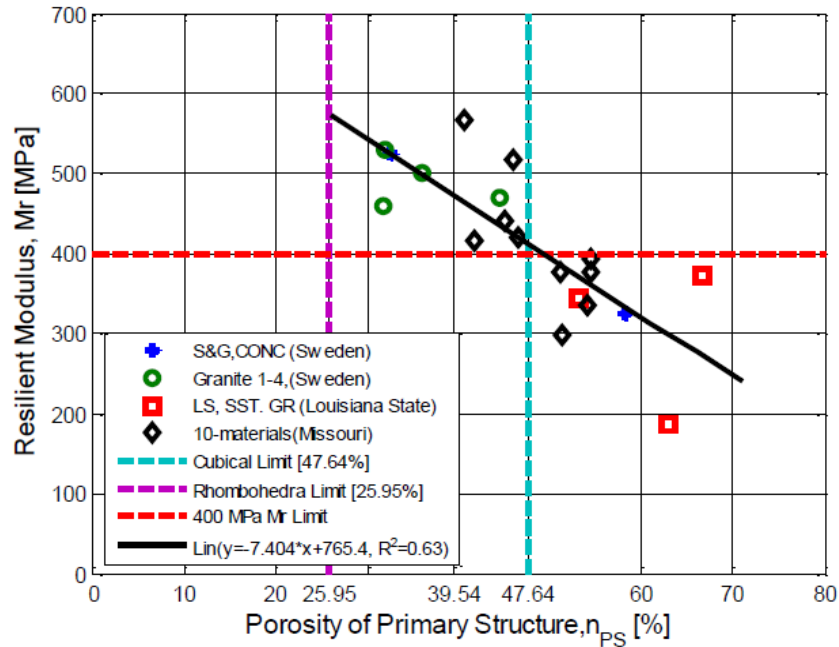
Figure A-26 - Relationship between PS porosity and Resilient Modulus (Yideti et al. 2014)
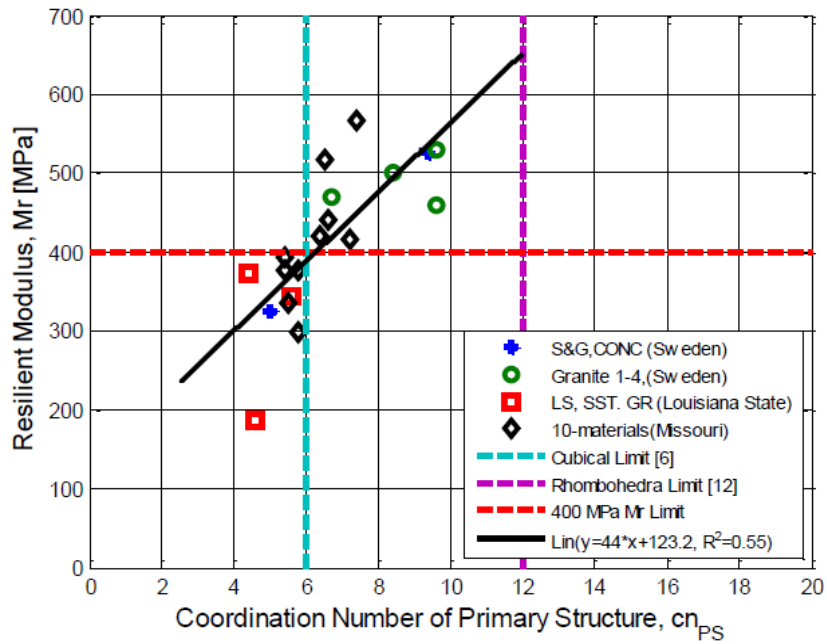
Figure A-27 - Relationship between PS coordination number and M$_R$ (Yideti et al. 2014)

Discrete Element Method (DEM)

The Discrete Element Method (DEM) is a numerical technique for investigating the mechanical behavior of granular materials. DEM treats materials as an assemblage of discrete, distinct particles behaving independently while interacting with each other at

contacts. It has been gaining popularity mainly because it allows simulation of the discontinuous and discrete paths of load transfer between particles to directly link mechanical behavior to the material microstructure. Moreover, it permits monitoring of particle movement in terms of displacements and rotations through the simulation process. DEM modeling will be used in the current project to connect the observed laboratory results with the results from the aggregate packing theories.

Laboratory tests on granular material are used to simulate field conditions in the laboratory. Interpretation of these tests is limited because the results only consist of the material response at specimen boundaries. Often, it is difficult to know why a specimen behaves in a certain manner because of the lack of information at the particle scale. Numerical models of granular media were developed to understand the microscopic mechanisms of granular material behavior. The flexibility of numerical modelling extends to loading configurations, particle sizes, size distributions and physical properties of the particles.

DEM was first introduced by Cundall and Strack (1971) for the analysis of rock-mechanics problems and then applied to soils by Cundall and Strack (1979). It has been proven that the DEM method is a useful and powerful tool that is capable of analyzing discontinuous/fracturing bodies and large deformation systems while capturing the microstructure changes and particle-scale behaviors (e.g., particle rotation and displacement).

Fundamentals of the discrete element method

In the discrete element method, particles are simulated as circular elements in 2D space or spherical elements 3D space. A model consists of arbitrarily shaped particles that displace independent of one another, and interact only at contacts or interfaces between the particles. The interaction of the particles is treated as a dynamic process with states of equilibrium developing whenever the internal forces balance. The contact forces and displacements of a stressed assembly of particles are found by tracing the movements of the individual particles. Bulk movements result from the propagation of displacements through the individual particle system of disturbances caused by specified wall and particle motion and/or body forces. This is a dynamic process in which the speed of propagation depends on the physical properties of the discrete system.

In describing the above dynamic behavior numerically, time steps are taken over which velocities and accelerations are assumed to be constant. The solution scheme is identical to that used by the explicit finite-difference method for continuum analysis. The DEM is based upon the idea that the chosen timestep may be so small that during a single timestep, disturbances cannot propagate from any particle further than its immediate neighbors. Then, at all times, the forces acting on any particle are determined exclusively by its interaction with the particles with which it is in contact. Since the speed at which a disturbance can propagate is a function of the physical properties of the discrete system, the timestep can be chosen to satisfy the above constraint.

The calculations performed in the DEM alternate between the application of Newton's Second Law to individual particles and a force-displacement law at the particle contacts. Newton's Second Law prescribes the motion of a particle resulting from the forces acting on it. The force-displacement law is used to find contact forces from displacements. The calculation cycle is illustrated in Figure A-28.
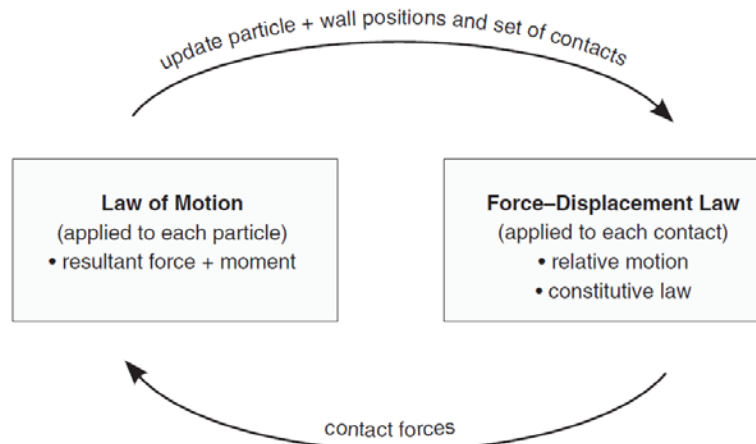
update particle + wall positions and set of contacts

Law of Motion	Force–Displacement Law
(applied to each particle)	(applied to each contact)
• resultant force + moment	• relative motion
	• constitutive law

contact forces

Figure A-28 - Calculation Cycle of DEM (Itasca 2008)

Computer program PFC³ᴰ

DEM modeling will be implemented using PFC³ᴰ-4.0: Particle Flow Code in Three dimensions version 4.0 (Itasca 2008) in this project. The PFC³ᴰ is a popular software to study the behavior of granular materials because of its well-verified performance, excellent documentation, flexibility, and ease of use. The PFC³ᴰ implements a particle-flow model utilizing the following assumptions:

1- The particles are treated as rigid bodies.
2- The walls are straight and rigid and interact only with particles but not with each other.
3- The contacts occur at a point.
4- Rigid particles are allowed to overlap at contacts but the magnitude of the overlap is small relative to particle size (the so-called 'soft contact' approach).

The assumption of particle rigidity is logical since the deformation in a granular assembly results primarily from the sliding and rotation of the particles as rigid bodies and the opening and interlocking at interfaces, and not from individual particle deformation.

The displacements of the particles and the forces at the contacts are found by tracing the movement of every particle in the assembly and the interaction of the particles is treated as a dynamic process. This dynamic behavior is represented by a time stepping algorithm which was discussed earlier. Centered finite-difference scheme is used to calculate the motions of the particles. The critical timestep is estimated on the basis of a multiple mass-spring system by a simplified procedure which can be expressed as:

$$t_{critical} = \begin{cases} \sqrt{m / k^{tran}} & (translational.motion) \\ \sqrt{I / k^{rot}} & (rotational.motion) \end{cases} \quad (A\text{-}17)$$

where m is the mass, k^{tran} is the translation stiffness, I is the moment of inertia, and k^{rot} is the rotational stiffness. The actual timestep used is taken as a fraction of the estimated critical value and this fraction can be specified.

Each particle in the assembly of particles modeled by PFC³ᴰ may have a different mass and stiffness, so various critical time steps may be found for each particle in the assembly by applying Equation A-A-17 separately to each degree of freedom, and assuming that the degrees of freedom are uncoupled. The final critical time step is taken to be the minimum of all critical time steps computed for all degrees of freedom of all particles.

Newton's Second Law and the force-displacement law are the two basic calculations that are performed alternately to each particle and at each contact in each timestep. Newton's second law gives the motions of the particles resulting from the known (and fixed) forces acting on them and the force-displacement law is used to find contact forces from known (and fixed) displacements. This calculation cycle is repeated by a timestepping algorithm, and it is illustrated in Figure A-28.

The contact constitutive model is of great importance in DEM because the overall constitutive behavior of the system is dependent on the constitutive model at each contact. The constitutive model of each contact consists of three parts: a stiffness model, a slip model, and a bonding model. The stiffness model including the linear contact model and the Hertz-Mindlin contact model is used to define a relation between the contact force and the relative displacement in both normal and shear directions. The slip model defines the relation between shear and normal contact forces and allows slip to occur by limiting the shear force. Slip occurs when the shear stress at the contact is greater than the maximum allowable shear contact force which is the product of the friction coefficient and the normal contact force at the contact. Particles can be bonded together at the contacts and the bonding model is used to limit the total normal and shear forces that the contact can carry by limiting the bond strength. Two bonding models, the contact-bond model which can only transit a force and the parallel-bond model which can transit both a force and a moment, can be used. Some alternative contact models such as simple viscoelastic model, simple ductile model, and displacement-softening model can also be used to simulate more complex contact behaviors.
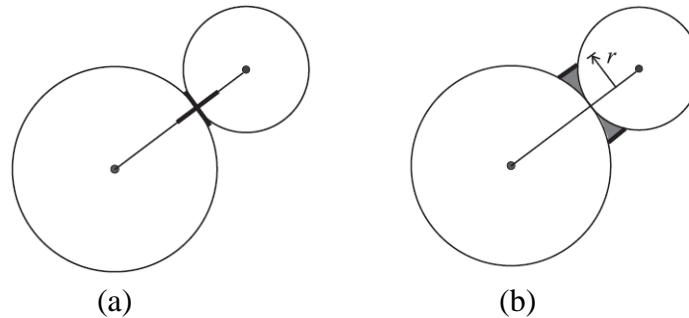

(a)   (b)

Figure A-29 - Bonding logic in PFC: (a) Contact bond – (b) Parallel bond

In order to simulate real materials using PFC^{3D}, properties of the particles comprising the sample of interest must be specified. In continuum models, such as finite-element or finite-difference, these properties can be derived directly from measurements on laboratory samples. However, PFC^{3D} works at a more basic level. It "synthesizes" material behavior from the micro-components (equivalent grains) that make up the material. If the properties and geometry of these micro-components are known, then they can be used directly as input to PFC^{3D}. However, simulating the response of a solid, such as rock, the properties of the microscopic constituents may be unknown. In this case, "inverse modeling" is used (i.e., perform a number of tests on samples with assumed properties, and compare the results with the desired response of the real intact material). When a match has been found, the corresponding set of properties may be used in the full simulation.

Aggregate Imaging Measurement System

Physical properties affect ABC performance. Studies have shown that surface texture, angularity, and particle form (Meininger and Nichols 1990) are key characteristics that affect performance of pavements. These properties can be tested by traditional methods such as roughness (texture), roundness of corners (angularity), and aspect ratio (flat and elongated) (Kuo 2000). These methods have been shown to be difficult, time-consuming, and subjection (Gates, et al. 2011). Thus, by utilizing image analysis, data can be obtained that is consistent, quick, and efficient.

The Aggregate Imaging Measurement System (AIMS) is a relatively new device used to characterize the geometric properties of aggregate particles. It is a simple, quick and a non-destructive procedure. It can measure physical properties such as texture, surface angularity, and particle form. Through its implementation, aggregates can be classified using an objective and automated procedure.

History

The first AIMS device was developed as a prototype system to investigate the use of digital image analysis to classify aggregate physical characteristics (Gates, et al. 2011). The original design focused on the development and not on operational ease of use or cost. Therefore, the original AIMS system was ultimately expensive and difficult to operate. As a result, the AIMS2 was designed to meet project and industry standards. The AIMS2 is affordable, easy to use, and effective at classifying aggregate particle geometric characteristics.

The original system utilized a variable magnification microscope and camera system with two different lighting modes in order to image aggregate particles. One of the light modes creates a backlit image to give the particle's silhouette. Shape characteristics such as angularity and cross-sectional form can be obtained from this silhouette. The second lighting mode, a top light, helps create a high-magnification, gray-scale image of the particle surface. From the position of the focal plane in the texture image, the height and a three-dimensional form of the particle is attained. The original system utilized an x-y-z gantry system which proved to be expensive and difficult to align (Gates et al. 2011).

Problems arose in the original system not only from the cost and operational ease, but also design. Multiple interconnections between the system (Figure A-30) made set up and troubleshooting a challenge. There was also no component for omitting ambient laboratory lighting from altering the results. The original system's lighting schemes were found to be difficult to control and hence led to non-uniformity in results.

Figure A-30 - AIMS1 equipment and set-up (Gates et al. 2011).

The new system has been upgraded significantly to address the problems with the original system. A turntable is used for placing aggregate particles to be imaged, which decreases the size requirements of the backlight area. Particles can be loaded directly on the turntable in different slots instead of on specific points within a grid which is simpler and accommodates a greater number of aggregate particles. The tray system also makes cleaning easier. Fine particles can be placed on colored trays to see them with sufficient contrast. A better camera was employed as well as LED technology for the lighting. The operator interface was streamlined to address user difficulty. The new AIMS2 system is shown in Figure A-31. All of these upgrades have made the AIMS2 a viable option for automated determination of aggregate particle geometric properties in practice which can further improve specifications in asphalt pavements.

Figure A-31 - AIMS2 equipment and set-up (Gates et al. 2011)

Properties Characterized and Traditional Methods

The AIMS2 measures aggregate particle shape, surface texture, and particle angularity. Figure A-32 depicts the geometric characteristics used to describe an aggregate particle. These properties are important to the performance of the aggregates in asphalt base course in pavement. The aggregate base course provides structural stability to the layers above the base course.
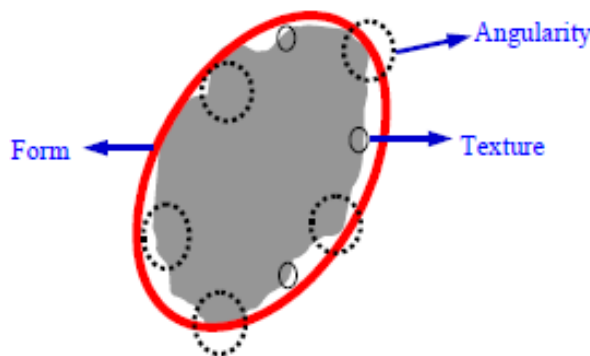
Figure A-32 - Physical characteristics of aggregate particles (Little et al. 2003)

Particle Form

The variations in the proportions of an aggregate particle is considered the particle form. The particle form of coarse aggregates is often examined to determine the quantity of flat or elongated particles. These particles can affect compaction and can break under compaction, (which can change the gradation of the aggregate) (Little, et al. 2003). There is an ASTM standard test to determine the proportion of flat and elongated coarse aggregate particles: STM D 4791: Flat Particles, Elongated Particles, or Flat and Elongated Particles in Coarse Aggregates (Saeed, et al. 2001).

ASTM D 4791 Method A classifies the particles into four groups: (1) flat particles, (2) elongated particles, (3) particles that meet the criteria of both groups, and (4) particles that are neither flat nor elongated that do not meet the criteria of either group (ASTM D 4791, 2010). A proportional caliper device is used to examine a representative set of coarse aggregate particles. For the flat particle test, the caliper's larger opening is set equal to the maximum particle width and then the particle is deemed flat if the maximum thickness can be placed in the smaller opening. For the elongated particle test, the larger opening of the caliper is set to the maximum particle length and then the particle is deemed elongated if the maximum width can be placed through the smaller opening of the caliper (ASTM D 4791, 2010). Method B has the particles placed in only two groups: (1) flat and elongated or (2) not flat and elongated. The test has the larger caliper opening set to the maximum particle length and the particle is deemed flat and elongated if the maximum thickness can be placed through the smaller opening of the caliper. Once the particles have been classified by either method, the fraction of the sample that is considered flat and elongated is determined.
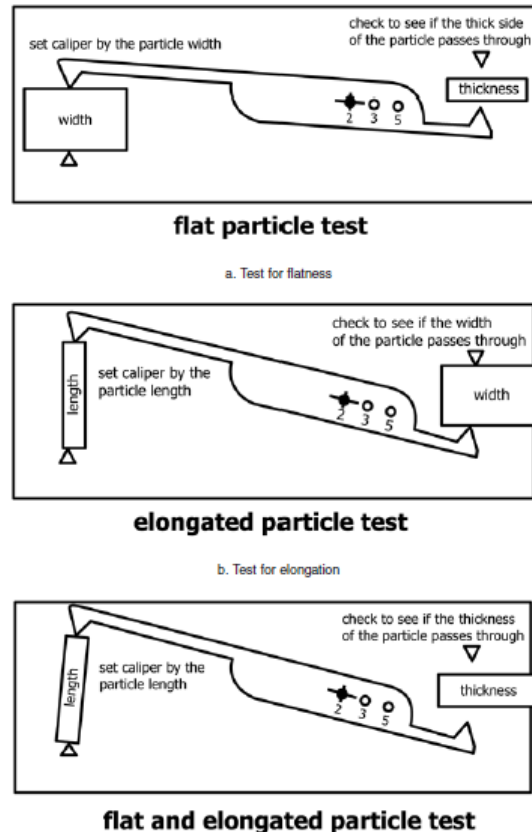
Figure A-33 - Demonstration of Method A and Method B for Particle Form (ASTM D 4791 2010)

Surface Texture

Surface texture is related to an aggregate particle's surface irregularity at a microscopic scale. Surface texture does not affect the overall particle shape but does affect the friction between particles. In an NCHRP synthesis of "Practices of Unbound Aggregate Pavement Layers" there is indication that increasing particle roughness, (along with particle angularity), increases the resilient modulus and at the same time decreases Poisson's ratio (Tutumluer, 2013). In hot-mix asphalt, a rougher texture increases strength and requires more asphalt to achieve workability compared to smoother aggregates. There is also a higher void content in compacted aggregates with a rougher texture than smooth which provides more space for asphalt cement (Little, et al. 2003). Without proper surface texture in the base course, rutting and fatigue cracking can occur (Saeed, et al. 2001).

Surface texture is difficult to measure because it relates to a microscopic level. Janoo (1998) reports that surface texture can be indirectly evaluated by coating the surface of a sawed aggregate surface with asphalt and then scraping to the surface of the aggregate. The quantity of leftover asphalt on the particle can be used as an indicator of surface texture.

Angularity

Angularity is the differences in the corners of an aggregate particle. Angularity is critical to the performance of the unbound pavement layer because angularity drive interlocking between particles. Interlocking of particles increases resistance to rutting and fatigue (Saeed, et al. 2001). Angularity increases the contact points between aggregate

particles which increases resilient modulus and distributes loads better than less angular particles (Tutumluer, 2013). There are two standards to quantify the angularity of an aggregate particle: AASHTO T 335: Determining the Percentage of Fractured Particles in Coarse Aggregates and AASHTO T 304: Un-compacted Void Content of Fine Aggregates.

AASHTO T 335 requires visual inspection of a representative set of coarse aggregate particles. Coarse aggregates are inspected and separated into the three categories: fractured particles meeting the criteria, particles not meeting the criteria, and borderline particles. Criteria are based on a minimum number of fractured faces (AASHTO T 335, 2012). A fractured face is an angular, rough, or broken surface of the particle obtained by crushing or another mechanism. A particle is considered a fractured face when one-half or more of the projected area is fractured with sharp and well-defined edges (AASHTO T 335, 2012). Once the aggregate particles have been separated into the three categories, the dry mass is determined for each to the nearest 0.1 g. If the borderline category is greater than 15% of the total mass of the sample, the sorting procedure is repeated until it is less than 15%. AASHTO T 304 involves using a calibrated container (100 mL) that is filled with fine aggregate and allows the sample to flow through a funnel from a fixed height in the container. The mass is determined and the un-compacted void content is the difference between the volume of the container and the absolute volume of the fine aggregate obtained in the container. At least two replicates are completed and the results are averaged. A higher void content indicates a higher angularity, rougher surface texture, less roundness, or a combination of the three factors. These inferences are only applied to Methods A and B in the standard (AASHTO T 304, 2015).

AIMS2 Test Procedure

The AIMS2 employs the use of algorithms to analyze the particles being studied. The AIMS2 uses a variable magnification camera system and two lighting configurations to capture aggregate particles. The device also utilizes a turntable within a closed box system. The device is simple to use in that particles are placed in the chamber on the tray and the system then automatically obtains the images needed for analysis. Method A analyzes coarse aggregates using a 0.25X objective lens and camera to obtain images. Method B is used for fine aggregate angularity and a 0.5X objective lens is utilized for capturing images. A few grams of fine aggregate particles are uniformly spread out so that individual particles are not touching. Backlighting is used to obtain the images (Masad, 2005).

Surface Texture

Surface texture analysis is done by wavelet analysis and used to define a texture index. A short-duration basis function separates fine variations in texture while long-duration functions provide coarse details of texture. Wavelet analysis include short, high-frequency basis functions and long, low-frequency basis functions. This produces images that can be blurred to remove the fine details while retaining the coarse details and the remaining images still have the data "lost" in the blurred image analysis. Through wavelet analysis, detail coefficients are obtained and a texture index number is calculated (Masad, 2005). Equation A-17 shows how the texture index is calculated where n is the level of decomposition, and *i* takes a value of 1, 2 or 3 for the direction of texture and *j* is the wavelet coefficient.

$$Texture\ Index = \frac{1}{3N}\sum_{i=1}^{3}\sum_{j=1}^{N}(D_{i,j}(x,y))^2 \qquad\qquad \text{(A-18)}$$

Angularity

  Angularity is determined in the AIMS2 using the gradient method. Gradient vectors are calculated at each edge-point using a Sobel mask. A Sobel mask operates at each point on the edge and the surrounding eight points. The angle or orientation numbers (theta) of the edge-points and the magnitude of the difference in these numbers for neighboring points on the edge are used to describe how sharp the corner is. This corresponds to large changes in theta. All the angularity values for the boundary points are measured. The sum of these values around the edge makes up the angularity index. Equation A-18 defines how the Angularity Index is calculated. N is the total number of points on the edge of the particle and i is the ith point on the edge of the particle. The number three is from the step-size of the particular example but represents the angle of orientation of every third point on the boundary of the aggregate (Masad, 2005).

$$Angularity\ Index\ (Gradient\ Method) = \sum_{i=1}^{N-3}|\theta_i - \theta_{i+3}| \qquad\qquad \text{(A\_19)}$$

Particle Form

  Particle form is determined by the measurement of the three dimensions of the particle: the longest dimension (d_L), the intermediate dimension (d_I), and the shortest dimension (d_S). The form is defined in terms of sphericity of these three dimensions (Equation A-19).

$$Sphericity = \sqrt{\frac{d_S d_I}{d_L^2}} \qquad\qquad \text{(A-20)}$$

  AIMS2 provides a chart to determine flat and elongated particles as sphericity alone cannot be used. The chart is shown in Figure A-34 (Masad 2005).
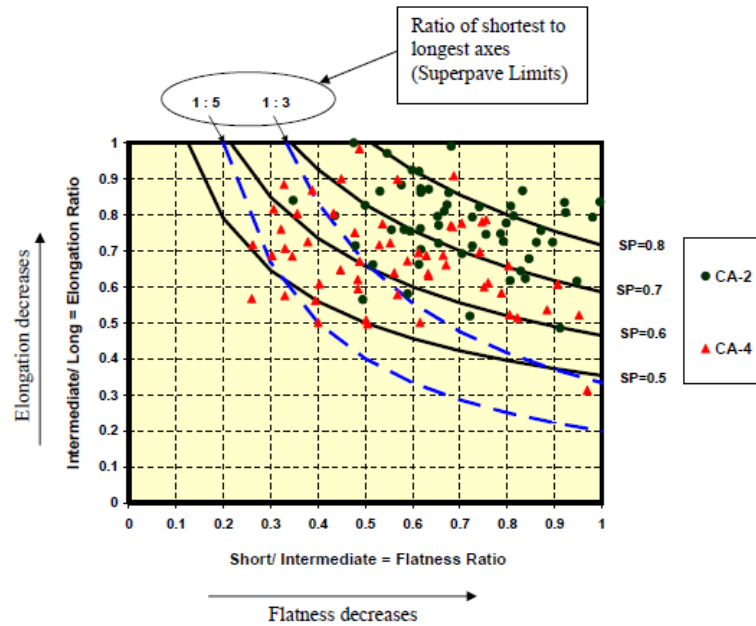
Figure A-34 - Chart for identifying flat, elongated or flat and elongated particles (Masad 2005)

Applications

The AIMS2 has the potential to allow comprehensive and efficient characterization of aggregate geometric properties. Two AASHTO Standards have been proposed: (1) PP64-10: Determining Aggregate Source Shape Values from Digital Image Analysis Shape Properties and (2) TP81-10: Determining Aggregate Shape Properties by Means of Digital Analysis. It was shown in studies done by Little et al. and Saeed, et al. that many of the geometric characteristics quantified affect the performance of asphalt concrete and unbound pavement layers (Little et al. 2003, Saeed et al. 2001).

Example Data

Example AIMS2 data obtained from Pine Instruments are shown in Figure A-35 to Figure A-37. Figure A-35 for three aggregate sources: river gravel, limestone, and crushed granite. The surface texture is characterized between zero and 10,000. It can be seen that the gravel has the lowest texture measurements with the crushed granite having the highest. Figure A-36 shows the angularity chart for the same three materials as in Figure A-35. The crushed granite has the highest angularity which makes sense because crushed aggregate usually has more angular surface unlike river gravel. Finally, Figure A-37 is a representation of particle form characterization and presents the 3D data in multiple formats (Pine Instruments, Inc.) Most samples in the particle shape fall within the ratio of 1:3 for a less flat and less elongated particles. This goes to show that you cannot rely on one physical characteristic alone. Collectively the properties of an aggregate should be taken into account as a summation of all the properties.
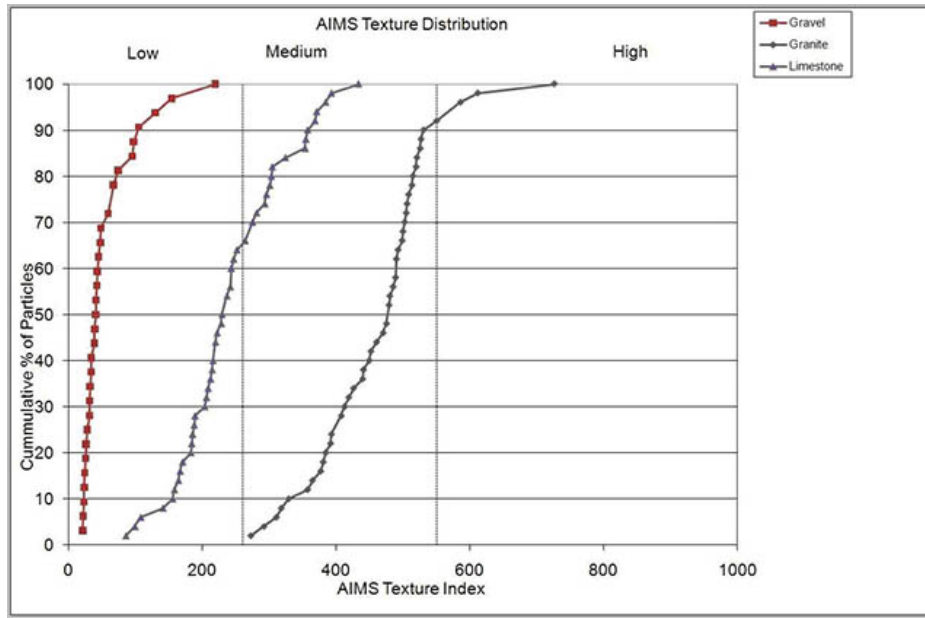
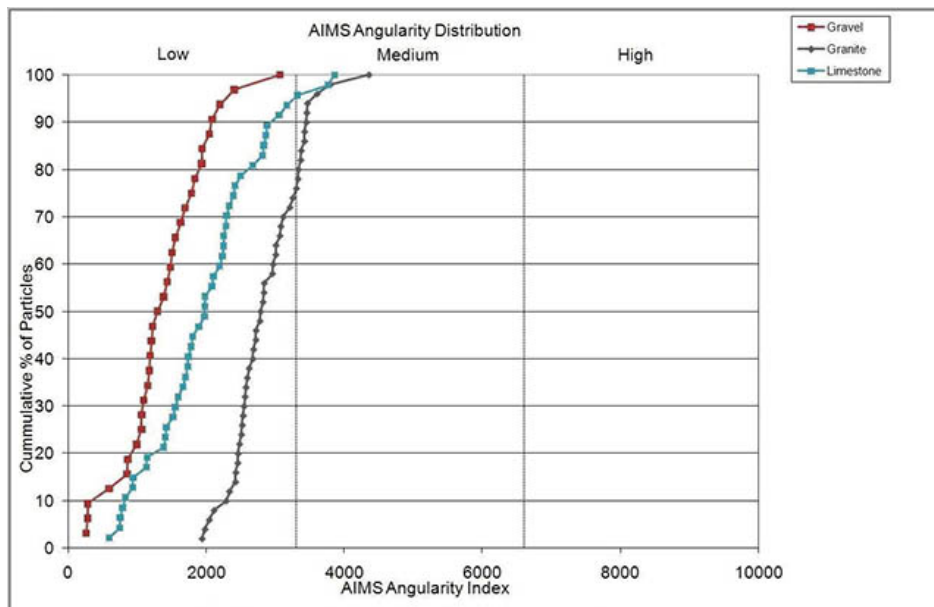**Figure A-35 - Aggregate surface texture example data (Pine Instruments, Inc.)**

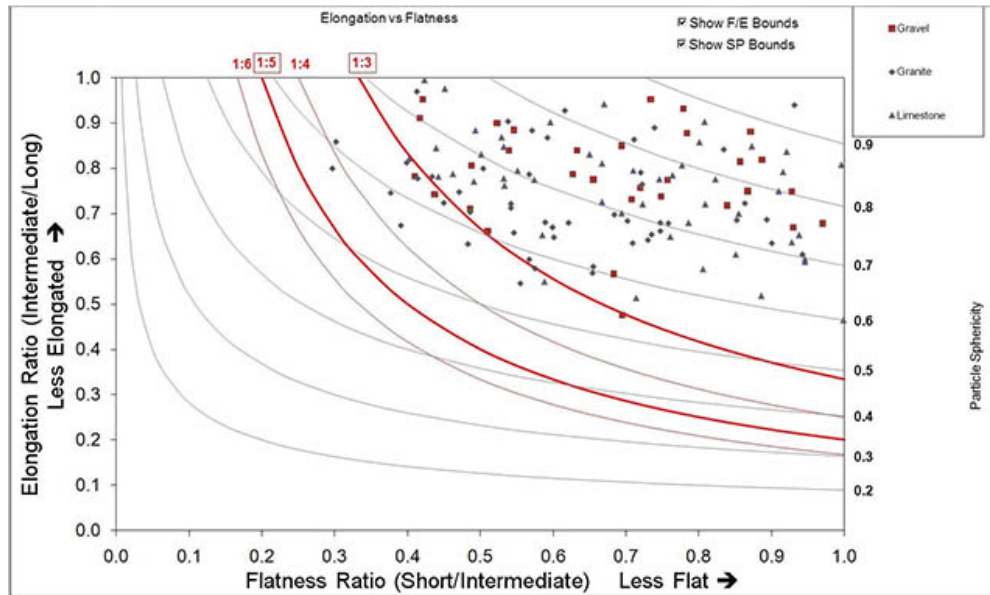**Figure A-36 - Aggregate angularity example data (Pine Instruments, Inc.)**

Figure A-37 - Particle shape example data (Pine Instruments, Inc)

Digital Imaging Analysis

Introduction and Purpose

Digital Imaging Analysis (DIA) is a technique that can be used to visualize aggregate packing characteristics. An ABC's behavior is largely determined by its fabric and structure. The aggregate fabric is considered the arrangement of the particles, particle groups, and pore spaces in the aggregate specimen (Yang 2002). The aggregate structure is considered the fabric, composition, and inter-particle forces combined (Yang 2002). The geometric layout and the physical properties of the aggregate particles is important as it influences the loading resistance of the aggregate base course (Kuo 2000). The aggregate skeleton is formed by the interconnected particles in the loading direction. Without proper interconnection, the load will not be transferred effectively, resulting in deformation. During loading, contact forces are formed between particles and if the resistance to shear is lower than the forces applied, permanent deformation can occur. The packing characteristics of the ABC will be influenced by the gradation and geometric characteristics of the aggregate (Yideti 2014).

The DIA procedure uses a two-dimensional surface to visualize layout of aggregate particles in a compacted aggregate sample. The information obtained includes the number of contacts among particles within the skeleton, the orientation of the contacts, the length of the contacts, and the particle orientation and distribution.

Methods

Various methods exist within the framework of digital imaging analysis. Methods can either be destructive or non-destructive. The non-destructive method utilizes X-ray tomography (Sefidmazgi 2011). The destructive method, the one that will be used in this research, will involve cutting the specimen to display the internal structure of the unbound material. The main outcomes will be aggregate orientation, segregation, contact points, and air void distribution (Coenen 2011).

There are three methods that can be classified as automated, semi-automated, and manual to describe the process of processing the images. Automated processing uses pre-written algorithms with limited pre-processing of inputs of the mixture characteristics. Semi-automated methods requires the user to change the numerical values of filters and operators that are applied by pre-written algorithms. Finally, manual methods usually require the user to identify the perimeter of each coarse aggregate particle and changing the color intensity of individual pixels to differentiate between each phase (Coenen 2011).

Procedure

For analysis of aggregate particle packing, digital image analysis is generally conducted on a physically cut triaxial sample. To allow slicing of a sample without destroying the particle structure, the sample must first be impregnated with resin to create a stiff mold. Yang (2002) and Evans (2005) provided detailed descriptions of a two-step impregnation method. The overall procedure is depicted in Figure A-38 Yang (2002). The general steps of the two-step method are as follows:

1. Flush the aggregates with a dilute solution of glue (e.g., Elmer's Carpenter Glue was used) under a small vacuum. This draws the solution from the bottom to the top of the sample where excess glue solution is emptied into a waste container. (Figure A-39)
2. Once the container is ½-1 the pore volume of solution, the release the vacuum to allow excess glue to drain from the pores.
3. Reactivate vacuum to push desiccated air through the pores. Monitor the relative humidity from the top (Figure A-40). If the relative humidity is above 40% the specimen is not fully cured.
4. Once the relative humidity is below 40% the glue has cured. This drying process will take anywhere from 1-7 days depending on the initial moisture condition and the total volume of the specimen.
5. Apply vacuum to the top and bottom plates of the sample and release the confining stress from the cell.
6. Impregnate the sample with epoxy resin. Before impregnation, the sample is cut from the triaxial set up. The sample membrane is removed. The specimen is placed in a shallow basin, and resin is slowly added until it is filled up. It cures for 24 hours. (Yang, 2002, Evans, 2005).
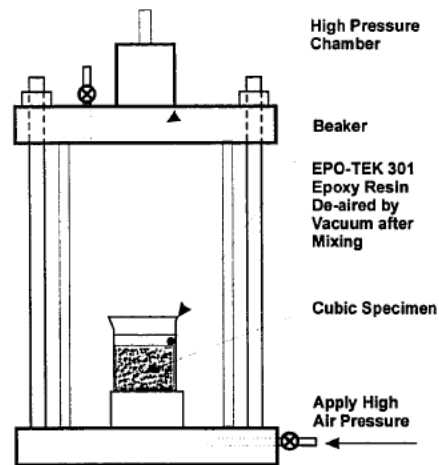7. Samples are cut, ground, and polished.
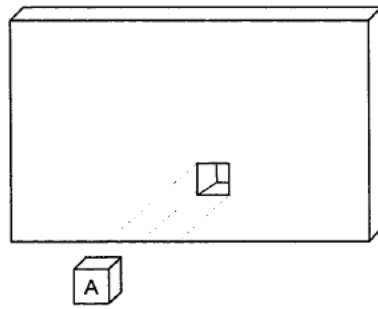
Step 1: Extract a (or several) 2in. Cubic Specimen(s) from Preselected Location(s) in a Sandblow Specimen preserved by Elmer Glue
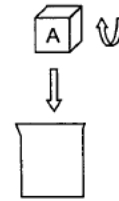
Step2: Rotate the Cubic Specimen 90° to Let the Front Side (A) of the Cube to Face Up and Put it into a Disposable Beaker
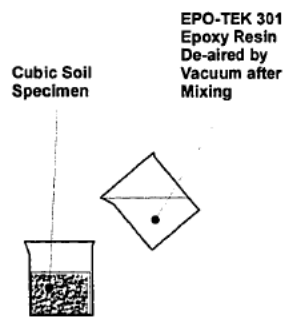
Step 3: Pour De-aired Epoxy Resin into the Beaker Carefully

Step 4: Move the Breaker to a High Pressure Chamber and Apply High Pressure to Reduce the Size of Air Bubbles
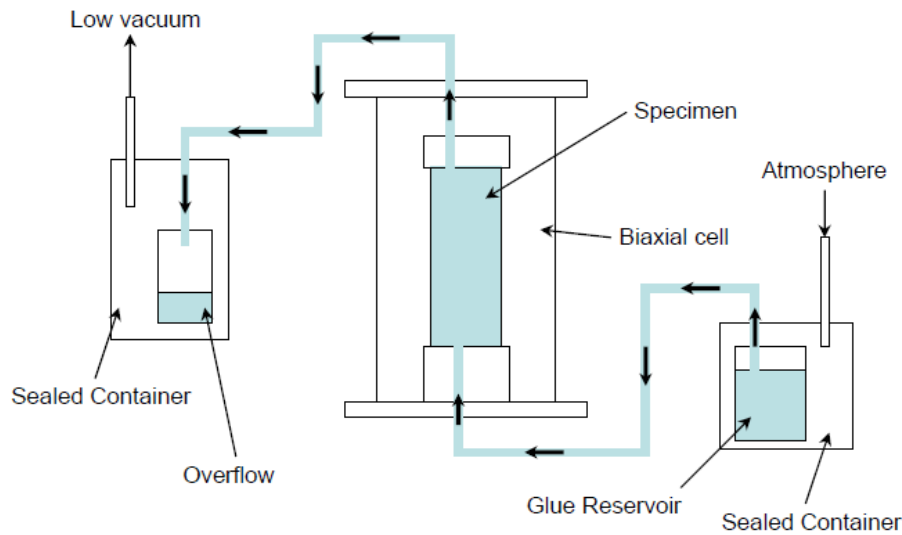
Figure A-38 - Two-step impregnation procedure done by Yang (2002).

Figure A-39 - Glue impregnation process done by Evans (2005)
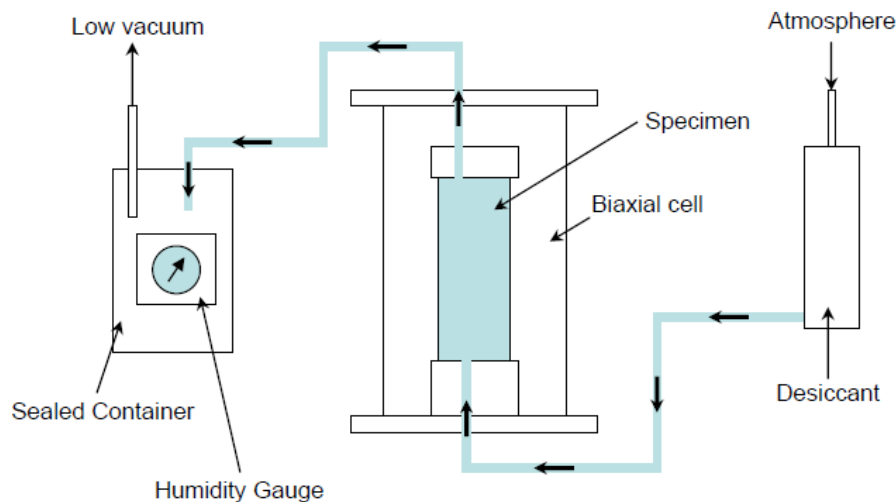
Figure A-40 - Desiccation process schematic (Evans 2005)

After the sample is prepared, images can be taken and processed. During processing, the image is converted into gray scale due to difference in color intensity of the phases (resin and aggregate). Once converted to gray scale, it will be converted to black and white to allow isolation of individual aggregate particles. To convert to black and white the gray scale intensity of the pixels of the image are categorized. The higher intensity pixels are considered aggregates. During processing, the images used should be from the middle as outside edges can provide erroneous results.

Certain basic measurements are obtained for each aggregate particle: area, perimeter, ferret diameters, and coordinates. In addition to those measurements important fabric quantities are: the number of aggregate contact points, the contact length/area, the normal to contact plane orientation, and the stress paths within the skeleton (Sefidmazgi 2011).

In the image analysis, the area is considered the sum of the pixels within the aggregate boundary. The perimeter is the sum of the pixels on the aggregate boundary (Kuo 2000). The ferret diameter is determined by Equation A-20.

$$Ferret\ Diameter = (4 * area/\pi)^{0.5} \qquad (A-21)$$

The number of contacts that an aggregate sample contains as connections facilitate load transfer (Sefidmazgi 2011). The more contacts an aggregate has, the better the stress distribution will be for the base course. However, the contact length must also be taken into account because it impacts the effectiveness of the contact point. The greater the contact length, the more friction and interlocking of the aggregates. The normal to contact plane orientation is demonstrated in Figure A-41. If the normal to contact plane orientation is closer to the loading direction, the better the sample will be better at resisting deformation. Finally, the overall stress path within the aggregate skeleton is important to the performance of the aggregate base course. The stress path is important because if only a few aggregate particles are carrying the load, the structure will be weaker. The aggregate skeleton is composed of the aggregates connected in the loading direction (Sefidmazgi 2011). This is illustrated in Figure A-42 as the aggregates not part of the skeleton, the ones that only have one contact point or aggregates not connected to the top and bottom of the sample, are neglected (Sefidmazgi 2011).
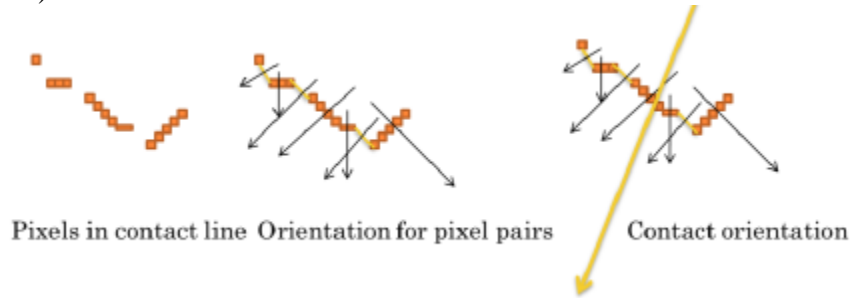

Pixels in contact line Orientation for pixel pairs   Contact orientation

Figure A-41 - Demonstration of the normal to contact particle orientation (Sefidmazgi 2011)
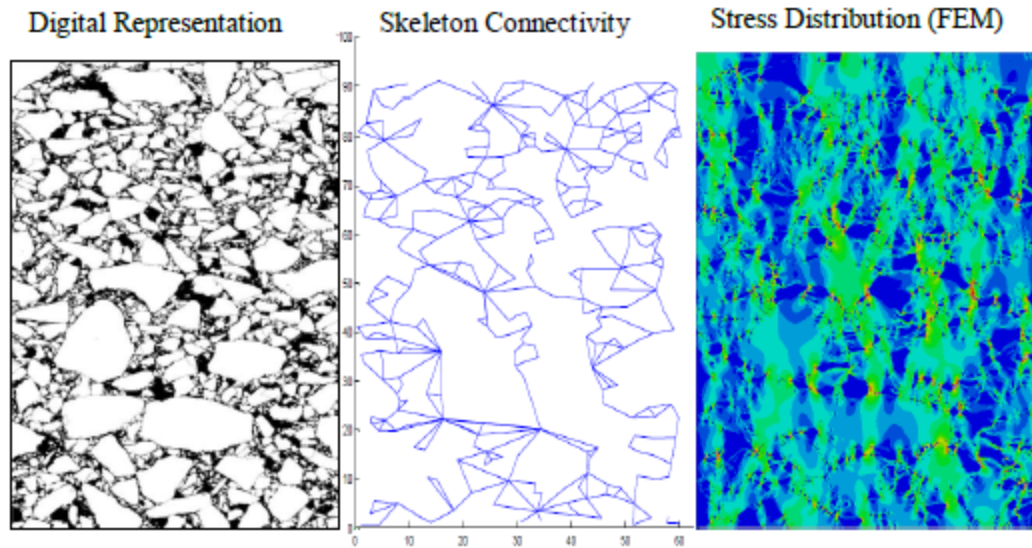
Figure A-42 - The aggregate skeleton with non-skeleton aggregates being neglected (Sefidmazgi 2011).

Previous Applications of Digital Imaging Analysis

Previous research has applied DIA to study aggregate structure in sands and in asphalt mixtures. However, these techniques can also be applied to ABC. The internal structure is crucial as it determines the ability of the aggregate to resist deformation upon loading.

Asphalt Mixtures

Asphalt concrete is a mixture of asphalt binder, air, and aggregates (fine and course). Studies have shown that the spatial distribution of aggregate particles is an important factor in the rutting performance of asphalt mixtures (Coenen 2011). Sefidmazgi (2011) found that rutting performance of asphalt mixtures is dependent upon the internal structure and that digital imaging can be used to effectively quantify that structure. The number of aggregate contact points has a key influence on the load distribution to prevent permanent deformation.

Coenen (2011) found that despite asphalt mixtures having the same aggregate gradation and compaction effort, aggregate structure still varied greatly. The variation was found to differ with binder types indicating that binder type has a significant impact on aggregate structure within the mixture. The binder's lubricity plays a controlling part in the initial aggregate structure formation instead of viscosity (Sefidmazgi 2011).

Sands

In sands, the digital imaging process allows for analyzing internal structure and pore space. Yang (2002) used the two step impregnation procedure to look at sand triaxial samples. This was necessary as the first bonding was weaker but reduced the shrinkage during the epoxy impregnation. Also, to impregnate the sample with resin without damaging the equipment, the glue allowed for smaller specimens to be extracted. This reduces the amount of resin needed, thus, the cost (Yang 2002). Aggregate base course will be easier to impregnate than sand due to the larger size of particles and the fact that samples will be tested without prior loading to failure.

Application to Aggregate Base Course

This research work will focus on aggregate base course and quantifying the packing structure through digital imaging analysis. Four items will be evaluated: (1) number of contacts between particles in the aggregate skeleton, (2) orientation of the particles, (3) length of the contacts, and (4) particle orientation and distribution. The impregnation procedure developed for sands will be adapted to ABC to allow for obtaining specimens. Impregnated specimens will be sliced and imaged using a digital scanner.

Summary

Gradation alone is insufficient to adequately capture the sensitivity of different ABC materials' mechanical properties, including stress and moisture sensitivity. Incorporating physical characteristics of the ABC (e.g., angularity, shape, and texture) and aggregate packing theory into the material specification will better link the constituent material properties to mechanical behavior of ABC.

References from Literature Review

AASHTO T 304. Un-compacted Void Content of Fine Aggregates, *American Association of State Highway and Transportation Officials*.

AASHTO T 335. Determining the Percentage of Fractured Particles in Coarse Aggregates, *American Association of State Highway and Transportation Officials*.

ASTM D 4791. Standard Method of Test for Flat Particles, Elongated Particles, or Flat and Elongated Particles in Coarse Aggregate, *ASTM International*.

Barksdale, R. D., and Itani, S. Y. (1989). Influence of aggregate shape on base behavior. *Transportation Research Record* (1227).

Cundall, P. A. (1971). The measurement and analysis of accelerations in rock slopes. Imperial College London (University of London).

Cundall, P. A., and Strack, O. D. (1979). A discrete numerical model for granular assemblies. *Geotechnique*, 29(1), 47-65.

Cunningham, C. N., Evans, T. M., and Tayebali, A. A. (2013). Gradation effects on the mechanical response of crushed stone aggregate. *International Journal of Pavement Engineering*, 14(3), 231-241.

Daniel, J. S., and Rivera, F. (2009). Application of the Bailey Method to New Hampshire Asphalt Mixtures.

Dawson, A., Thom, N., and Paute, J. (1996). Mechanical characteristics of unbound granular materials as a function of condition. *Gomes Correia, Balkema, Rotterdam*, 35-44.

Guarin, A., Roque, R., Kim, S., and Sirin, O. (2013). Disruption factor of asphalt mixtures. *International Journal of Pavement Engineering*, 14(5), 472-485.

Heydinger, A., Xie, Q., Randolph, B., and Gupta, J. (1996). Analysis of resilient modulus of dense-and open-graded aggregates. *Transportation Research Record: Journal of the Transportation Research Board*(1547), 1-6.

Hicks, R. G., and Monismith, C. L. (1971). Factors influencing the resilient response of granular materials. *Highway research record* (345).

Itasca (2008). PFC-2D: Particle Flow Code in Tree Dimensions. Itasca Consulting Group Inc.

Jorenby, B. N., and Hicks, R. G. (1986). *Base course contamination limits*.

Kamal, M., Dawson, A., Farouki, O., Hughes, D., and Sha'at, A. (1993). Field and Laboratory Evaluation of the Mechanical Behavior of Unbound Granular Materials in Pavements. *Transportation Research Record*, 88-88.

Kim, S. (2006). Identification and Assessment of the Dominant Aggregate Size Range of Asphalt Mixture. University of Florida.

Kim, S., Roque, R., Guarin, A., and Birgisson, B. (2006). Identification and Assessment of the Dominant Aggregate Size Range (DASR) of Asphalt Mixture (With Discussion). *Journal of the Association of Asphalt Paving Technologists*, 75.

Kolisoja, P. (1997). Resilient deformation characteristics of granular materials. Tampere University of Technology.

Lekarp, F., Isacsson, U., and Dawson, A. (2000). State of the art. I: Resilient response of unbound aggregates. *Journal of transportation engineering*, 126(1), 66-75.

Lira, B., Jelagin, D., and Birgisson, B. (2013). Gradation-based framework for asphalt mixture. *Materials and structures*, 46(8), 1401-1414.

Mishra, D., Tutumluer, E., and Butt, A. (2010). Quantifying effects of particle shape and type and amount of fines on unbound aggregate performance through controlled gradation. *Transportation Research Record: Journal of the Transportation Research Board*(2167), 61-71.

Rada, G., and Witczak, M. W. (1981). Comprehensive evaluation of laboratory resilient moduli results for granular material.

Rada, G., and Witczak, M. W. (1982). Material layer coefficients of unbound granular materials from resilient modulus.

Saeed, A., Hall Jr, J., and Barker, W. (2001). Performance-related tests of aggregates for use in unbound pavement layers.

Santamarina, J. C. (2003). Soil behavior at the microscale: particle forces. *Geotechnical Special Publication*, 25-56.

Talbot, A. N., and Richart, F. E. (1923). The strength of concrete - its relation to the cement, aggregate, and water. *Illinois Univ Eng Exp Sta Bulletin*.

Thom, N., and Brown, S. The effect of grading and density on the mechanical properties of a crushed dolomitic limestone. *Proc., Australian Road Research Board (ARRB) Conference, 14th, 1988, Canberra*.

Thom, N., and Brown, S. F. (1987). Effect of moisture on the structural performance of a crushed-limestone road base.

Tian, P., Zaman, M., and Laguros, J. (1998). Gradation and moisture effects on resilient moduli of aggregate bases. *Transportation Research Record: Journal of the Transportation Research Board*(1619), 75-84.

Vavrik, W. R. (2002). Bailey method for gradation selection in hot-mix asphalt mixture design, Transportation Research Board, National Research Council.

Vuong, B. (1992). Influence of density and moisture content on dynamic stress-strain behaviour of a low plasticity crushed rock. *Road and Transport Research*, 1(2).

Yideti, T. F. (2014). Packing theory-based Framework for Performance Evaluation of Unbound Granular Materials.

Yideti, T. F., Birgisson, B., Jelagin, D., and Guarin, A. (2013). Packing theory-based framework to evaluate permanent deformation of unbound granular materials. *International Journal of Pavement Engineering*, 14(3), 309-320.

Yideti, T. F., Birgisson, B., Jelagin, D., and Guarin, A. (2014). Packing theory-based framework for evaluating resilient modulus of unbound granular materials. *International Journal of Pavement Engineering*, 15(8), 689-697.

Zaman, M., Chen, D.-H., and Laguros, J. (1994). Resilient moduli of granular materials. *Journal of Transportation Engineering*, 120(6), 967-988.

Zeghal, M. (2000). Variability of resilient moduli of aggregate materials due to different gradations.

Appendix B – Draft Paper

"Investigating the use of packing theories to evaluate the mechanical performance of aggregate base course materials"

Submitted to International Journal of Pavement Engineering, Spring 2018

Abstract

Several past studies have proposed packing theory frameworks to evaluate the mechanical performance of granular mixtures in pavements based on their grain size distribution. Previous studies have validated that the packing theory frameworks relate to the mechanical performance of bound and unbound mixtures. However, past efforts have focused on the comparison of typical gradations used in pavement applications to atypical gradations. In contrast, this study evaluates the relationship between packing theory frameworks and mechanical performance for typical Aggregate Base Course (ABC) gradations. ABC materials were obtained from three quarries in North Carolina (NC) and four engineered gradations that fall within the NC Department of Transportation (NCDOT) gradation specification were evaluated. Three different packing theory frameworks were considered: the Bailey method, the Dominant Aggregate Size Range (DASR), and the Yideti framework. Resilient modulus tests were used as a performance indicator of the ABC. The three packing theories predict relatively different performance of the four ABC gradations evaluated. However, the rankings of the relative performances of the gradations evaluated based on the packing theory do not match the trends in the resilient modulus test results. The resilient modulus was found to be relatively insensitive to the different aggregate gradations falling within the NCDOT band specification for ABC.

Keywords: aggregate base course; resilient modulus; packing theories; rain size distribution

Introduction

Packing theories are used to describe how particles within a given gradation will interact. Packing theories have been used in a wide range of engineering fields (Yu, Standish 1988, Scott, Kilgour 1969, De Larrard 1999). Within pavement engineering, packing theories have been proposed to optimize the grain size distribution (GSD) of aggregate blends within Aggregate Base Course (ABC) and asphalt mixtures (Vavrik 2002, Kim et al. 2006, Lira et al. 2013, Guarin et al. 2013, Yideti et al. 2013, Yideti et al. 2014).

The ABC layer constitutes a primary structural component of a pavement. A primary function of the ABC layer is to distribute the wheel load, which is achieved by creating an aggregate skeleton where adjacent aggregates interlock. Numerous studies have reported that the GSD of the ABC affects its mechanical performance (Thom, Brown 1988, Kolisoja 1997, Lekarp, Isacsson 2001, Xiao et al. 2012).

Initially, researchers hypothesized that the primary factor driving the mechanical performance of an aggregate blend is the density. Correspondingly, empirical equations, such as the Talbot equation (Talbot, Richart 1923), were developed to facilitate the design of GSDs to achieve maximum density. However, later studies indicate that a denser aggregate

blend does not necessarily correlate to better performance (Santamarina 2003). Experimental studies have revealed that the majority of the load is transferred through a primary chain of particles when an external pressure is applied to ABC as illustrated in Figure B-1 (Santamarina et al. 2001). The other particles play a secondary role by preventing the load-bearing chain from buckling. Therefore, several more recent research studies have sought to use packing theory frameworks to identify the particles that constitute the load-bearing chain of an aggregate blend and evaluate its stability. In this study, three packing theory frameworks proposed to evaluate the GSD of granular materials for pavement applications are evaluated using ABC materials: the Bailey method (Vavrik 2002), the Dominant Aggregate Size Range (DASR) method (Kim et al. 2006), and the packing theory framework proposed by Yideti et al. (Yideti et al. 2014) (herein after referred to as the Yideti framework).
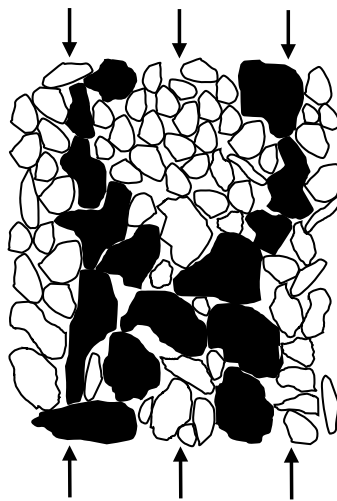
Figure B-1 - Load-bearing chain in granular material under compression

The Bailey method was one of the first packing theories proposed for use in pavement engineering (Vavrik 2002). The method was proposed for the design and evaluation of aggregate gradations in asphalt mixtures but also has merit in unbound granular material applications such as ABC. The Bailey method assumes that larger particles create voids within a mixture and that smaller particles fill these voids. Correspondingly, the Bailey method divides the particles within a mixture into coarse fractions (CF) and fine fractions (FF) where the CF is assumed to create voids that are filled by the FF. The critical particle size division between the CF and FF was derived using 2D and 3D packing analysis of particles with different shapes (i.e., flat and round faces). The size of the void within three mono-sized particles in contact was used to define the maximum size of aggregates within the FF based on the nominal maximum aggregate size (NMAS) of the CF. The Bailey method identifies the load-bearing chain of a mixture as either the CF or FF and evaluates its stability using a unit weight analysis of both the CF and FF. The unit weight analysis is based on simple laboratory measurements of loose unit weight (LUW) and rodded unit weight (RUW). The Bailey method postulates that the CF constitutes the load-bearing chain if the unit weight of CF within the compacted aggregate blend is higher than 95 percent of its LUW. Also, the Bailey Method proposes that the FF must exceed 100 percent of its RUW within a compacted aggregate blend to provide stability for the CF. While the definition for the division between

coarse and fine particles is based on an analysis of ideal particles, the RUW and LUW used in the Bailey method captures the influence of aggregate angularity, shape, and texture on packing. Previous research suggests that the Bailey method can characterizes the interlocking and resilient deformation characteristics of ABC materials with drastically different gradation (Bilodeau, Doré 2012, Cook et al. 2016).

An alternative packing theory framework, called the DASR method, was proposed by Kim et al. (2006) to identify and evaluate the load-bearing chain of aggregates in an asphalt mixture. The DASR method was derived using a numerical 2D spatial analysis of a binary mixture of spherical particles with a size ratio of 2:1. The DASR method uses the relative mass of aggregate retained on two successive sieves, with a size ratio of 2:1, to evaluate the interaction between aggregates and identify the load-bearing chain in a mixture. The load-bearing chain in this method is called dominant aggregate size ratio (DASR). If the relative proportion of the aggregate retained on two successive sieves is larger than 30/70 and smaller than 70/30, the two aggregates are considered part of the load-bearing chain (termed the DASR by Kim et al. (2006)).

To evaluate the stability of the load-bearing chain, the DASR method applies the well-known fact in soil mechanics that the porosity of granular materials in the loose state, (similar to LUW state in the Bailey method), will not exceed 50 percent regardless of the GSD of the particles. Therefore, the DASR method proposes that the porosity of the load-bearing chain should be less than 50 percent to ensure interaction between the load-bearing particles within the aggregate blend. The DASR framework was validated by comparing the porosity of the load-bearing chain of aggregate blends within asphalt mixtures to rutting performance (Kim et al. 2006). While the DASR method was initially proposed for the evaluation of aggregate blends within asphalt mixtures, it can theoretically be extended to ABC materials.

The porosity of the load-bearing chain in the DASR method framework is defined in Equation (1).

$$n = \frac{V_{V.LBC}}{V_{T.LBC}} \tag{1}$$

where $V_{V.LBC}$ is the volume of the voids within the load-bearing chain and $V_{T.LBC}$ is the total volume occupied by the load-bearing chain in the mixture. These volumes are depicted in the Figure B-2 and can be determined using specific gravity and density of the mixture.
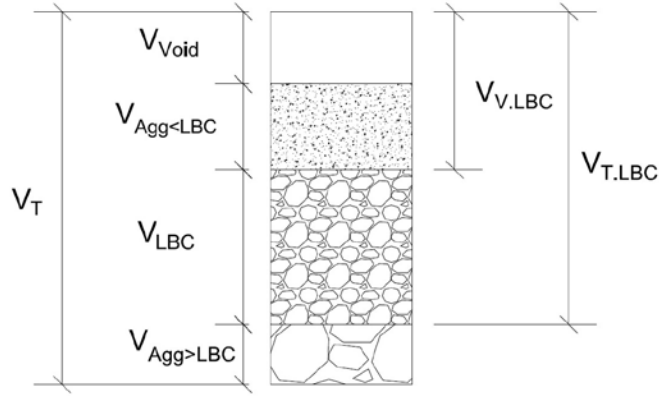
Figure B-2 - Schematic view of volumetrics in ABC

Yideti et al. (2013) recently proposed a packing theory framework to identify and evaluate the load-bearing chain within ABC materials. The Yideti framework is similar to the DASR method in that the relative proportion of aggregate retained on successive sieves is used to identify the load-bearing chain. The interaction of particles within the load-bearing chain is evaluated based on its porosity. However, the Yideti framework was derived using a numerical 3D spatial analysis of spherical particles with differing size ratios (not necessary 2:1 ratio). Equation (2) was developed to evaluate the interaction of two consecutive aggregate sizes within an ABC blend.

$$\frac{1.1 \times D_1 D_2}{\sqrt[3]{D_2^3 + 2.36 \times D_1^3}} \leq d_{w.avg} \leq \frac{1.1 \times D_1 D_2}{\sqrt[3]{2.36 \times D_2^3 + D_1^3}} \tag{2}$$

where D_1 is the larger sieve size of interest, D_2 is smaller sieve size of interest, and $d_{w.avg}$ is the weighted average void diameter between the weighted average diameter of particles with diameter of D_1 and D_2 which is $D_{w,avg}$ and is calculated using Equations (3) and (4).

$$D_{w,avg} = D_1 D_2 \sqrt[3]{\frac{\varphi_1 + \varphi_2}{\varphi_1 D_2^3 + \varphi_2 D_1^3}} \tag{3}$$

$$d_{w.avg} = 0.732 \times D_{w,avg} \tag{4}$$

where φ_1 and φ_2 are the percentage by volume retained on the two successive sieves.

The potential of the load-bearing chain to be disrupted by smaller particles, termed the Disruption Potential (DP), was also proposed as a useful means to evaluate the load-bearing chain stability by Yideti et al (2013). The DP is defined as the ratio between the volume of disruptive particles to the volume of free voids within the load-bearing chain. To calculate the DP, the volume of disruptive particles is obtained as the volume of particles ranging from the smallest chain particle to 0.225 times the smallest chain particle in the mixture. Also, the volume of free voids within the chain is obtained by multiplying the aggregate blend's void ratio to the volume of particles constructing the chain. Yideti et al

(2013) showed that the DP can be divided into three ranges: DP<0.5 as unstable, 0.5<DP<1.0 as stable, and DP>1.0 as disruptive. Also they showed when the DP exceeds one, the permanent deformation of granular materials increases as the DP increases.

In addition, the Yideti framework has been validated with resilient modulus (M_R) test results by comparing published M_r test results preformed on unbound granular materials and the porosity of primary structure of the materials; however, the gradations used to validate this framework spanned a range outside of what DOTs across the US typically use for ABC (Yideti et al. 2014).

The current study seeks to investigate the application of the three packing theory frameworks to evaluate the mechanical performance of ABC. To rigorously evaluate the packing theory frameworks, ABC material was acquired from several quarries in NC to cover a broad range of materials from the Piedmont region in the state. The mechanical performance of ABC is evaluated using the M_R in this study because the M_R is the most common value used to assess the behaviour of ABC and is a key input to the mechanistic-empirical design method (i.e., PavementME).

Materials and methods

In this study, three commonly used ABC materials from the state of North Carolina (NC) were obtained from various quarries. These quarries are designated as A, B, and C. Four gradations were developed by sieving and recomposing the materials. Three well graded gradations were selected to be the upper (UB), middle (MB), and lower boundaries (LB) of the gradation band specified by the NCDOT. Also, a gap graded gradation (GG) was evaluated for source A as an extreme gradation to critically evaluate the packing theory frameworks. The chosen gradations are presented in Figure B-3. The index properties of each ABC material and gradation evaluated are presented in Table B-1. The compaction (moisture-density) characteristics of the tested gradations were performed according to AASHTO T-180 with one modification; 86 blows were applied to each layer to compact the specimen to be consistent with the practice employed by the NCDOT instead of the 56 blows per layer specified by AASHTO T-180.
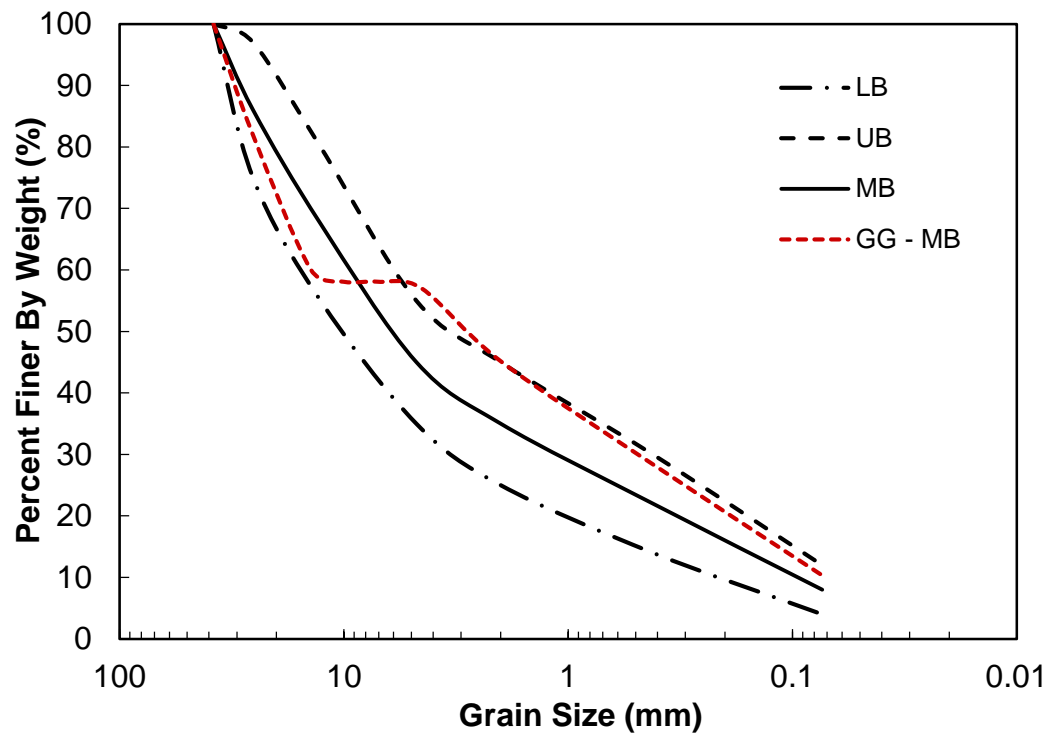
Figure B-3 - Tested grain size distributions

Table B-1 - Mixtures index properties

Source	Gradation	G_S (CF/FF)	G_S	MDD (gr/cm^3)	OWC (%)
A	UB	2.94/2.88	2.90	2.45	4.5
	MB	2.94/2.88	2.91	2.46	4.2
	LB	2.94/2.87	2.92	2.48	4.3
	GG	2.90/2.90	2.90	2.40	4.4
B	UB	2.71/2.70	2.71	2.25	6.3
	MB	2.72/2.71	2.72	2.28	5.5
	LB	2.72/2.70	2.71	2.31	5.5
C	UB	2.68/2.68	2.68	2.24	5.0
	MB	2.70/2.71	2.71	2.27	5.5
	LB	2.67/2.67	2.67	2.31	5.0
G_S: specific gravity, CF: coarse fraction, FF: fine fraction, MDD: maximum dry density, OWC: optimum water content,					

The morphological properties, including angularity index (AI), surface texture index (ST), and sphericity (SP), of course aggregates were evaluated using an aggregate image measurement system (AIMS2) (Gates et al. 2011). The AI describes variations at the particle boundary that influence the overall shape and ranges from 0 (rounded) to 10^4 (extremely angular) (Masad 2005). The ST describes the relative smoothness or roughness of coarse particles and ranges from 0 (smooth) to 10^3 (rough) (Masad 2005). The SP of particles describes the overall 3D shape of a particle by measuring the particle's shortest (d_S), intermediate (d_I), and largest (d_L) dimensions and ranges from 0 to 1.0 (spherical). The results are described for MB gradation of each source as the composite indices of the aggregates obtained by the procedure described by Gu et al. (2014). The results indicate that on average, based on the 50% of particles, the morphological properties of the three aggregate sources evaluated are generally within a similar range, demonstrating moderate angularity, moderate texture, and high sphericity. As the main assumption in the Yideti and DASR frameworks is that the particles are spherical, these conditions are roughly met for the material evaluated. Furthermore, the similarity of morphological properties indicate that the packing of the aggregates from these three sources will only be affected by the physical properties of particles and any differences are due to gradation. It should be mentioned that the composite index of each source was not sensitive to the gradation of the mixture.
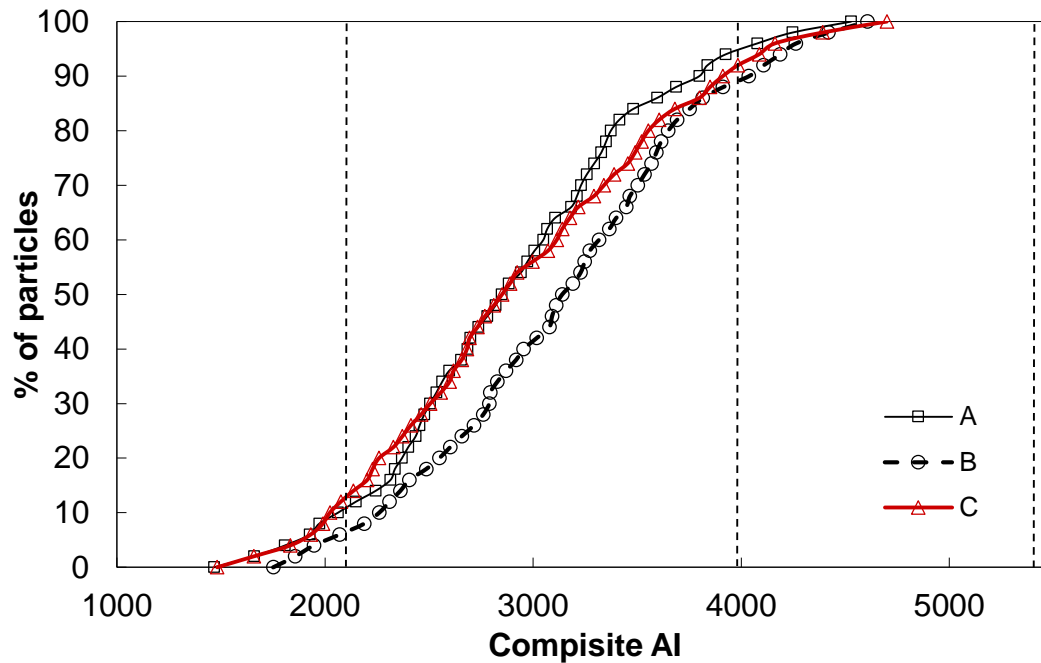
Figure B-4 – Angularity index of aggregate (0<low<2100, 2100<moderate<3975, 3975<high<5400, 5400<extreme<10^4)
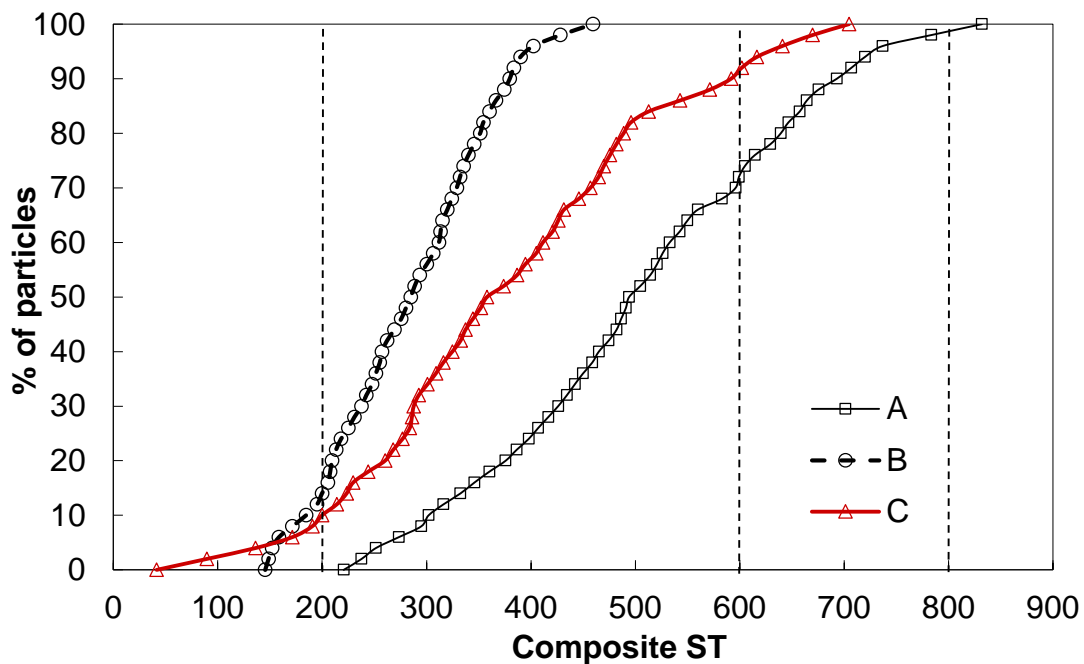
Figure B-5 – Coarse aggregate surface texture (0<low<200, 200<moderate<500, 500<high<750, 750<extreme<10^3)
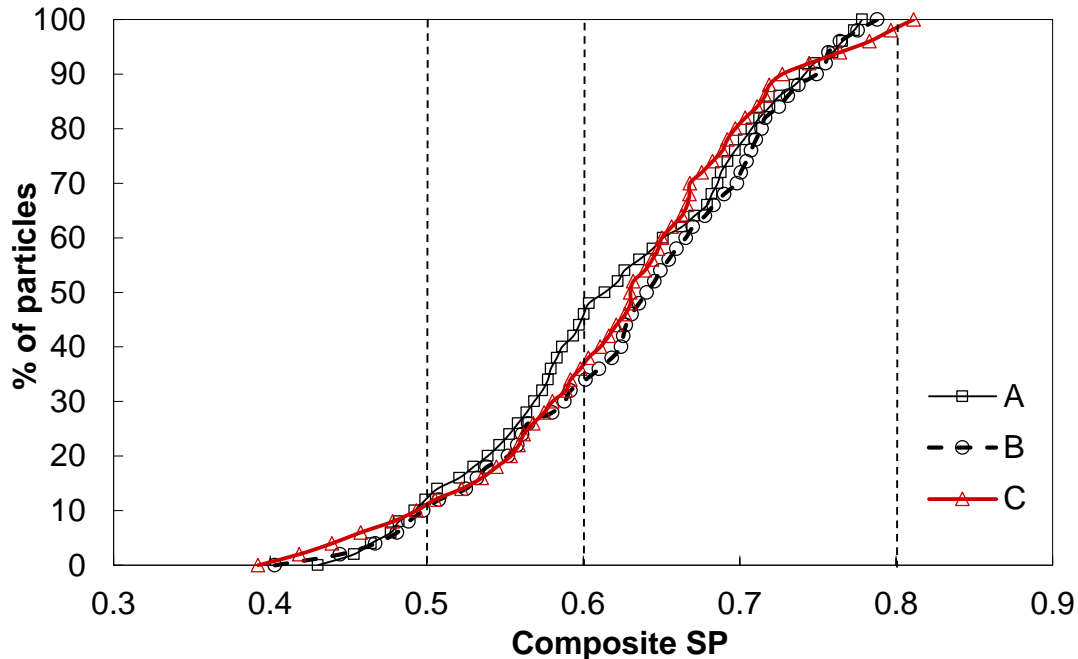
Figure B-6 - Coarse aggregate sphericity (0<low<0.5, 0.5<moderate<0.6, 0.6<high<0.8, 0.8<extreme<1.0)

The LUW and RUW were measured for the fine and coarse fractions of each gradation and source according to AASHTO T-19 as required for the Bailey method.

M_R tests were conducted for each source and gradation evaluated in accordance with AASHTO T-307. The M_R test samples were compacted using the impact hammer method to achieve 100 percent of their maximum dry density at the optimum moisture content.

Results and discussion

Analytical results based on the packing theories

The packing theory frameworks were first applied on the three well-graded gradations (e.g., UB, MB, LB) to identify the load-bearing chain (abbreviated as LBC in following tables) and its stability for the three aggregate sources, then the frameworks were applied to the gap-graded gradation.

Bailey method

To evaluate the ABC materials using the Bailey method, a volumetric analysis was performed on the compacted ABC blends using the LUW and RUW tests results following the method proposed by Bilodeau and Dore (2013). For all of the gradations evaluated, the boundary between the CF and FF was the #4 sieve, which happens to coincide with the conventional definition of course and fine aggregates used in soil mechanics. The results of the RUW and LUW analyses are shown in Table B-2.

For all of the ABC sources and gradations considered, the percentage of the loose unit weight of CF (%LUW_CF) of the LB gradations is higher than 95 percent; therefore, the load-bearing chain in the LB gradations is constructed by coarse aggregate according to the Bailey method. In addition, the results suggest that strong interlocking exists within the load-

119

bearing chain because the $\%LUW_{CF}$ of all the aggregate sources exceed 100% for the LB gradation; this indicates that the particles constituting the load-bearing chain are in contact. Also, the percentage of the rodded unit weight of the FF within the aggregate blend ($\%RUW_{FF}$) of the LB gradations of all the aggregate sources are equal or higher than 100%, which indicates the fine particles are compacted within the voids of the load-bearing structure and thus, are expected to provide stability for the CF. As the gradation becomes finer (i.e., MB and UB), the results suggest that not all of the coarse aggregate will be in contact because the $\%LUW_{CF}$ of all the aggregate sources are less than 95%. Therefore, the Bailey method suggests that the fine fraction of the aggregate constitutes the load-bearing chain for the MB and UB gradations. While the Bailey method does not stipulate whether a coarse or fine load-bearing chain is better, past studies suggest that coarser gradations result in higher resilient moduli (Lekarp et al. 2000). Also, as the gradation becomes finer, the $\%RUW_{FF}$ increases. A higher $\%RUF_{FF}$ indicates that the fine aggregate has greater particle-to-particle connectivity within the aggregate blend which provide more stability for the load-bearing chain.

Table B-2 – Volumetric analysis results of ABC materials

Source	GSD	RUW_{FF}	LUW_{CF}	$\%RUW_{FF}$	$\%LUW_{CF}$
		gr/cm3	gr/cm3	(>100%)	(>95%)
A	UB	1.76	1.53	122%	72%
	MB	1.83	1.56	113%	87%
	LB	1.90	1.52	101%	106%
B	UB	1.50	1.39	132%	73%
	MB	1.57	1.42	122%	89%
	LB	1.64	1.42	103%	103%
C	UB	1.67	1.38	113%	71%
	MB	1.73	1.42	110%	88%
	LB	1.75	1.43	100%	102%

DASR method

The DASR method is based on the analysis of the relative proportion of aggregates with a size ratio of 2:1. Therefore, to apply this method to the gradations in the current study, the tested gradations were first re-evaluated based on 2:1 sieve size ratios using interpolation of measured values. The results are shown in Table B-3.

Table B-3 - Re-evaluated gradations

1:2 ratio sieves (mm)	Percent passing			Percent retained		
	LB	MB	UB	LB	MB	UB
38.1	100%	100%	100%	0%	0%	0%
19.05	66%	78%	91%	35%	22%	9%
9.53	48%	60%	72%	18%	18%	19%
4.76	35%	45%	55%	13%	15%	17%
2.38	27%	37%	47%	9%	9%	9%
1.19	21%	31%	40%	6%	6%	7%
0.60	16%	25%	33%	5%	5%	7%
0.30	12%	19%	26%	4%	6%	7%
0.15	8%	14%	19%	4%	5%	7%
0.074	4%	8%	12%	4%	6%	7%

The GSD shown in Table B-3 was used to construct the so-called interaction diagram shown in Figure B-7. The interaction diagram was constructed using the relative proportions aggregates retained on each pair of consecutive sieves. For example, for the LB gradation, 35% and 18% of particles are retained on the 19.05 mm sieve and the 9.53 mm sieve, respectively,; therefore, the relative proportion of the 19.05 mm and 9.53 mm particle sizes is (35%)/(35%+18%) = 66% = 33/50. It should be noted that the relative proportion of particles with a size ratio of 2:1 is only affected by the gradation and is not a function of the material source; therefore, the interaction diagram is identical for all three material sources evaluated in this study. The interaction diagram is used to identify the load-bearing chain (DASR) in the three gradations by observing the aggregate sizes where the relative proportion of particles falls within the bounds of 30/70 and 70/30. Thus, all particles are interacting and forming the primary load-bearing chain (DASR) based on the DASR method. The minimum particle size which can be considered as a part of the load-bearing chain (DASR) was chosen to be 4.75 mm based on the division between fine and coarse particles based on the Bailey method. Therefore, based on the interaction diagram, in all the gradations, the aggregates larger than 4.75 mm were considered to be the load-bearing chain (DASR).

Figure B-7 – Interaction diagram for UM, MB, and LB gradations

The porosity of the load-bearing chain (DASR) for each material and gradation was calculated using Equation 1. In contrast with the interaction diagram, the porosity of load-bearing chain (DASR) is a function of the aggregate specific gravity and maximum dry density and therefore, differs among material sources.

The load-bearing chain (DASR) porosities of the materials and gradations evaluated and shown in Table B-4. According to the results, only the porosity of the LB gradation is less than 50 percent for all materials evaluated, which indicates that a strong interlock exists between the particles in the load-bearing chain (DASR). It is also observed that the porosity of the load-bearing chain (DASR) of aggregate particles increases and exceeds 50 percent as the gradation moves from the UB to LB. Therefore, the DASR framework suggests that among the three gradations within the NCDOT, only the load-bearing chain (DASR) in the LB gradation possesses a strong interlock, and the chain in the other gradations, MB and UB, have lower degree of interlock and are disrupted by other particles. These results are in agreement with the Bailey method results.

Table B-4 - DASR porosity

Gradation	LBC, range (mm)	A	B	C
UB		62.1%	62.1%	63.8%
MB	38.1 - 4.75	53.5%	53.1%	53.4%
LB		44.8%	44.5%	45.8%

Yideti framework

In the Yideti framework, the load-bearing chain of the gradations, called primary structure (PS), is identified using Equation (1), following the procedure described by Yideti et al. (2013). The range of particle sizes that comprise the load-bearing chain (PS) and the corresponding load-bearing chain (PS) porosities of all sources and gradations evaluated according to the Yideti framework are shown in Table B-5. Similar to DASR method, the load-bearing chain (PS) particle size range is also independent of aggregate properties and is only related to the gradation. The results indicate that the UB gradation load-bearing chain (PS) is comprised of less particle sizes than the MB and LB gradations. In addition, the results indicate that the porosity increases as the gradation becomes finer within the NCDOT specification band; this indicates that better performance is expected with the use of coarser gradations within the NCDOT specification band.

Table B-5 – PS and theory porosities for different gyrations and sources

Gradation	LBC, range (mm)	PS porosity		
		A	B	C
UB	25.4 - 4.75	63.2%	63.0%	65.3%
MB	38.1 - 2.00	44.1%	46.0%	45.4%
LB	38.1 - 2.00	35.5%	36.9%	36.7%

To evaluate the disruption of the load-bearing chain (PS) by the fine particles, the DP values were calculated for each gradation and material source evaluated. The DP results are shown in Table B-6. The DP values were between 0.5 and 1.0 in LB which shows the stability of the load-bearing chain (PS) in this gradation, and for MB and UB were more than 1.0 (except for MB of source B). The later showed that the load-bearing chain (PS) of MB and UB are disrupted by fine particles (disruptive material), and the disruption is more in UB.

Table B-6 – DP of mixtures

Gradation	DP, range (mm)	DP		
		A	B	C
UB	4.75 - 2.00	1.46	1.51	1.05
MB	2.00 - 0.42	1.23	0.98	1.05
LB	2.00 - 0.42	0.90	0.77	0.79

The different packing theories lead to some differences in the aggregate size range identified as the load-bearing chain. As summarized in Table B-7, according to Bailey method, the load-bearing chain is constructed in LB gradation by particles larger than 4.75 mm and smaller than 38.1 mm (CF), and in MB and UB gradations, the chain consists of particles smaller than 4.75 mm (FF). This is because Bailey method identifies the chain to be either comprised by CF or FF of a mixture. The DASR method identified similar load-bearing chain for the three gradations as particles smaller than 38.1 mm and larger than 4.75 mm; however, using the Yideti framework, it was found that the load-bearing chain in the three gradation is constructed with different particle sizes; particles smaller than 25.4 mm and larger than4.57 for UB gradation, and particles smaller than 38.1 mm and larger than 2.0 for MB and LB gradations.

The evaluation results, shown in Table B-7, indicate that the Bailey and DASR methods identified LB gradation as the gradation with the load-bearing chain constructed by stable CA and highest degree of interlock, respectively, among others. In addition, the Bailey method showed that load-bearing chains within MB and UB gradations are constructed by FA. Yideti framework results suggested that decreased porosity of the load-bearing chain as the gradation becomes coarser within the NCDOT band specification.

In summary, the results of all of the packing theory frameworks indicate that the load-bearing chain is stronger in coarser gradations within the NCDOT band specification for ABC and that the load-bearing chain becomes (more) porous as the gradation moves toward finer bound of the NCDOT band specification. Therefore, the LB gradation is expected to have better mechanical performance than the MB and the UB gradations.

Table B-7 - Summary of the packing theory results

Gradation	LBC, range (mm)			LBC criteria*		
	Bailey	DASR	Yideti	Bailey	DASR	Yideti
UB	< 4.75 (FF)		25.4 - 4.75	%LUW$_{CF}$ = 72%	$\bar{n}$ =62.7%	$\bar{n}$ =63.4%
MB	< 4.75 (FF)	38.1 - 4.75	38.1 - 2.00	%LUW$_{CF}$ = 88%	$\bar{n}$ =53.3%	$\bar{n}$ =45.2%
LB	38.1 - 4.75 (CF)		38.1 - 2.00	%LUW$_{CF}$ = 104%	$\bar{n}$ =45.0%	$\bar{n}$ =36.4%

*The LBC criteria in this table are average values of criterion of all the sources.

Mechanical performance test results

To evaluate the practical implications of the packing theory framework results, M_R tests were performed. The resilient modulus test results of the different gradations and sources are shown in Figure B-8 to Figure B-10. Each points in these figures indicate the M_R of each sample at a certain bulk stress. In addition, each test were repeated once, except the MB gradation of source A which was repeated 3 times, and each plotted point represents the average values of the repetitions The sensitivity of the M_R to gradation for each aggregate source varies with the bulk stresses. For all of the material sources, the M_R values of the different gradations are close at low bulk stresses but as bulk stress increases, there tends to be more sensitivity in the M_R to gradation. Similar trends were also observed in a previous study within the same gradation band (Cunningham et al. 2013). The packing theory frameworks evaluated all indicate that the LB gradation is expected to perform better than

the MB and UB gradations. However, the LB gradation exhibited the highest M_R values for only the ABC material from source C. Therefore, packing theory frameworks alone do not have the ability to predict the trends in M_R. Due to the relatively low sensitivity of M_R test results to the gradations evaluated herein, it is recommended that future work investigate other performance measures when evaluating the relative performance of ABC materials (Mishra et al. 2012, Chow et al. 2014).
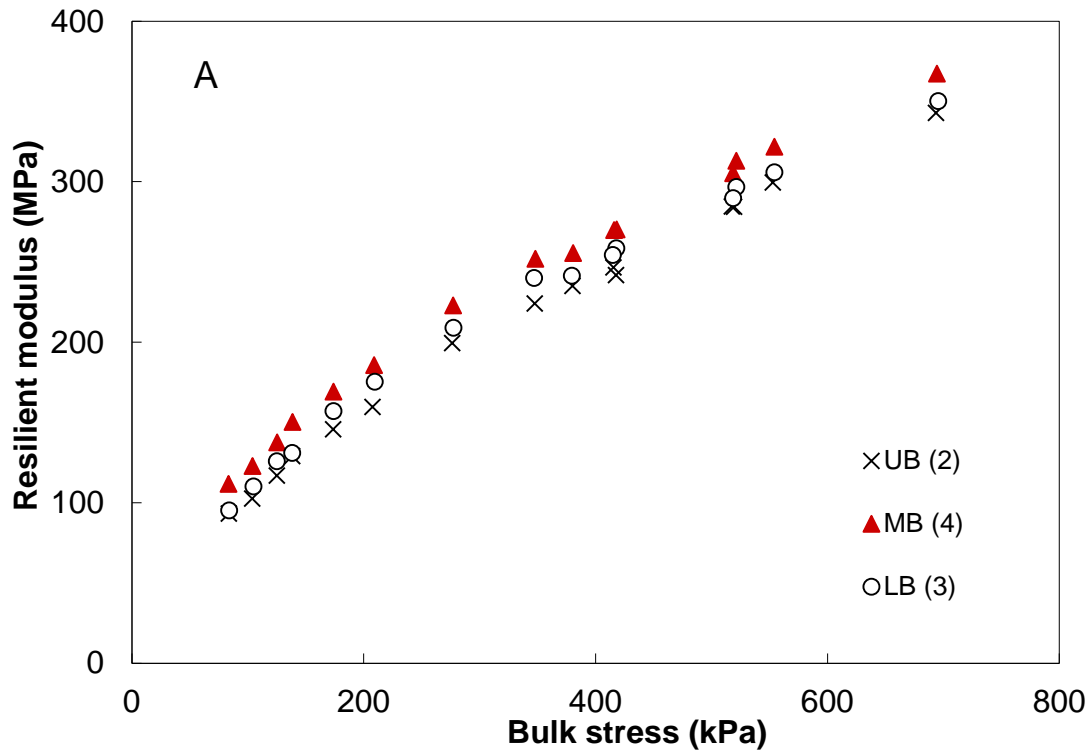

Figure B-8 - M_R test results on materials from source A
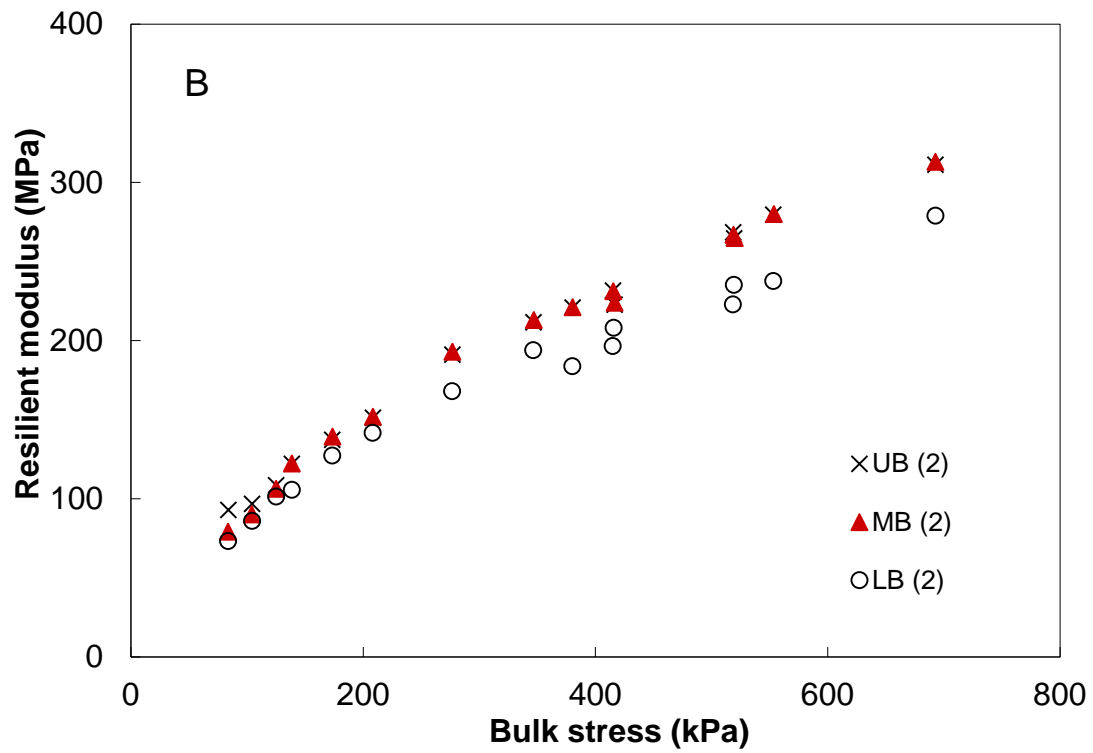
Figure B-9 - M$_R$ test results on materials from source B
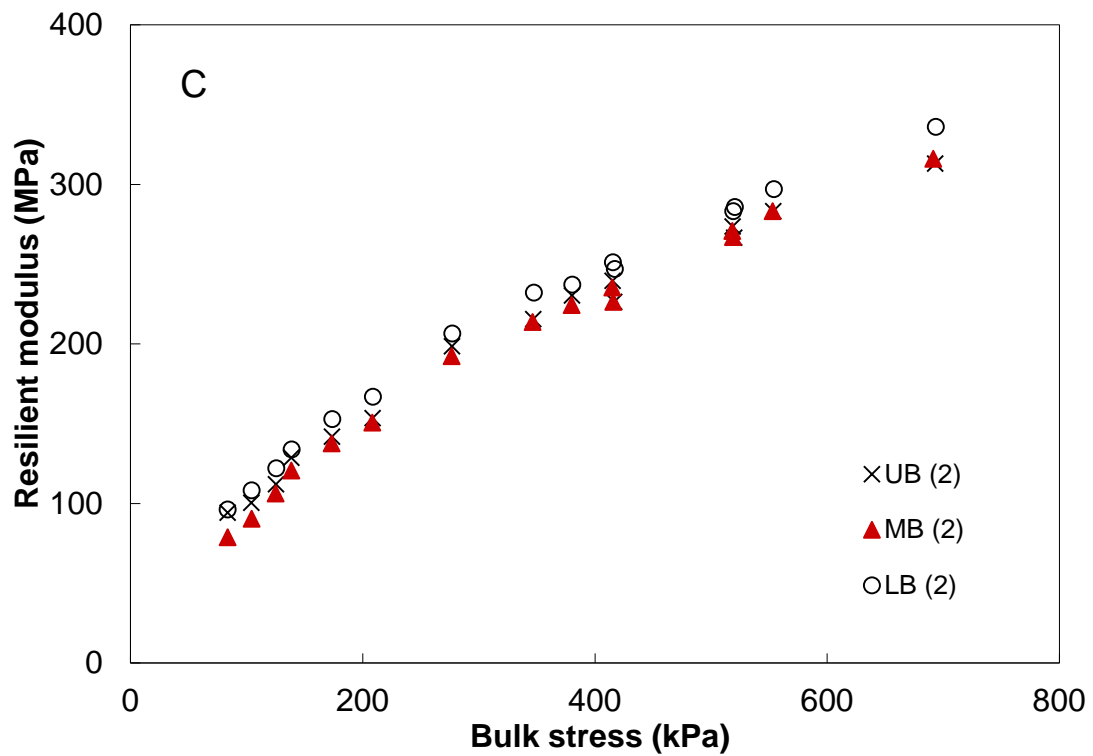
Figure B-10 - M$_R$ test results on materials from source C

Evaluating an extreme gradation

The UB, MB, and LB gradations all represent typical well-graded ABC gradations. Therefore, to further evaluate the relationship between the packing theory frameworks and mechanical performance, an additional gap gradation comprised of ABC material from source A was designed, evaluated, and tested. The gap gradation was created using the MB gradation but excluding aggregate smaller than 12.7 mm and larger than 4.75 mm which was found by all the packing theory frameworks to be a large portion of the load-bearing chain. The gap gradation still fell within the NCDOT band specification for ABC as shown in Figure B-3.

The Bailey method results of the gap gradation (GG) from source A compared to the MB gradations are shown in Table B-8. The results show that the $\%LUW_{CA}$ of the GG was less than 95 percent which suggests that the coarse fraction in a compacted GG blend is highly disrupted by the fine fraction of the mixture. However, the $\%LUW_{CA}$ of GG gradation (71%) is close to the $\%LUW_{CA}$ of UB (72%) as shown in Table B-8. In addition, the volumetric analysis showed that the fine fraction of GG was highly compacted in the mixture ($\%RUW_{FA}$ of 118%). Based on the volumetric analysis on the gap graded gradation, the load-bearing chain in this gradation is constructed by the FF which is highly compacted.

Table B-8 – Volumetric analysis results on MB and GG gradations – source A

Gradation	RUW_{FA}	LUW_{CA}	$\%RUW_{FA}$	$\%LUW_{CA}$
	gr/cm^3	gr/cm^3		
MB	1.79	1.42	107%	88%
GG	1.80	1.42	118%	71%

The interaction diagram resulting from applying the DASR method to the MB and GG gradations is shown in Figure B-11. The results indicate that load-bearing chain in the GG is not constructed because the aggregate larger than the 4.75 mm sieve fall outside of the 70/30 limit for the relative proportion of aggregates from two contiguous sieves with a size ratio of 2:1. The DASR and Yideti framework results for porosity of the load-bearing chain of particles and DP are shown in Table B-9. The Yideti framework also suggests a reduction in the range of particle sizes included within the load-bearing chain. It can be seen that the porosity of the load-bearing chain in the GG is significantly higher than 50 percent according to both the Yideti framework, suggesting poor performance. The expected poor performance was also confirmed by the high DP (1.43) of the GG gradation.
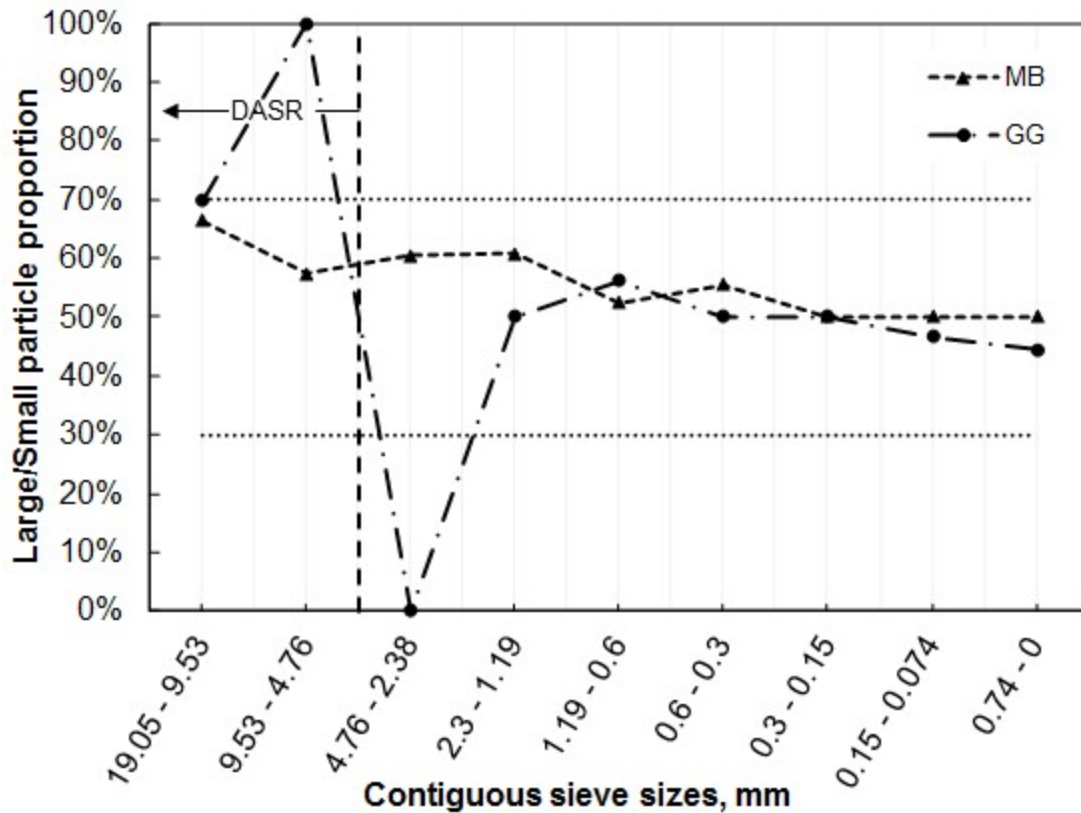
Figure B-11 – Interaction diagram, comparing MB and GG from source A

Table B-9 – DASR and Yideti frameworks for GG and MB mixtures - Source A

Gradation	DASR		Yideti			
	DASR, range (mm)	n (%)	PS, range (mm)	n (%)	DM, range (mm)	DP
MB	38.1-1.19	41.0%	38.1 - 2.00	45.0%	2.00 - 0.42	1.23
GG	-	-	38.1 - 12.7	54.9%	12.7 - 2.00	1.43

The M_R test results of the GG and MB gradations comprised of materials from source A are shown in Figure B-12. The M_R values of the GG are generally very similar to the MB gradation. Thus, while the packing theory frameworks suggest that the GG gradation does not have a strong load-bearing chain of particles, the performance test results indicate comparable performance to the MB gradation.
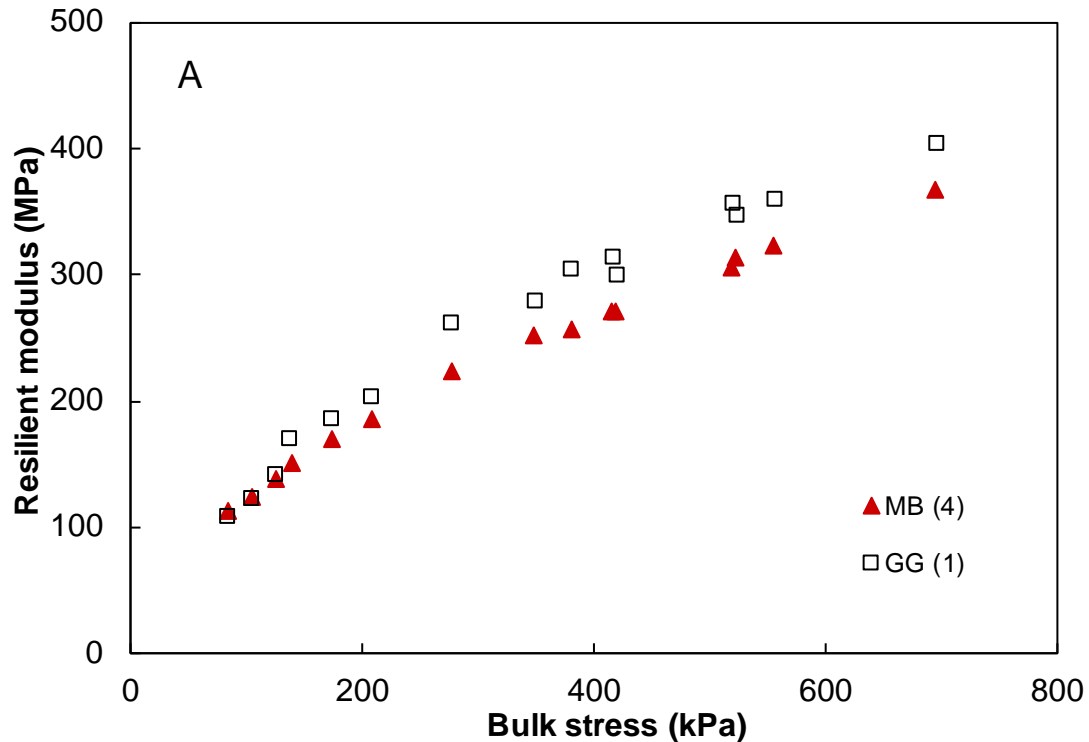
Figure B-12 - M_R test results on GG and MB mixtures – Source A

     The comparison between the packing analysis and M_R test results indicate that within the NCDOT band specification for ABC, the packing theory frameworks do not provide results that relate to M_R. The experimental results indicate that the variation of M_R is insignificant for all gradations evaluated within the NCDOT band specification. Therefore, packing theory frameworks alone are insufficient to effectively design and evaluate the resilient behaviour of ABC materials falling within typical gradation band specifications.

Conclusions

The following conclusions are drawn from this study:

1. The three packing theories evaluated (i.e., Bailey method, DASR method, Yideti framework) predict the same expected relative performance of three typical ABC gradations.
2. The three packing theories do not adequately predict the observed trends in the M_R test results.
3. The packing theories only consider the influence of the gradation. However, M_R test results suggests that physical and morphological aggregate properties also influence ABC resilient behavior. Therefore, packing theory alone is insufficient to elucidate ABC resilient behavior.

References

Bilodeau, J. and Dore, G., 2012. Relating resilient behaviour of compacted unbound base granular materials to matrix and interlock characteristics. *Construction and Building Materials,* 37, 220-228.

Chow, L.C., Mishra, D. and Turumluer, E., 2014. Aggregate base course material testing and rutting model development. Final Report to North Department of Transportation, 128 pp.

Cook, C.S., Tanyu, B.F. and Yavuz, A.B., 2016. Effect of particle shape on durability and performance of unbound aggregate base. *Journal of Materials in Civil Engineering*, pp. 04016221.

Cunningham, C.N., Evans, T.M. and Tayebali, A.A., 2013. Gradation effects on the mechanical response of crushed stone aggregate. *International Journal of Pavement Engineering,* 14 (3), pp. 231-241.

De Larrard, F., 1999. Concrete mixture proportioning: a scientific approach. CRC Press.

Gates, L., Masad, E., Pyle, R. and Bushee, D., 2011. Aggregate Imaging Measurement System 2 (AIMS2). Final Report: FHWA-HIF-11-030.

Gu, F., *et al.*, 2014. Estimation of resilient modulus of unbound aggregates using performance-related base course properties. *Journal of Materials in Civil Engineering,* 27 (6), 04014188.

Guarin, A., Roque, R., Kim, S. and Sirin, O., 2013. Disruption factor of asphalt mixtures. *International Journal of Pavement Engineering*, 14, 472-485.

Kim, S., Guarin, A., Roque, R., and Birgisson, B., 2006. Identification and Assessment of the Dominant Aggregate Size Range (DASR) of Asphalt Mixture. *Journal of Asphalt Paving Technologists,* 75, pp. 789–814.

Kolisoja, P., 1997. Resilient deformation characteristics of granular materials. Thesis (PhD). Tampere University of Technology.

Lekarp, F. and Isacsson, U., 2001. The effects of grading scale on repeated load triaxial test results. *International Journal of Pavement Engineering,* 2 (2), pp. 85-101.

Lekarp, F., Isacsson, U. and Dawson, A., 2000. State of the art. I: Resilient response of unbound aggregates. *Journal of Transportation Engineering,* 126, pp. 66-75.

Lira, B., Jelagin, D. and Birgisson, B., 2013. Gradation-based framework for asphalt mixture. *Materials and structures,* 46, pp. 1401-1414.

Masad, E.A., 2005. *Aggregate imaging system (AIMS): Basics and applications.* FHAWA/TX-05/5-1707-01-1. Texas Transportation Institute, Texas A & M University System.

Mishra, D. and Tutumluer, E., 2012. Aggregate physical properties affecting modulus and deformation characteristics of unsurfaced pavements. *Journal of Materials in Civil Engineering,* 24 (9), pp. 1144-1152.

Santamarina, J.C., Klein, A. and Fam, M.A., 2001. Soils and waves: Particulate materials behavior, characterization and process monitoring. *Journal of Soils and Sediments,* 1 (2), pp. 130-130.

Santamarina, J.C., 2003. Soil behavior at the microscale: particle forces. *Soil Behavior and Soft Ground Construction*, pp. 25-56.

Scott, G. and Kilgour, D., 1969. The density of random close packing of spheres. *Journal of Physics D: Applied Physics,* 2 (6), pp. 863-866.

Talbot, A.N. and Richart, F.E., 1923. The strength of concrete-its relation to the cement, aggregates and water. University of Illinois at Urbana Champaign, College of Engineering. Engineering Experiment Station.

Thom, N. and Brown, S., 1988. The effect of grading and density on the mechanical properties of a crushed dolomitic limestone. *14th Australian Road Research Board (ARRB) Conference,* Canberra 1988.

Vavrik, W.R., 2002. Bailey method for gradation selection in hot-mix asphalt mixture design. Transportation Research Board, National Research Council.

Xiao, Y., Tutumluer, E., Qian, Y. and Siekmeier, J., 2012. Gradation effects influencing mechanical properties of aggregate base-granular subbase materials in Minnesota. *Transportation Research Record: Journal of the Transportation Research Board*, pp. 14-26.

Yideti, T.F., Birgisson, B., Jelagin, D. and Guarin, A., 2013. Packing theory-based framework to evaluate permanent deformation of unbound granular materials. *International Journal of Pavement Engineering,* 14 (3), pp. 309-320.

Yideti, T.F., Birgisson, B., Jelagin, D. and Guarin, A., 2014. Packing theory-based framework for evaluating resilient modulus of unbound granular materials. *International Journal of Pavement Engineering*, 15, pp. 689-697.

Yu, A. and Standish, N., 1988. An analytical-parametric theory of the random packing of particles. *Powder Technology,* 55 (3), pp. 171-186.

Appendix C – Additional Resilient Modulus Results at varying Degrees of Saturations

In this section, the M_R test results of each stage is shown; for comparison, the variability of the M_R for samples tested at the OMC is also illustrated (i.e., plotted variability brackets).
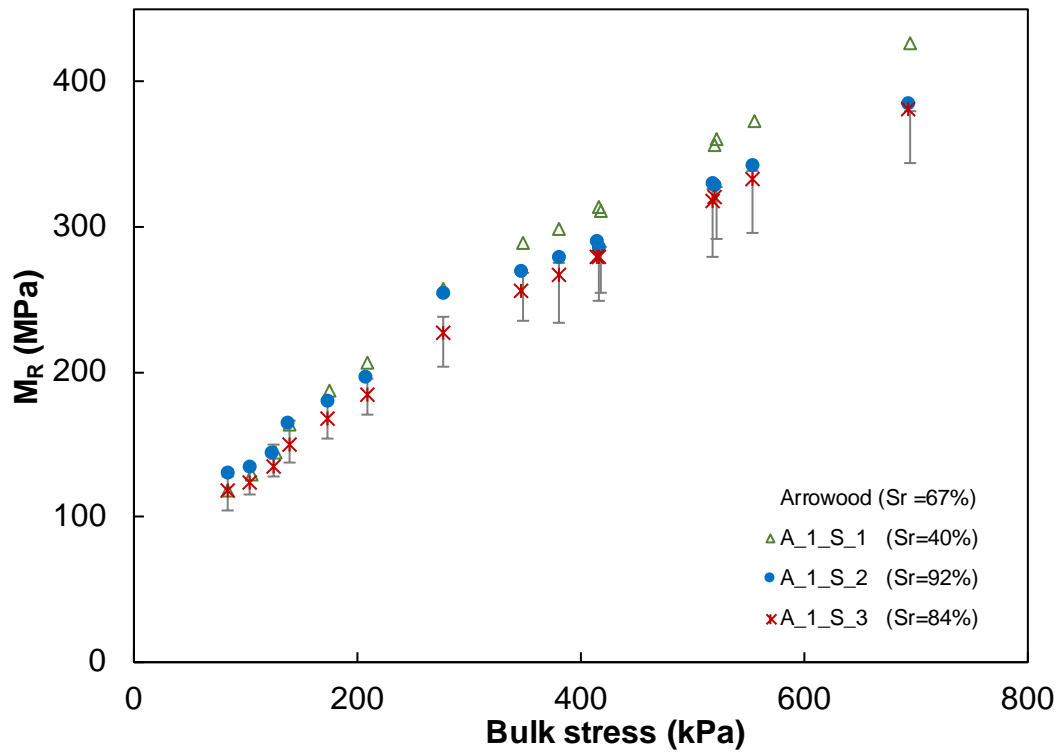
Figure C-1 - Arrowood aggregate - Test 1 - Stages 1, 2, and 3
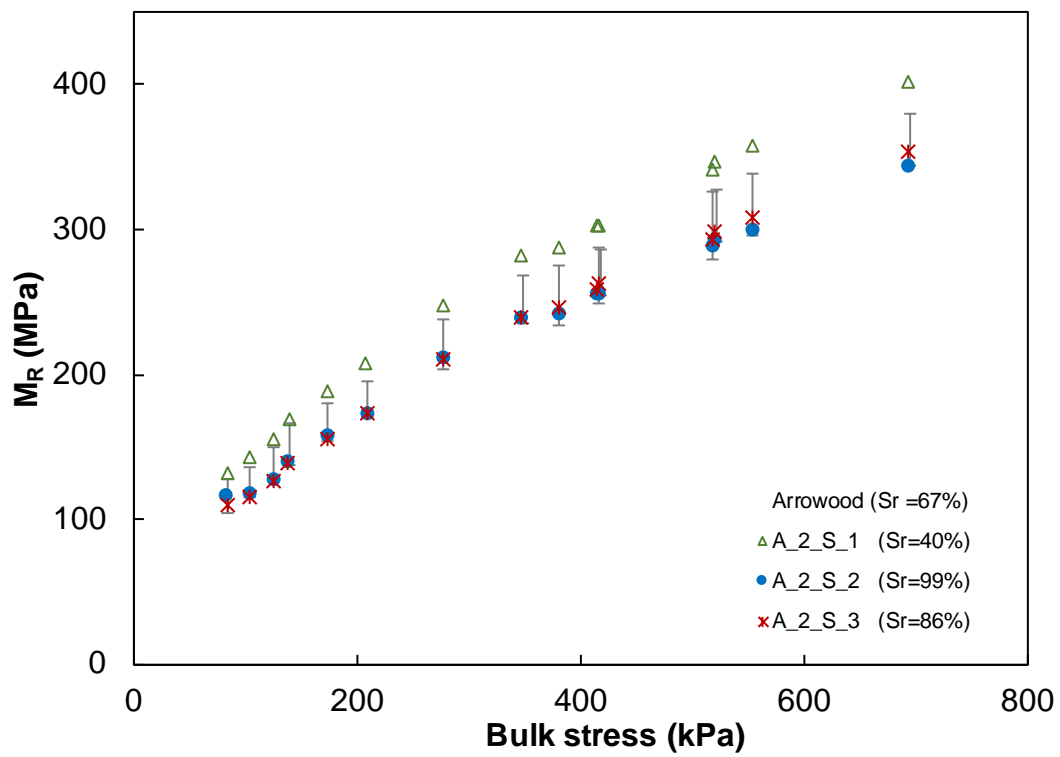
Figure C-2 – Arrowood aggregate – Test 2 – Stages 1, 2, and 3
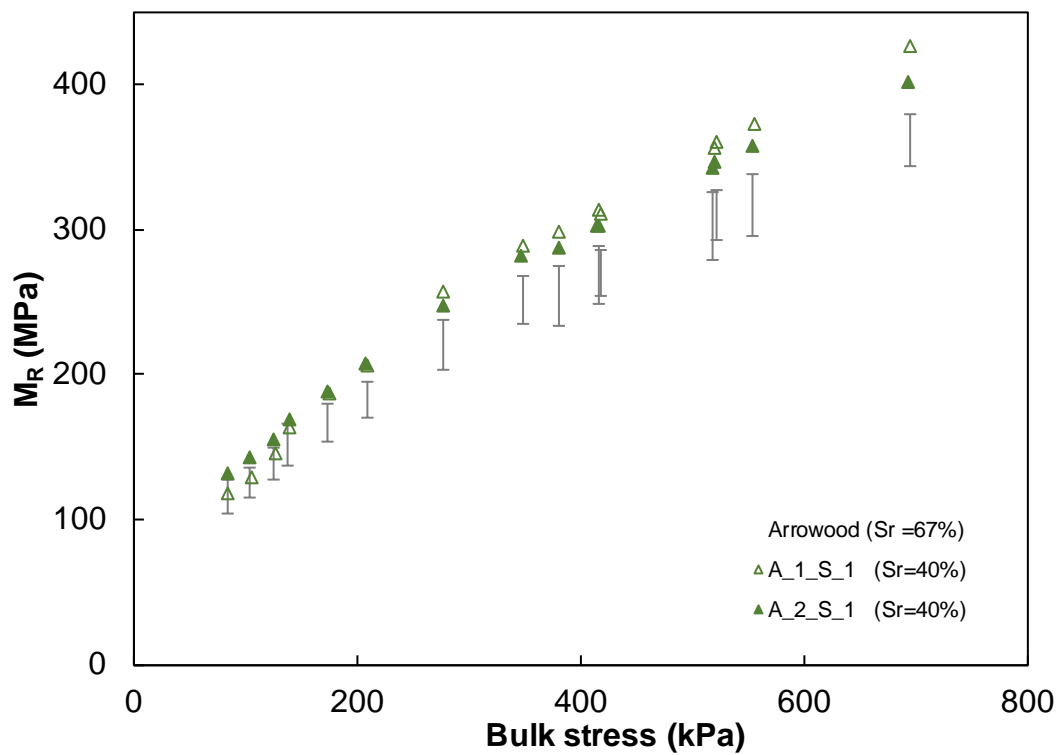
Figure C-3 – Arrowood aggregate – Stage 1 – Tests 1 and 2
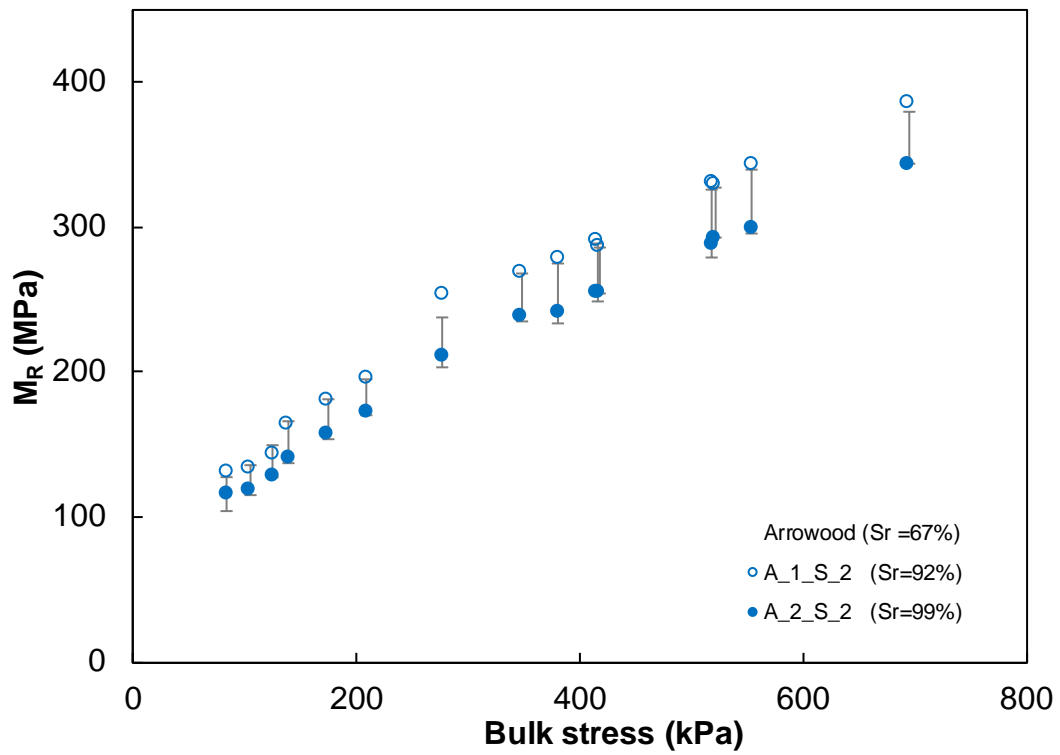
Figure C-4 – Arrowood aggregate – Stage 2 – Tests 1 and 2
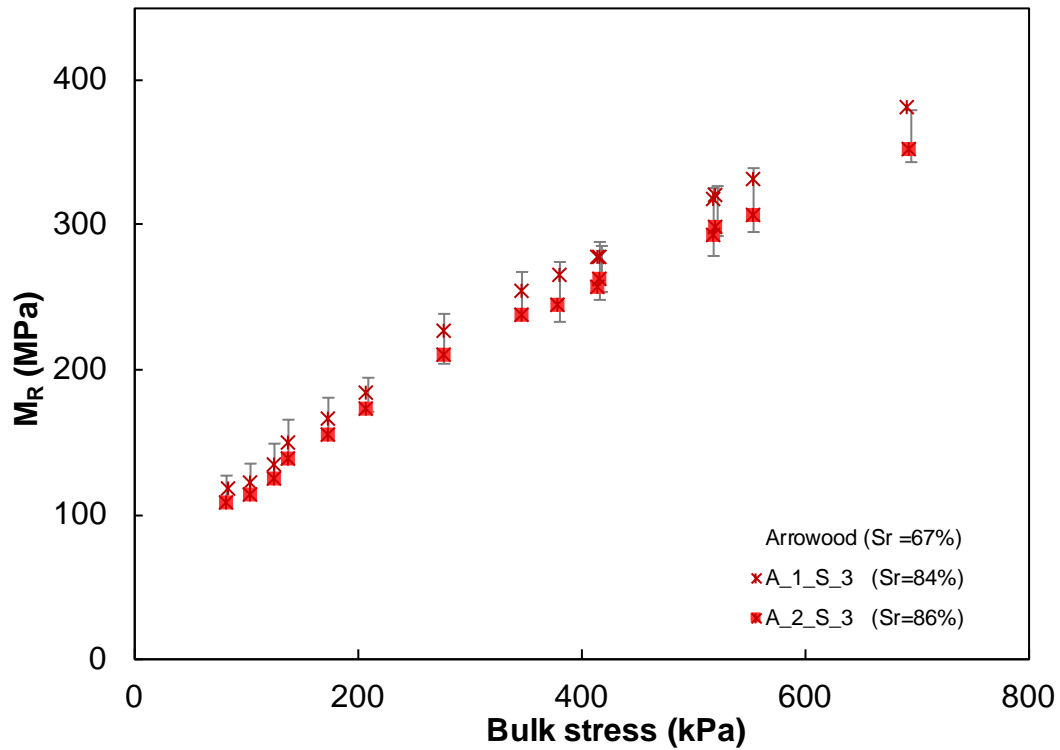
Figure C-5 – Arrowood aggregate – Stage 3 – Tests 1 and 2
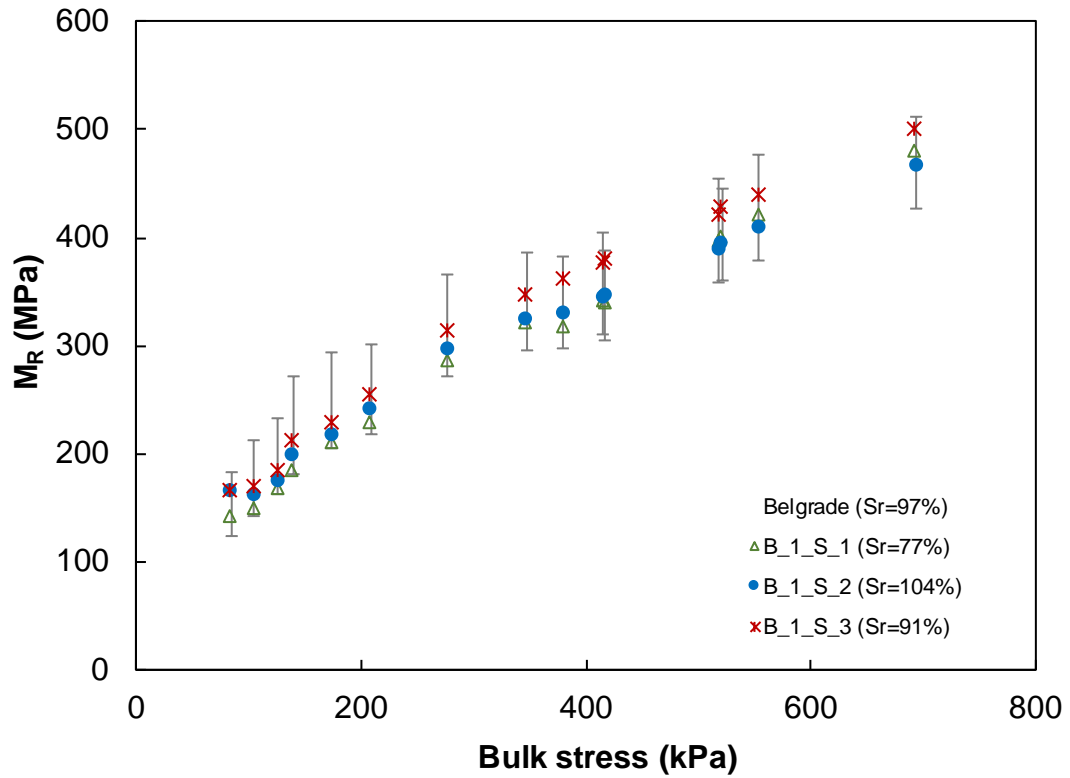
Figure C-6 – Belgrade aggregate – Test 1 – Stages 1, 2, and 3
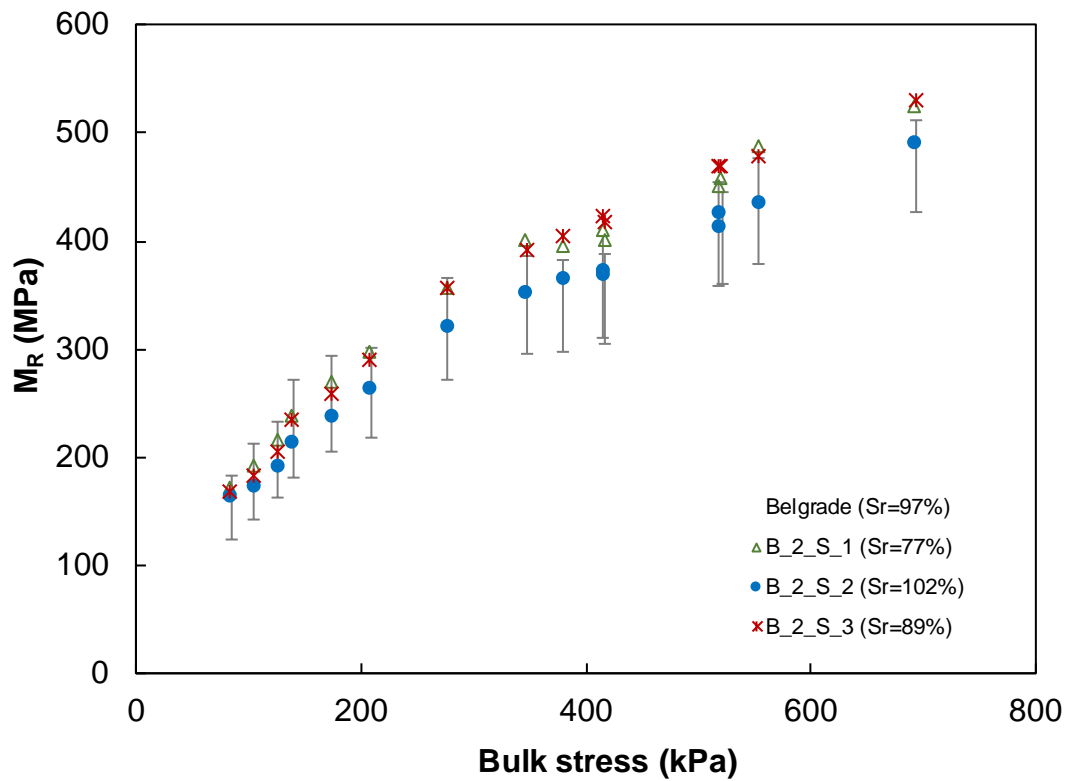
Figure C-7 – Belgrade aggregate – Test 2 – Stages 1, 2, and 3
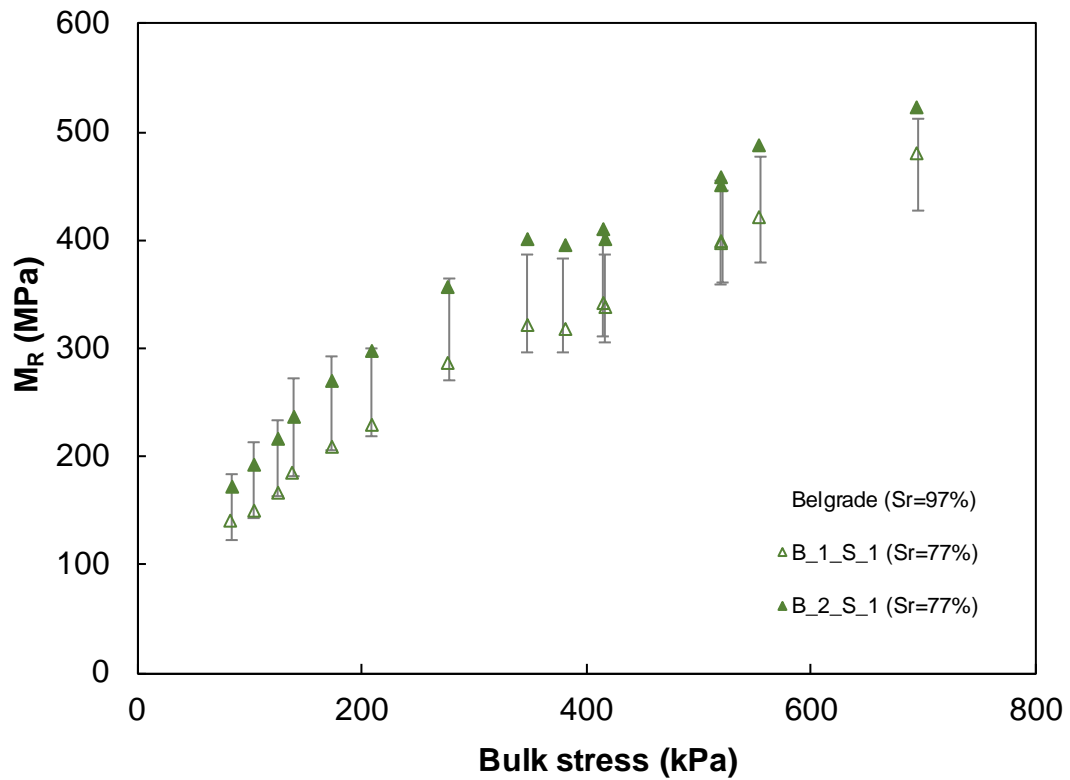
Figure C-8 – Belgrade aggregate – Stage 1 – Tests 1 and 2
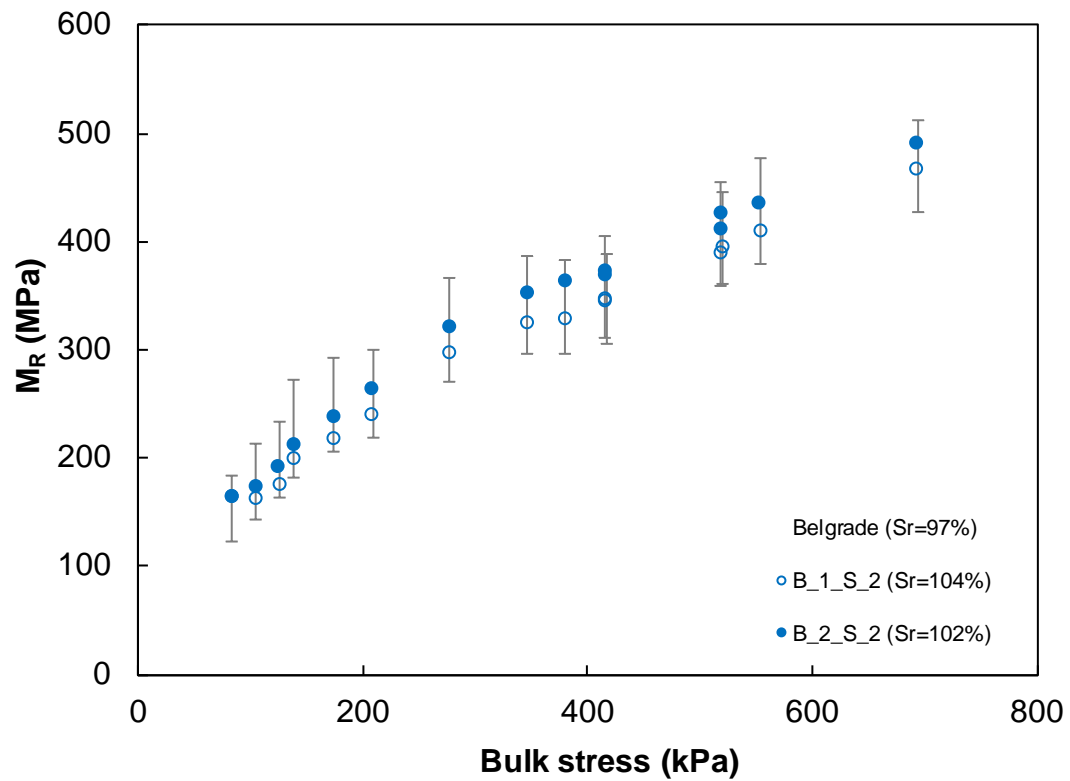
Figure C-9– Belgrade aggregate – Stage 2 – Tests 1 and 2
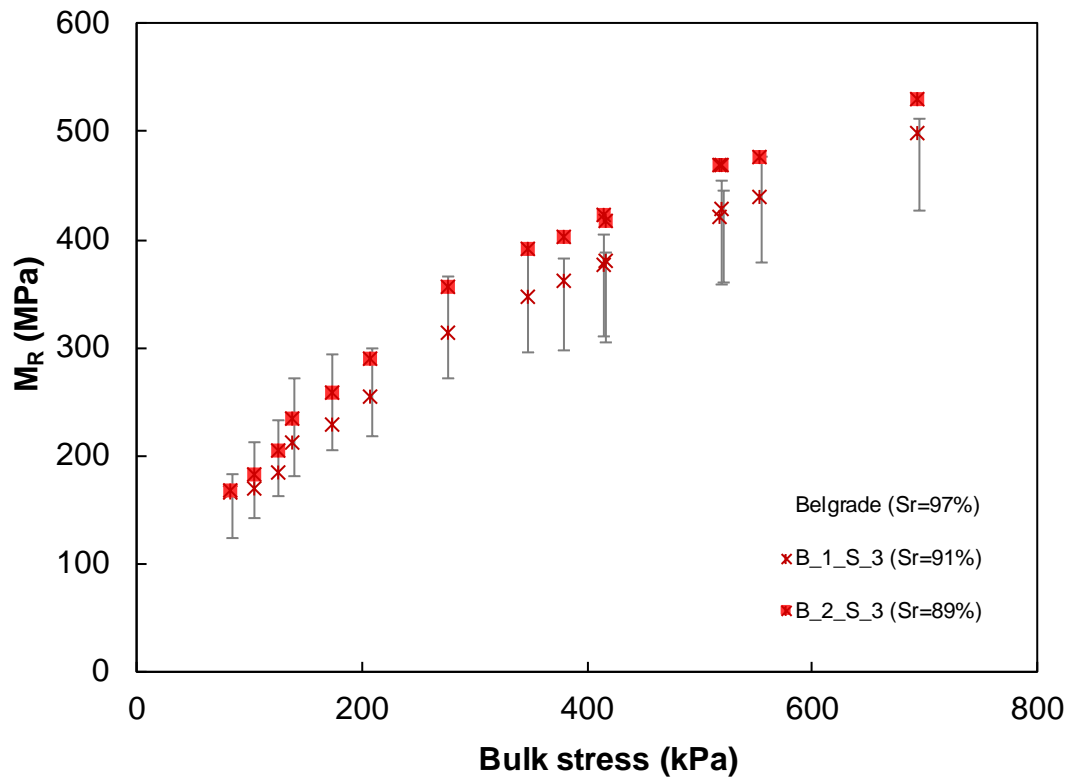
Figure C-10 – Belgrade aggregate – Stage 3 – Tests 1 and 2

Appendix D – Mineralogy Test Results

BOWSER-MORNER, INC.

Delivery Address: 4518 Taylorsville Rd • Dayton, Ohio 45424 Mailing Address: P.O. Box 51 • Dayton, Ohio 45401

AASHTO/ISO 17025 Accredited • USACE Validated ACIL

LABORATORY REPORT

Report To: North Carolina State University
Attn: Arash Bozorgi
Engineering Department

Report Date: 07/19/17
Job No.: 180253
Report No.: 112480
No. of Pages: 1

Report On: Elemental Analysis of One Crushed Stone Sample
Source: Martin Marietta Aggregates
Sample ID: Arrowood Quarry

Date Received: 06/26/17

Procedure: Chemical Analysis of Limestone, Quicklime and Hydrated Lime (ASTM C 25)

Analysis Description	Test Results
Calcium (Ca), %:	5.44
Calcium Oxide (CaO), %:	7.61
Calcium Carbonate ($CaCO_3$), %:	13.59
Magnesium (Mg), %:	2.48
Magnesium Oxide (MgO), %:	4.11
Magnesium Carbonate ($MgCO_3$), %:	8.60
Iron Oxide (Fe_2O_3), %:	12.47
Aluminum Oxide (Al_2O_3), %:	17.35
Silica (Si), %:	22.49
Silicon Dioxide (SiO_2), %:	48.10

For the chemical analysis of limestone, ASTM test methods C 25 (classical methods), C 1301 (atomic absorption), and C 1271 (x-ray emission) all measure the concentration of elements. In reporting the results, each test method assumes that the elements in the limestone are present as specific mineralogical oxides and carbonates. For some materials, these mineralogical assumptions may not be applicable and the sum of the compounds may be less than or greater than a theoretical 100%.

Should you have any questions, or if we may be of further service, please contact me at 937-236-8805, extension 322.

Respectfully submitted,

BOWSER-MORNER, INC.

KAF/gls/jlh
112480
1-File
1-abozorg@ncsu.edu

Karl A. Fletcher, Manager
Construction Materials and
Geotechnical Laboratories

BOWSER-MORNER, INC.

AASHTO/ISO 17025 Accredited • USACE Validated ACIL

LABORATORY REPORT

Report To:	North Carolina State University	**Report Date:**	07/19/17
	Attn: Arash Bozorgi	**Job No.:**	180253
	Engineering Department	**Report No.:**	112481
		No. of Pages:	1

Report On:	Elemental Analysis of One Crushed Stone Sample	**Date Received:**	06/26/17
Source:	Martin Marietta Aggregates		
Sample ID:	Belgrade Quarry		
Procedure:	Chemical Analysis of Limestone, Quicklime and Hydrated Lime (ASTM C 25)		

Analysis Description	Test Results
Calcium (Ca), %:	26.84
Calcium Oxide (CaO), %:	37.55
Calcium Carbonate ($CaCO_3$), %:	67.03
Magnesium (Mg), %:	0.45
Magnesium Oxide (MgO), %:	0.75
Magnesium Carbonate ($MgCO_3$), %:	1.56
Iron Oxide (Fe_2O_3), %:	0.40
Aluminum Oxide (Al_2O_3), %:	0.59
Silica (Si), %:	14.52
Silicon Dioxide (SiO_2), %:	31.06

For the chemical analysis of limestone, ASTM test methods C 25 (classical methods), C 1301 (atomic absorption), and C 1271 (x-ray emission) all measure the concentration of elements. In reporting the results, each test method assumes that the elements in the limestone are present as specific mineralogical oxides and carbonates. For some materials, these mineralogical assumptions may not be applicable and the sum of the compounds may be less than or greater than a theoretical 100%.

Should you have any questions, or if we may be of further service, please contact me at 937-236-8805, extension 322.

Respectfully submitted,

BOWSER-MORNER, INC.

Karl A. Fletcher, Manager
Construction Materials and
Geotechnical Laboratories

KAF/gls/jlh
112481
1-File
1-abozorg@ncsu.edu

BOWSER-MORNER, INC.

LABORATORY REPORT

Report To: North Carolina State University	**Report Date:**	07/19/17
Attn: Arash Bozorgi	**Job No.:**	180253
Engineering Department	**Report No.:**	112482
	No. of Pages:	1

Report On: Elemental Analysis of One Crushed Stone Sample   **Date Received:** 06/26/17

Source: Martin Marietta Aggregates

Sample ID: Fountain Quarry

Procedure: Chemical Analysis of Limestone, Quicklime and Hydrated Lime (ASTM C 25)

Analysis Description	Test Results
Calcium (Ca), %:	1.02
Calcium Oxide (CaO), %:	1.43
Calcium Carbonate ($CaCO_3$), %:	2.55
Magnesium (Mg), %:	0.20
Magnesium Oxide (MgO), %:	0.33
Magnesium Carbonate ($MgCO_3$), %:	0.69
Iron Oxide (Fe_2O_3), %:	3.62
Aluminum Oxide (Al_2O_3), %:	10.68
Silica (Si), %:	35.36
Silicon Dioxide (SiO_2), %:	75.65

For the chemical analysis of limestone, ASTM test methods C 25 (classical methods), C 1301 (atomic absorption), and C 1271 (x-ray emission) all measure the concentration of elements. In reporting the results, each test method assumes that the elements in the limestone are present as specific mineralogical oxides and carbonates. For some materials, these mineralogical assumptions may not be applicable and the sum of the compounds may be less than or greater than a theoretical 100%.

Should you have any questions, or if we may be of further service, please contact me at 937-236-8805, extension 322.

Respectfully submitted,

BOWSER-MORNER, INC.

KAF/gls/jlh
112482
1-File
1-abozorg@ncsu.edu

Karl A. Fletcher, Manager
Construction Materials and
Geotechnical Laboratories

BOWSER-MORNER, INC.

Delivery Address: 4518 Taylorsville Rd • Dayton, Ohio 45424 Mailing Address: P.O. Box 51 • Dayton, Ohio 45401

AASHTO/ISO 17025 Accredited • USACE Validated ACIL

LABORATORY REPORT

Report To: North Carolina State University
Attn: Arash Bozorgi
Engineering Department

Report Date: 07/19/17
Job No.: 180253
Report No.: 112483
No. of Pages: 1

Report On: Elemental Analysis of One Crushed Stone Sample

Date Received: 06/26/17

Source: Martin Marietta Aggregates

Sample ID: Franklin Quarry

Procedure: Chemical Analysis of Limestone, Quicklime and Hydrated Lime (ASTM C 25)

Analysis Description	Test Results
Calcium (Ca), %:	1.66
Calcium Oxide (CaO), %:	2.32
Calcium Carbonate ($CaCO_3$), %:	4.15
Magnesium (Mg), %:	0.54
Magnesium Oxide (MgO), %:	0.90
Magnesium Carbonate ($MgCO_3$), %:	1.87
Iron Oxide (Fe_2O_3), %:	2.89
Aluminum Oxide (Al_2O_3), %:	15.61
Silica (Si), %:	33.38
Silicon Dioxide (SiO_2), %:	71.41

For the chemical analysis of limestone, ASTM test methods C 25 (classical methods), C 1301 (atomic absorption), and C 1271 (x-ray emission) all measure the concentration of elements. In reporting the results, each test method assumes that the elements in the limestone are present as specific mineralogical oxides and carbonates. For some materials, these mineralogical assumptions may not be applicable and the sum of the compounds may be less than or greater than a theoretical 100%.

Should you have any questions, or if we may be of further service, please contact me at 937-236-8805, extension 322.

Respectfully submitted,

BOWSER-MORNER, INC.

Karl A. Fletcher, Manager
Construction Materials and
Geotechnical Laboratories

KAF/gls/jlh
112483
1-File
1-abozorg@ncsu.edu

BOWSER-MORNER, INC.

Delivery Address: 4518 Taylorsville Rd • Dayton, Ohio 45424 Mailing Address: P.O. Box 51 • Dayton, Ohio 45401

AASHTO/ISO 17025 Accredited • USACE Validated ACIL

LABORATORY REPORT

Report To:	North Carolina State University	**Report Date:**	07/19/17
	Attn: Arash Bozorgi	**Job No.:**	180253
	Engineering Department	**Report No.:**	112484
		No. of Pages:	1

Report On:	Elemental Analysis of One Crushed Stone Sample	**Date Received:**	06/26/17
Source:	Martin Marietta Aggregates		
Sample ID:	Jamestown Quarry		
Procedure:	Chemical Analysis of Limestone, Quicklime and Hydrated Lime (ASTM C 25)		

Analysis Description	Test Results
Calcium (Ca), %:	2.95
Calcium Oxide (CaO), %:	4.13
Calcium Carbonate (CaCO$_3$), %:	7.37
Magnesium (Mg), %:	0.80
Magnesium Oxide (MgO), %:	1.33
Magnesium Carbonate (MgCO$_3$), %:	2.77
Iron Oxide (Fe$_2$O$_3$), %:	2.94
Aluminum Oxide (Al$_2$O$_3$), %:	16.40
Silica (Si), %:	33.90
Silicon Dioxide (SiO$_2$), %:	72.51

For the chemical analysis of limestone, ASTM test methods C 25 (classical methods), C 1301 (atomic absorption), and C 1271 (x-ray emission) all measure the concentration of elements. In reporting the results, each test method assumes that the elements in the limestone are present as specific mineralogical oxides and carbonates. For some materials, these mineralogical assumptions may not be applicable and the sum of the compounds may be less than or greater than a theoretical 100%.

Should you have any questions, or if we may be of further service, please contact me at 937-236-8805, extension 322.

Respectfully submitted,

BOWSER-MORNER, INC.

KAF/gls/jlh
112484
1-File
1-abozorg@ncsu.edu

Karl A. Fletcher, Manager
Construction Materials and
Geotechnical Laboratories